AD NUMBER
AD889048
LIMITATION CHANGES
TO: **Approved for public release; distribution is unlimited.**
FROM: **Distribution authorized to U.S. Gov't. agencies only; Test and Evaluation; NOV 1971. Other requests shall be referred to Air ForceArmament Laboratory, Attn: DLGC, Eglin AFB, FL 32542.**
AUTHORITY
AFAL ltr, 21 Jun 1974

AEDC-TR-71-244
AFATL-TR-71-142

cy 2

SEPARATION CHARACTERISTICS OF THE SUU-51 LASER-GUIDED DISPENSER MUNITION WITH FIXED TAIL FINS FROM THE F-4C AIRCRAFT

Jerry Coble

ARO, Inc.

November 1971

PROPULSION WIND TUNNEL FACILITY
ARNOLD ENGINEERING DEVELOPMENT CENTER
AIR FORCE SYSTEMS COMMAND
ARNOLD AIR FORCE STATION, TENNESSEE

NOTICES

When U. S. Government drawings specifications, or other data are used for any purpose other than a definitely related Government procurement operation, the Government thereby incurs no responsibility nor any obligation whatsoever, and the fact that the Government may have formulated, furnished, or in any way supplied the said drawings, specifications, or other data, is not to be regarded by implication or otherwise, or in any manner licensing the holder or any other person or corporation, or conveying any rights or permission to manufacture, use, or sell any patented invention that may in any way be related thereto.

Qualified users may obtain copies of this report from the Defense Documentation Center.

References to named commercial products in this report are not to be considered in any sense as an endorsement of the product by the United States Air Force or the Government.

SEPARATION CHARACTERISTICS OF THE SUU-51 LASER-GUIDED DISPENSER MUNITION WITH FIXED TAIL FINS FROM THE F-4C AIRCRAFT

Jerry Coble
ARO, Inc.

FOREWORD

The work reported herein was sponsored by the Air Force Armament Laboratory (DLGC/Bob Hume), Armament Development and Test Center (ADTC), Air Force Systems Command (AFSC), under Program Element 64604F, Project 1120, Task 09.

The test results presented were obtained by ARO, Inc. (a subsidiary of Sverdrup & Parcel and Associates, Inc.), contract operator of the Arnold Engineering Development Center (AEDC), AFSC, Arnold Air Force Station, Tennessee, under Contract F40600-72-C-0003. The test was conducted from August 7 through 13, 1971, under ARO Project No. PC0157. The manuscript was submitted for publication on October 1, 1971.

This technical report has been reviewed and is approved.

George F. Garey
Lt Colonel, USAF
AF Representative, PWT
Directorate of Test

Duncan W. Rabey, Jr.
Colonel, USAF
Director of Test

ABSTRACT

Tests were conducted in the Aerodynamic Wind Tunnel (4T) using 0.05-scale models to investigate the separation characteristics of the SUU-51 Laser-Guided Dispenser Munition (LGDM) with fixed tail fins from several carriage configurations of the F-4C aircraft. Releases were studied from the outboard and inboard pylons and from Triple Ejection Rack and Multiple Ejection Rack locations on the inboard and centerline pylons, respectively. Captive-trajectory store separation data were obtained at Mach numbers from 0.66 to 0.90 and a simulated altitude of 5000 ft. At selected test conditions, a parent-aircraft dive angle of 45 deg was simulated. Free-stream force and moment data were also obtained on the SUU-51 (LGDM) model at Mach numbers of 0.66 and 0.90 at store angles of attack from -6 to 24 deg. Generally, the store initially separated from the parent aircraft without store-to-parent contact with most of the trajectories manually terminated. Changing fuel tank positions improved some undesirable trajectories.

CONTENTS

APPENDIXES

Figure Page

II. TABLES

NOMENCLATURE

BL	Aircraft buttock line from plane of symmetry, in., model scale
b	Store reference dimension, ft, full scale
C_ℓ	Store rolling-moment coefficient, rolling moment/$q_\infty Sb$
C_{ℓ_p}	Store roll-damping derivative, $dC_\ell/d(pb/2V_\infty)$
C_m	Store pitching-moment coefficient, referenced to the store cg, pitching moment/$q_\infty Sb$
C_{m_q}	Store pitch-damping derivative, $dC_m/d(qb/2V_\infty)$
C_N	Store normal-force coefficient, normal force/$q_\infty S$
C_n	Store yawing-moment coefficient, referenced to the store cg, yawing moment/$q_\infty Sb$
C_{n_r}	Store yaw-damping derivative, $dC_n/d(rb/2V_\infty)$
FS	Aircraft fuselage station, in., model scale
F_Z	MER/TER ejector force, lb
F_{Z_1}	Pylon forward ejector force, lb
F_{Z_2}	Pylon aft ejector force, lb
I_{xx}	Full-scale moment of inertia about the store X_B axis, slug-ft^2
I_{xz}	Full-scale product of inertia, X_B-Z_B axis, slug-ft^2
I_{yy}	Full-scale moment of inertia about the store Y_B axis, slug-ft^2
I_{zz}	Full-scale moment of inertia about the store Z_B axis, slug-ft^2
M_∞	Free-stream Mach number
$\overline{m}$	Full-scale store mass, slugs
p	Store angular velocity about the X_B axis, radians/sec
p_∞	Free-stream static pressure, psfa
q	Store angular velocity about the Y_B axis, radians/sec

q_∞	Free-stream dynamic pressure, 0.7 $p_\infty M_\infty^2$, psf
r	Store angular velocity about the Z_B axis, radians/sec
S	Store reference area, ft^2, full scale
T_E	Ejector force cutoff time, sec
t	Real trajectory time from initiation of trajectory, sec
V_∞	Free-stream velocity, ft/sec
WL	Aircraft waterline from reference horizontal plane, in., model scale
X	Separation distance of the store cg parallel to the flight axis system X_F direction, ft, full scale measured from the prelaunch position
X_{cg}	Full-scale cg location, ft, from nose of store
X_L	Ejector piston location relative to the store cg, positive forward of store cg, ft, full scale
X_{L_1}	Forward ejector piston location relative to the store cg, positive forward of store cg, ft, full scale
X_{L_2}	Aft ejector piston location relative to the store cg, positive forward of store cg, ft, full scale
Y	Separation distance of the store cg parallel to the flight axis system Y_F direction, ft, full scale measured from the prelaunch position
Z	Separation distance of the store cg parallel to the flight-axis system Z_F direction, ft, full scale measured from the prelaunch position
Z_E	Ejector stroke length, ft, full scale
α_p	Parent-aircraft model angle of attack relative to the free-stream velocity vector, deg
θ	Angle between the store longitudinal axis and its projection in the X_F-Y_F plane, positive when store nose is raised as seen by pilot, deg
$\bar{\theta}$	Simulated parent-aircraft climb angle. Angle between the flight direction and the earth horizontal, deg, positive for increasing altitude
ϕ	Angle between the projection of the store lateral axis in the Y_F-Z_F plane and the Y_F axis, positive for clockwise rotation when looking upstream, deg

ψ Angle between the projection of the store longitudinal axis in the X_F-Y_F plane and the X_F axis, positive when the store nose is to the right as seen by the pilot, deg

FLIGHT-AXIS SYSTEM COORDINATES

Directions

X_F Parallel to the free-stream wind vector, positive direction is forward as seen by the pilot

Y_F Perpendicular to the X_F and Z_F directions, positive direction is to the right as seen by the pilot

Z_F In the aircraft plane of symmetry, perpendicular to the free-stream wind vector, positive direction is downward

The flight-axis system origin is coincident with the aircraft cg and remains fixed with respect to the parent aircraft during store separation. The X_F, Y_F, and Z_F coordinate axes do not rotate with respect to the initial flight direction and attitude.

STORE BODY-AXIS SYSTEM COORDINATES

Directions

X_B Parallel to the store longitudinal axis, positive direction is upstream in the prelaunch position

Y_B Perpendicular to the store longitudinal axis, and parallel to the flight-axis system X_F-Y_F plane when the store is at zero roll angle, positive direction is to the right looking upstream when the store is at zero yaw and roll angles

Z_B Perpendicualr to both the X_B and Y_B axes, positive direction is downward as seen by the pilot when the store is at zero pitch and roll angles.

The store body-axis system origin is coincident with the store cg and moves with the store during separation from the parent airplane. The X_B, Y_B, and Z_B coordinate axes rotate with the store in pitch, yaw, and roll so that mass moments of inertia about the three axes are not time-varying quantities.

SECTION I
INTRODUCTION

This investigation was conducted in the Aerodynamic Wind Tunnel (4T) of the Propulsion Wind Tunnel Facility to obtain captive-trajectory store-separation data for the SUU-51 (LGDM) store. The 0.05-scale models were released from various F-4C inboard and centerline multiple carriage and outboard and inboard single carriage configurations. All separation trajectories were initiated from the launch position with simulated ejector forces acting on the store. The SUU-51 (LGDM) was modified from an earlier design that did not separate from the parent aircraft satisfactorily (Ref. 1). The data presented in Ref. 1 are for a SUU-51 (LGDM) configuration with the fins folded into the body during release, whereas the present configurations include fixed tail fins extending from the body.

To simulate the separation trajectories, the store models were attached to the Captive Trajectory System (CTS) in the 4T wind tunnel. Flight conditions were simulated at Mach numbers of 0.66, 0.74, 0.82, and 0.90 for an altitude of 5000 ft. At selected test conditions, a parent-aircraft dive angle of 45 deg was simulated. Free-stream static stability data for the store models were obtained at Mach numbers of 0.66 and 0.90 at store angles of attack from -6 to 24 deg.

SECTION II
APPARATUS

2.1 TEST FACILITY

The Aerodynamic Wind Tunnel (4T) is a closed-loop, continuous flow, variable density tunnel in which the Mach number can be varied from 0.2 to 1.3. At all Mach numbers, the stagnation pressure can be varied from 200 to 3400 psfa. The test section is 4 ft square and 12.5 ft long with perforated, variable porosity (0.5- to 10-percent open) walls. It is completely enclosed in a plenum chamber from which the air can be evacuated, allowing part of the tunnel airflow to be removed through the perforated walls of the test section.

For store separation testing, two separate and independent support systems are used to support the models. The parent-aircraft model is inverted in the test section and supported by an offset sting attached to the main pitch sector. The store model is supported by the CTS which extends down from the tunnel top wall and provides store movement (six degreees of freedom) independent of the parent-aircraft model. An isometric drawing of a typical store separation installation is shown in Fig. 1, Appendix I.

Also shown in Fig. 1 is a block diagram of the computer control loop used during captive trajectory testing. The analog system and the digital computer work as an integrated unit and, utilizing required input information, control the store movement during a trajectory. Store positioning is accomplished by use of six individual d-c electric motors. Maximum translational travel of the CTS is ±15 in. from the tunnel centerline in the lateral and vertical directions and 36 in. in the axial direction. Maximum angular

displacements are ±45 deg in pitch and yaw and ±360 deg in roll. A more complete description of the test facility can be found in Ref. 2. A schematic showing the test section details and the location of the models in the tunnel is shown in Fig. 2.

2.2 TEST ARTICLES

The test articles were 0.05-scale models of the F-4C parent aircraft and the SUU-51 (LGDM) store as shown in the tunnel installation photograph (Fig. 3). A sketch showing the basic dimensions of the F-4C parent model is shown in Fig. 4. For this test, only the right wing and fuselage centerline of the F-4C were equipped for store separation. Details and dimensions of the pylons are shown in Fig. 5. The surfaces of the fuselage centerline and inboard and outboard pylons are inclined at a 1.0-deg nose-down angle with respect to the aircraft waterline. The outboard pylon is canted 7.5-deg outboard (Fig. 4).

The Triple Ejection Rack (TER) and Multiple Ejection Rack (MER) were mounted on the inboard and centerline pylons, respectively, and matched to the 30-in. suspension lug of the pylons. Details and dimensions of the TER and MER are shown in Figs. 6 and 7, respectively.

Details and dimensions of the SUU-51 (LGDM) store models are shown in Fig. 8. Store configurations S-1 and S-2 are identical in dimensions but weigh 1000 and 812 lb, respectively. Stores S-1 and S-2 have a swept leading edge on the tail fins with a 36-in. full-scale span, whereas the S-3 configuration has a perpendicular leading edge on the tail fins with a 30-in. span.

Dimensional sketches of the 370- and 600-gal dummy fuel tanks used to simulate the desired aircraft configurations are shown in Figs. 9 and 10, respectively. Aircraft/weapons loading nomenclature used for describing the configurations is given in Fig. 11, and the loading configurations for which trajectory data were obtained are shown in Fig. 12. As shown in Fig. 12, load configurations 1, 3, 5, 6, 7, 9, 11, 13, and 14 are the actual left-wing loadings which were simulated during the test by reversing the launch sequence and releasing from the right wing. The right-wing load configurations presented in Fig. 12 were released as shown.

2.3 INSTRUMENTATION

A six-component, internal strain-gage balance was used to obtain the force and moment data on the SUU-51 (LGDM) models. Translational and angular positions of the store models were obtained from the CTS analog outputs. An angular position indicator in the F-4C aircraft was used to determine the parent-model angle of attack. The MER, TER, and appropriate pylons were instrumented with a touch wire at each station which aided in the positioning of the sting-mounted store model at the launch position on the rack. The system was also electrically connected to automatically stop the CTS movement if the model or sting contacted the rack or the aircraft-model surface.

SECTION III
TEST DESCRIPTION

3.1 TEST CONDITIONS

Separation trajectory data were obtained at Mach numbers from 0.60 to 0.90. Tunnel dynamic pressure was 500 psf at all Mach numbers, and tunnel stagnation temperature was maintained near 120°F.

Tunnel conditions were held constant at the desired Mach number and stagnation pressure while data for each trajectory were obtained. The trajectories were terminated when the store or sting contacted the parent-aircraft model, when a CTS limit was reached, or when manually stopped after the accumulation of sufficient data.

3.2 TRAJECTORY DATA ACQUISITION

To obtain a trajectory, test conditions were established in the tunnel and the parent model was positioned at the desired angle of attack. The store model was then oriented to a position corresponding to the store carriage location. After the store was set at the desired initial position, operational control of the CTS was switched to the digital computer which controlled the store movement during the trajectory through commands to the CTS analog system (see block diagram Fig. 1). Data from the wind tunnel, consisting of measured model forces and moments, wind-tunnel operating conditions, and CTS rig positions, were input to the digital computer for use in the full-scale trajectory calculations.

The digital computer was programmed to solve the six-degree-of-freedom equations to calculate the angular and linear displacements of the store relative to the parent-aircraft pylon. In general, the program involves using the last two successive measured values of each static aerodynamic coefficient to predict the magnitude of the coefficients over the next time interval of the trajectory. These predicted values are used to calculate the new position and attitude of the store at the end of the time interval. The CTS is then commanded to move the store model to this new position and the aerodynamic loads are measured. If these new measurements agree with the predicted values, the process is continued over another time interval of the same magnitude. If the measured and predicted values do not agree within the desired precision, the calculation is repeated over a time interval one-half the previous value. This process is repeated until a complete trajectory has been obtained.

In applying the wind-tunnel data to the calculations of the full-scale store trajectories, the measured forces and moments are reduced to coefficient form and then applied with proper full-scale store dimensions and flight dynamic pressure. Dynamic pressure was calculated using a flight velocity equal to the free-stream velocity component plus the components of store velocity relative to the aircraft, and a density corresponding to the simulated altitude.

The initial portion of each launch trajectory incorporated simulated ejector forces in addition to the measured aerodynamic forces acting on the store. The ejector force

functions for the SUU-51 (LGDM) stores are presented in Figs. 13 through 16. The ejector force was considered to act perpendicular to the rack or pylon mounting surface. The locations of the applied ejector forces and other full-scale store parameters used in the trajectory calculations are listed in Table I, Appendix II.

3.3 CORRECTIONS

Balance, sting, and support deflections caused by the aerodynamic loads on the store models were accounted for in the data reduction program to calculate the true store-model angles. Corrections were also made for model weight tares to calculate the net aerodynamic forces on the store model.

3.4 PRECISION OF DATA

The trajectory data are subject to error from several sources including tunnel conditions, balance measurements, extrapolation tolerances allowed in the predicted coefficients, and CTS positioning control. Maximum error in the CTS position control was ±0.05 in. for the translational settings, ±0.15 deg for angular displacement settings in pitch and yaw, and ±1.0 deg for angular displacement settings in roll. Extrapolation tolerances were ±0.10 for each of the aerodynamic coefficients. The maximum uncertainties in the full-scale position data caused by the balance precision limitations are given in Table II.

The estimated uncertainty in setting Mach number was no greater than ±0.005, and the uncertainty in parent-model angle of attack was estimated to be ±0.1 deg.

SECTION IV
RESULTS AND DISCUSSION

4.1 GENERAL

Data obtained during this test consisted of separation trajectories of the SUU-51 (LGDM) from the F-4C outboard, inboard, and centerline carriage positions. Data showing the linear and angular displacements of the store relative to the mate position on the racks or pylons are presented as functions of full-scale trajectory time in Figs. 17 through 33. All trajectories were initiated from the right wing, with left-wing loading configurations (1, 3, 5, 6, 7, 9, 11, 13, and 14) simulated by launching from the right wing with a reversed (1, 3, and 2) TER ejection sequence.

Positive X, Y, and Z displacements (as seen by the pilot) are forward, to the right (outboard), and down, respectively. Positive changes in pitch, yaw, and roll (as seen by the pilot) are nose up, nose right (outboard), and clockwise, respectively. The ejector-separated trajectories simulated releases from left-wing outboard and inboard pylons, left- and right-wing inboard TER, and centerline MER positions. No attempt is made in this report to establish the safe-separation envelopes or to qualify the SUU-51 (LGDM) as safe or unsafe for separation from the F-4C. The trajectory data are presented as obtained from the wind tunnel along with comments regarding the aerodynamics of the store in the aircraft flow field. The data plots presented have a symbol placed on every tenth data point obtained.

4.2 SUU-51 (LGDM) TRAJECTORIES

Thirteen loading configurations of the SUU-51 (LGDM) were tested. Most of the releases attempted resulted in clean trajectories (no store-to-parent contact) with the flight terminated manually at an arbitrary elapsed time.

Figure 17 presents a comparison between the trajectories of the 1000-lb (S-1) and 812-lb (S-2) stores at Mach number 0.66 when released from an outboard pylon and an inboard TER. The heavier configuration (S-1) was a deviation from the nominal 812-lb store (S-2) and was tested to investigate the effect of mass on the trajectories. Since the trajectories were essentially identical, the sponsor decided to conduct the remaining releases with the S-2 store.

Trajectories presented in Figs. 18 through 23 indicate the S-2 configuration exhibited an outboard yawing motion for all load configurations except configuration 4 (Fig. 21). It is also noted that significantly different trajectories were obtained when Mach number was varied from 0.66 to 0.90 for some of the loading configurations, for example, configuration 2 (Fig. 19).

The alternate SUU-51 (LGDM) configuration (S-3) was released from various load configuations, and the trajectories are presented in Figs. 24 through 28. In general, the trajectories were not of sufficient duration, because of manual termination or the sting interference with the parent aircraft, to determine the yaw and pitch recovery point. For load configurations 9, 10, and 11 (Figs. 26, 27, and 28), the yaw angular rates were significantly larger for Mach number 0.90 than Mach number 0.66.

Load configurations 13 and 14 were similar to configurations 1 and 3, respectively, except for the fuel tank locations. The basic trajectories from load configurations 13 and 14 are presented in Figs. 29 and 30, respectively, for Mach numbers of 0.66 and 0.90. Figures 31 and 32 are presented to show the effect of the fuel tank changes on the trajectories. Figure 31 shows that the outboard translation and yaw angle were reduced by shifting the fuel tank from the centerline to the outboard pylon. Figure 32b indicates that with the outboard fuel tank location, the store moved inboard and thus did not contact the pylon early in the trajectory.

From Fig. 33 it is noted that the dive angle of the parent aircraft had no significant effect on the Y and Z displacements and only slight influence on the other trajectory parameters.

4.3 STATIC STABILITY DATA

Free-stream static stability data are presented in Fig. 34 for the SUU-51 (LGDM) alternate design (S-3) model. At a Mach number of 0.66, the vehicle was statically unstable through zero angle of attack and exhibited a stable trim point at 8- or 10-deg angle of attack, depending on the fin orientation. At a Mach number of 0.90, the vehicle was neutrally stable near zero angle of attack and did not indicate a stable trim point over the angle-of-attack range of these tests.

Static stability characteristics were determined for a configuration similar to the (S-2) model during a previous entry, with the results documented in Ref. 3. The previously tested 0.25-scale model was built with a gimbaled seeker and canards having a 22.00-in. full-scale span, whereas the 0.05-scale model used in this test had a flat-faced disk in place of the seeker and canards with a 23.22-in. full-scale span.

REFERENCES

1. Roberts, Robert H. "Separation Characteristics of the SUU-51 Laser-Guided Dispenser Munition from the F-4C Aircraft." AEDC-TR-71-140 (AD886554L), also AFATL-TR-71-92, August 1971.

2. Test Facilities Handbook (Ninth Edition). "Propulsion Wind Tunnel Facility, Vol. 4." Arnold Engineering Development Center, July 1971.

3. Coble, Jerry. "Static Stability and Control Effectiveness of the SUU-51 Laser-Guided Dispenser Munition at Mach Numbers from 0.66 to 0.99." AEDC-TR-71-196 (AD517323L), also AFATL-TR-71-119, September 1971, Confidential Report.

APPENDIXES
I. ILLUSTRATIONS
II. TABLES

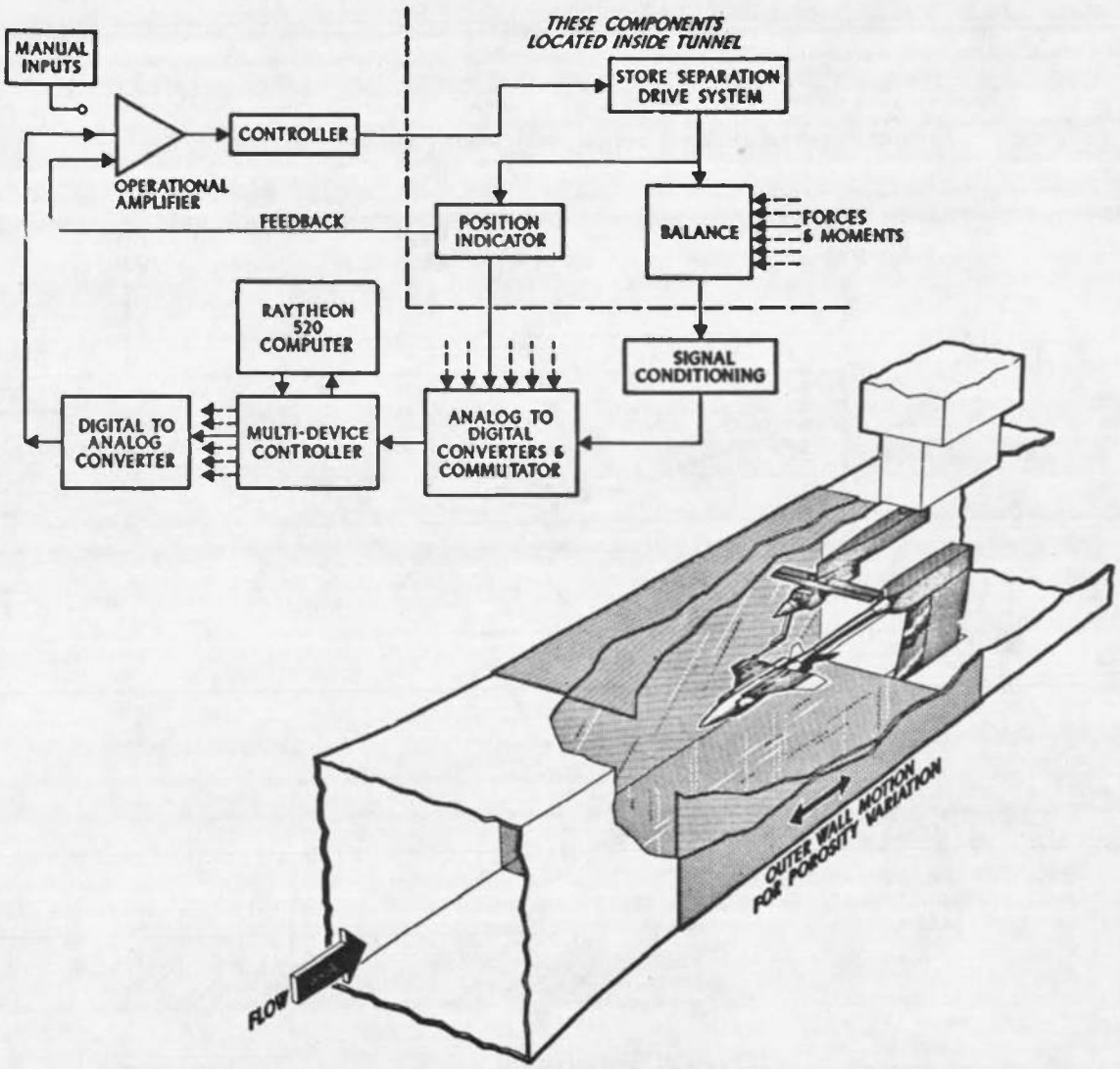

Fig. 1 Isometric Drawing of a Typical Store Separation Installation and a Block Diagram of the Computer Control Loop

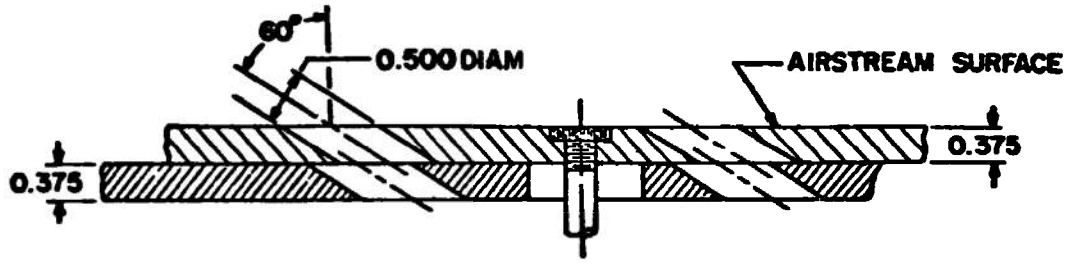

TYPICAL PERFORATED WALL CROSS SECTION

NOTE: TUNNEL STATIONS AND DIMENSIONS ARE IN INCHES

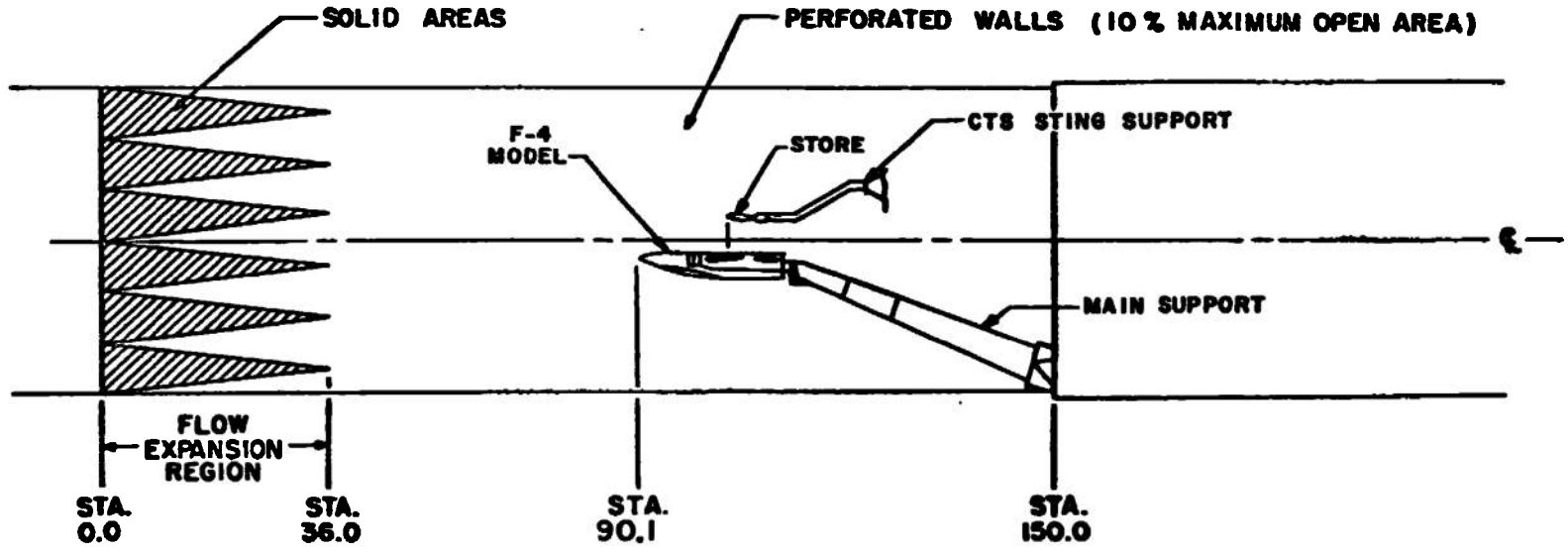

Fig. 2 Schematic of the Tunnel Test Section Showing Model Location

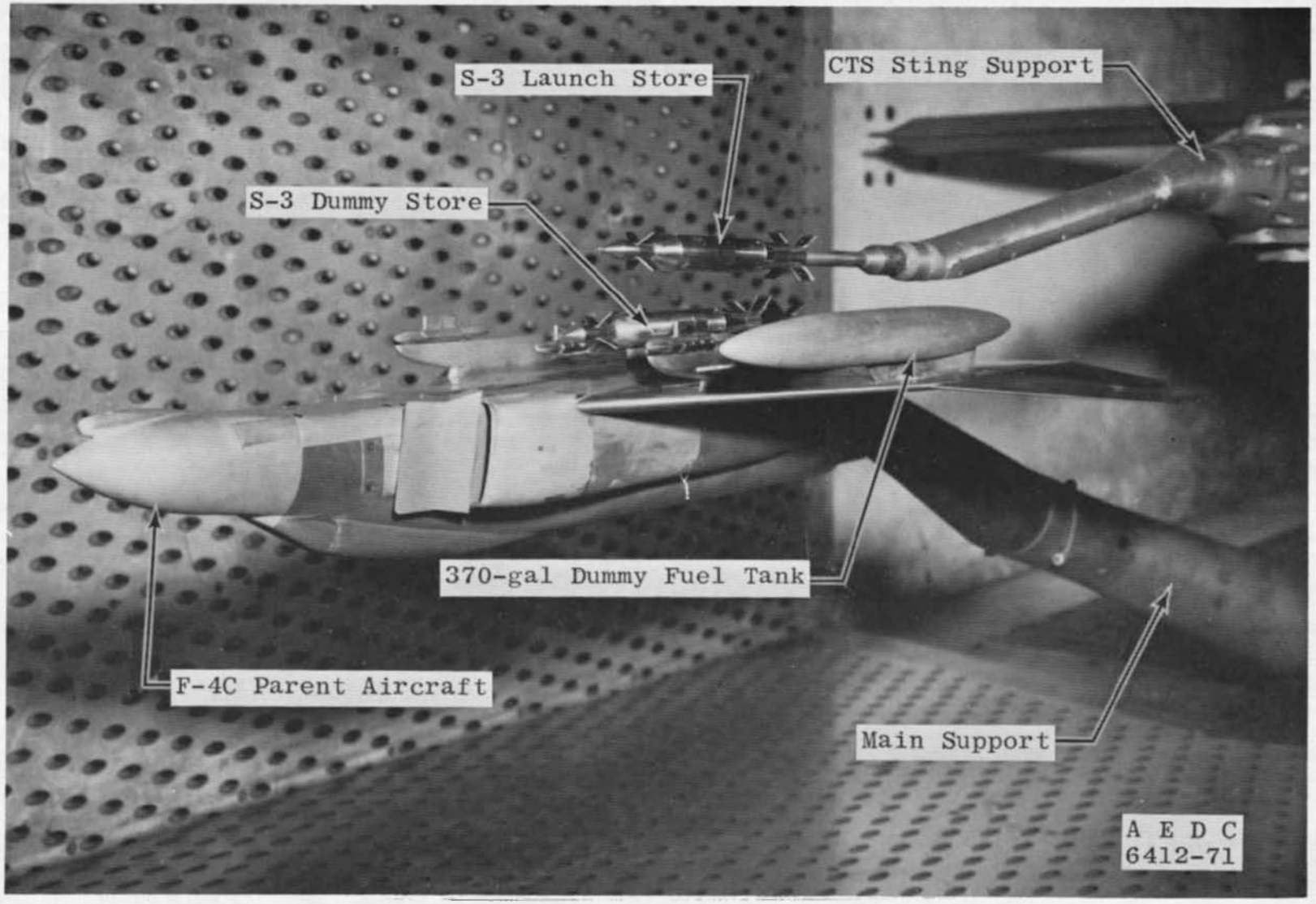

Fig. 3 Tunnel Installation Photograph

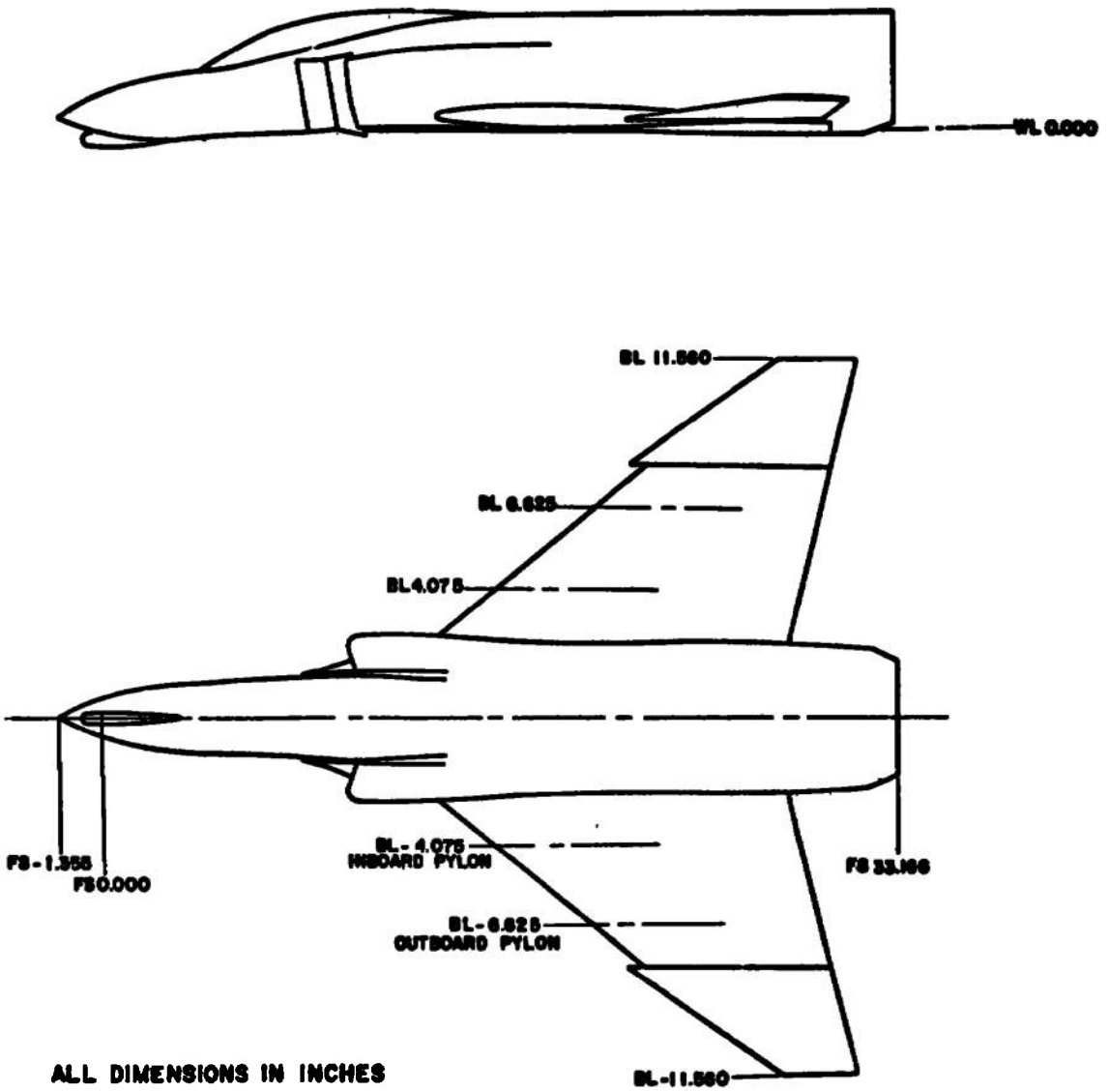

Fig. 4 Sketch of the F-4C Parent-Aircraft Model

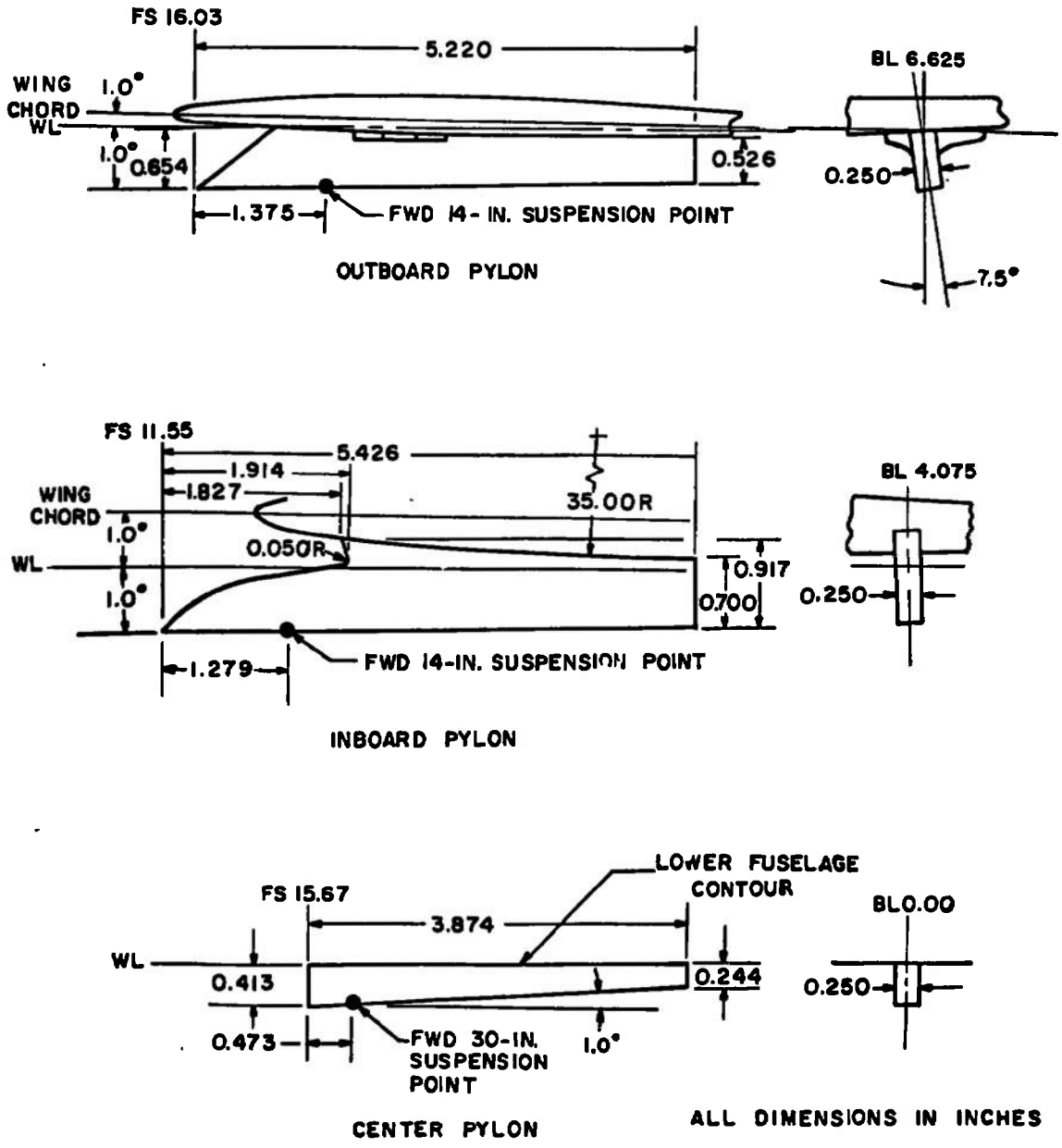

Fig. 5 Details and Dimensions of the F-4C Pylon Models

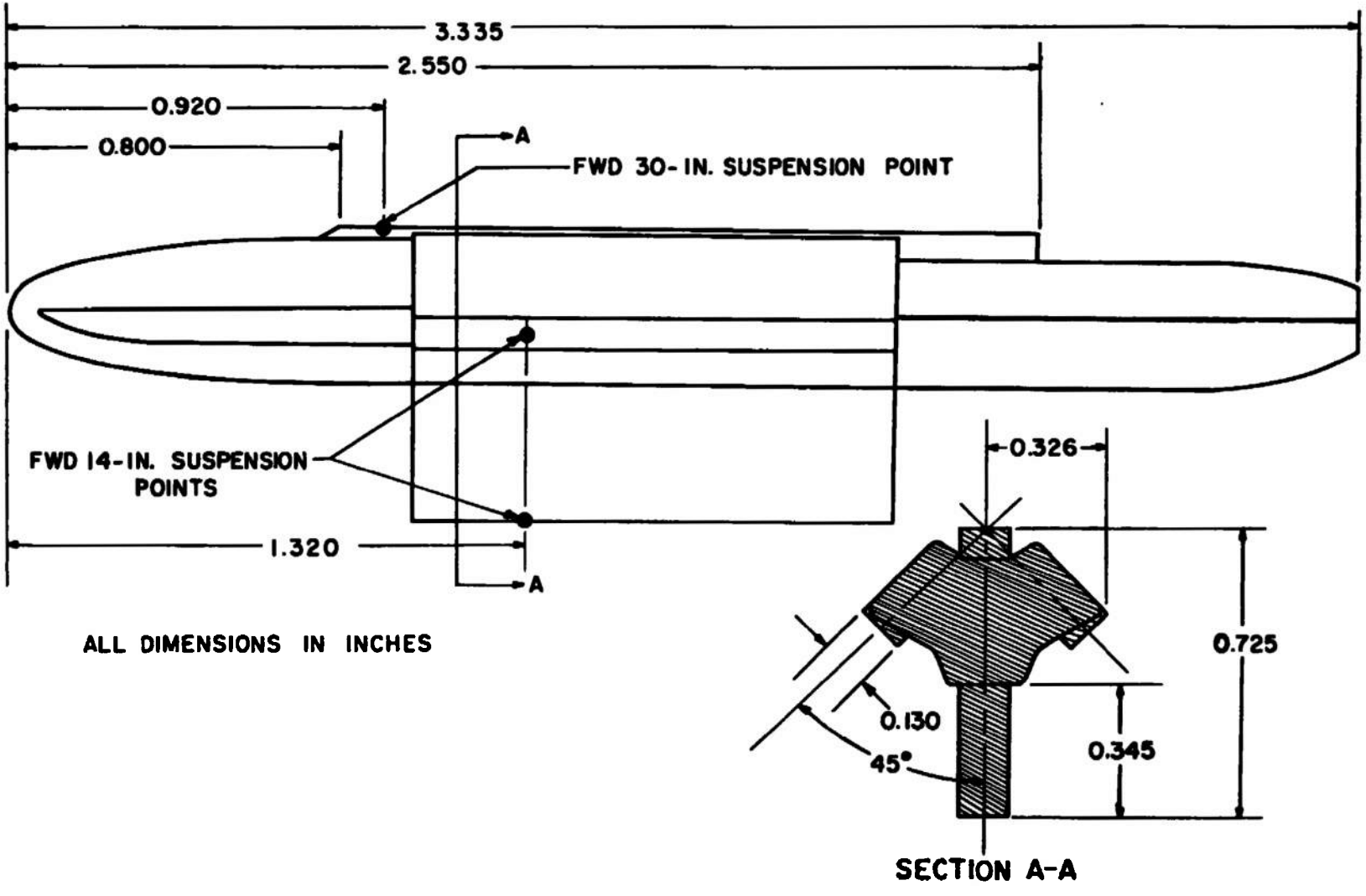

Fig. 6 Details and Dimensions of the TER Model

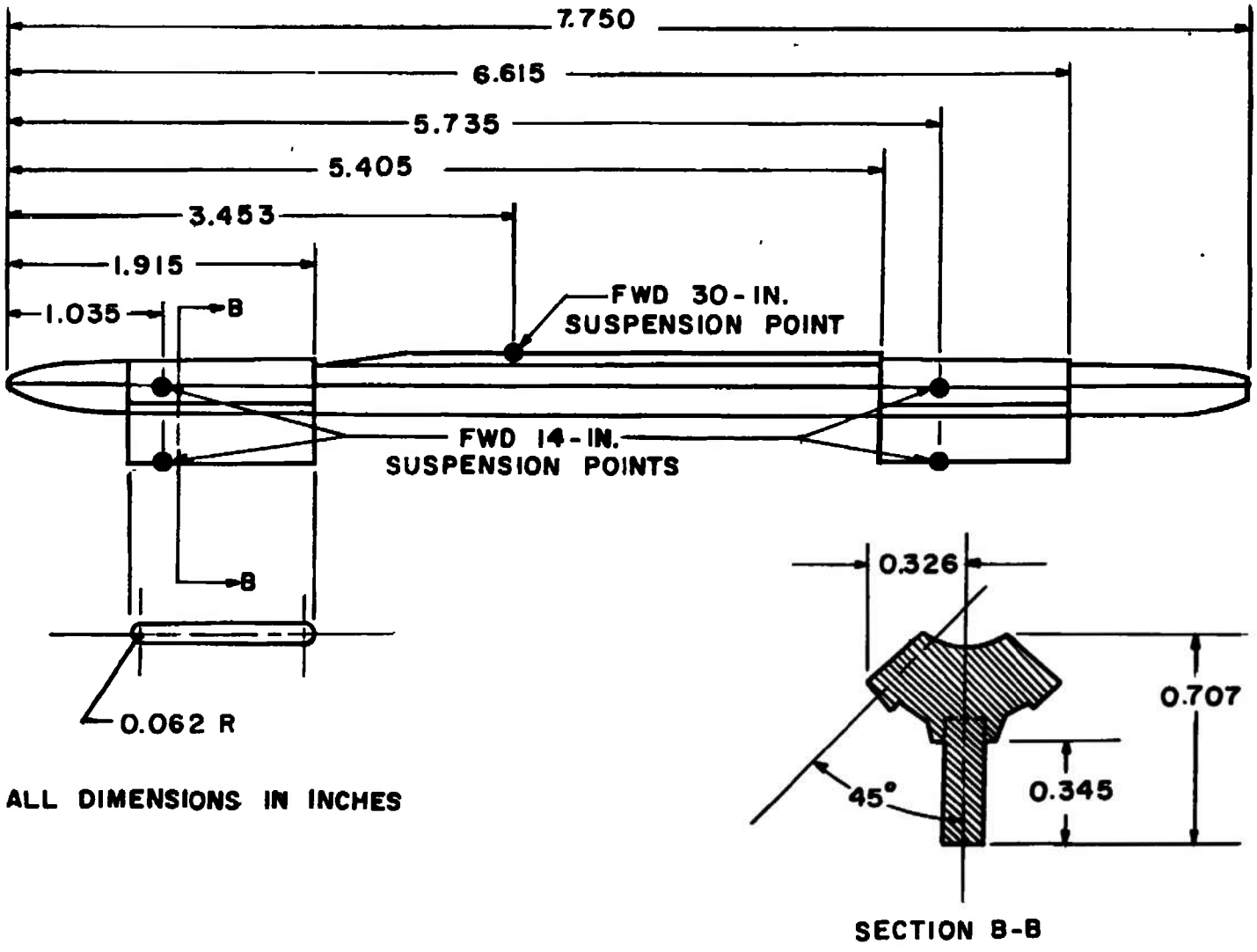

Fig. 7 Details and Dimensions of the MER Model

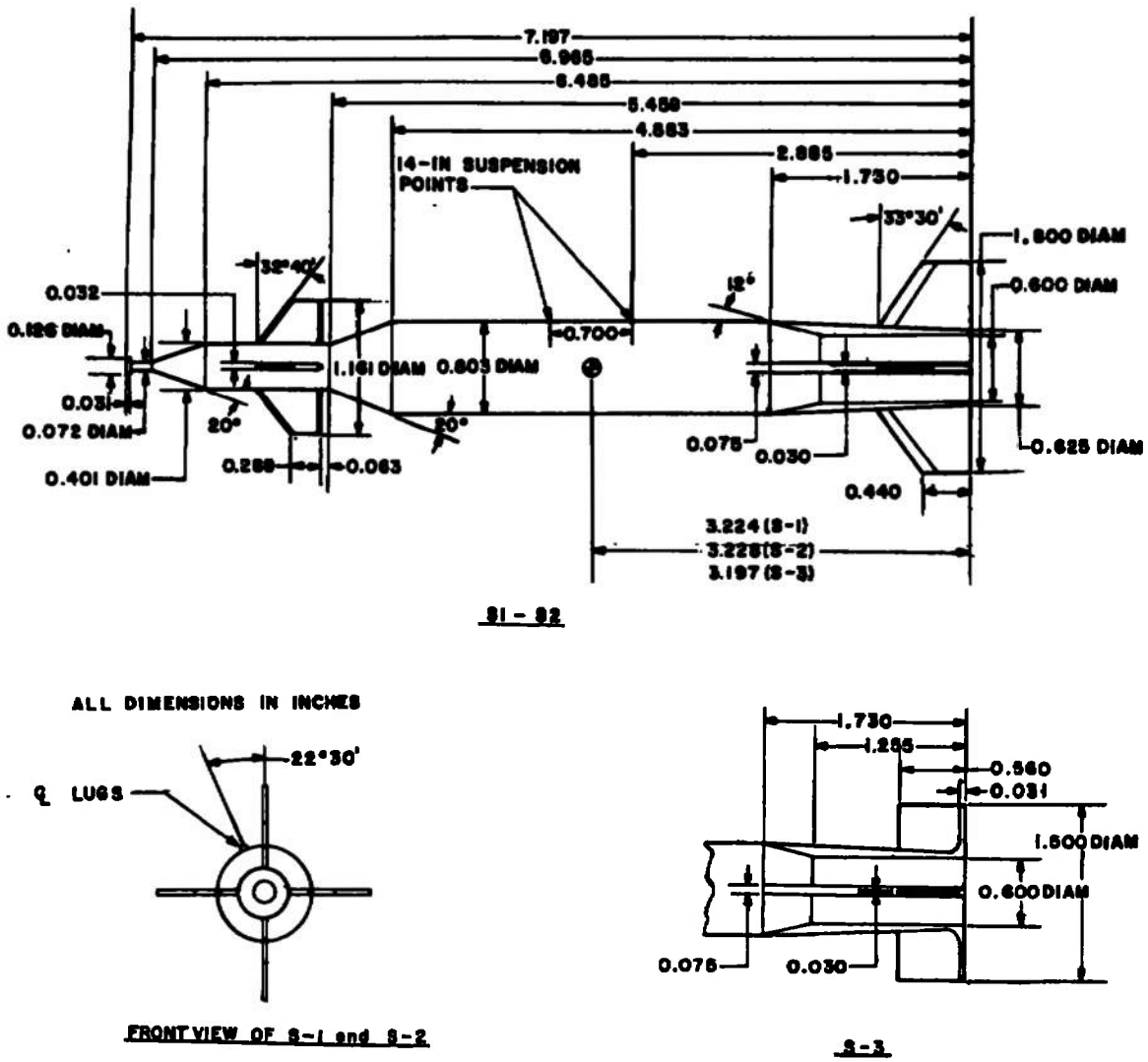

Fig. 8 Details and Dimensions of the SUU-51 (LGDM) Models

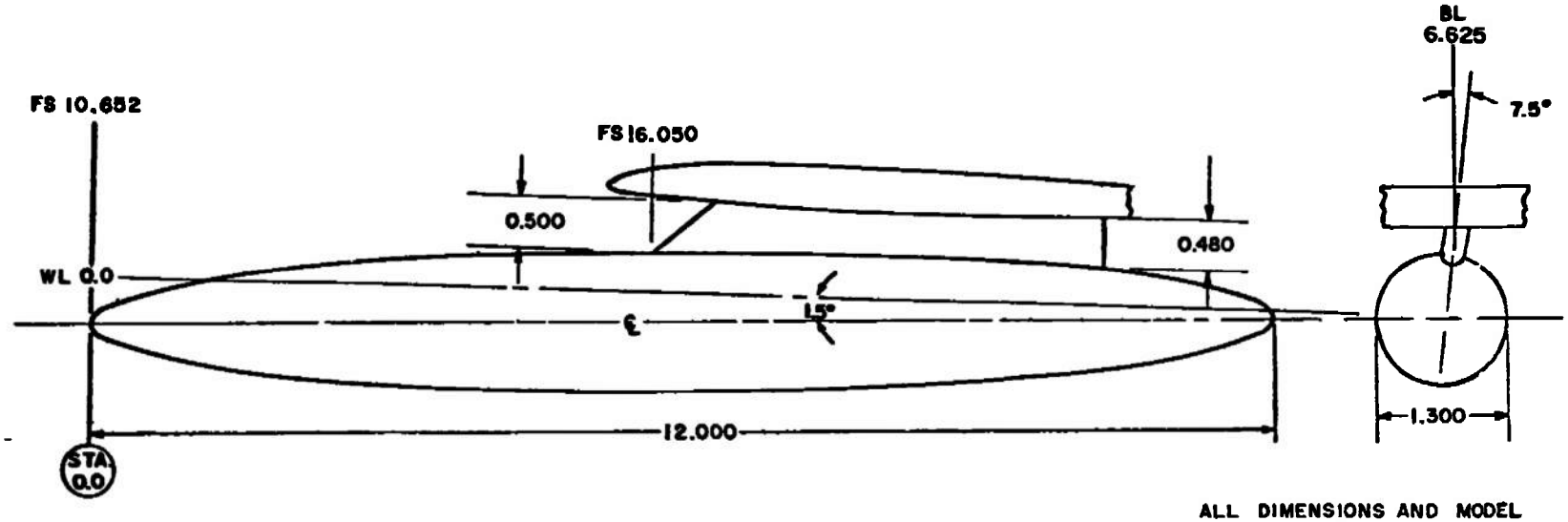

ALL DIMENSIONS AND MODEL STATIONS IN INCHES

BODY CONTOUR, TYPICAL BOTH ENDS

STATION	BODY DIAM	STATION	BODY DIAM
0.000	0.000	2.500	1.116
0.025	0.100	2.750	1.156
0.050	0.144	3.000	1.190
0.150	0.258	3.250	1.218
0.250	0.340	3.500	1.242
0.500	0.498	3.750	1.260
0.750	0.622	4.000	1.274
1.000	0.724	4.250	1.286
1.250	0.812	4.500	1.294
1.500	0.890	4.750	1.298
1.750	0.958	5.000	1.300
2.000	1.016	6.000	1.300
2.250	1.070		

Fig. 9 Details and Dimensions of the 370-gal Dummy Fuel Tank

BODY CONTOUR

Y	R	Y	R
0.000	0 000	4.250	0 827
0.050	0 049	4.500	0.838
0.100	0.077	4.750	0.847
0.150	0.101	5.000	0.854
0.200	0 122	5.250	0.859
0.250	0.143	5.500	0 960
0.500	0.232	6.250	0.860
0.750	0.308	6 500	0.859
1.000	0.376	6.750	0.856
1.250	0.438	7.000	0 852
1.500	0.494	7.250	0 846
1.750	0.546	7 500	0.839
2.000	0.593	7.750	0.830
2.250	0.637	8 000	0.820
2.500	0.679	8.250	0.809
2.750	0.713	8.500	0.796
3.000	0.740	8.750	0.781
3.250	0.762	9 000	0.765
3.500	0.782	9.250	0 745
3.750	0.799	13.000	0.400
4.000	0 814		

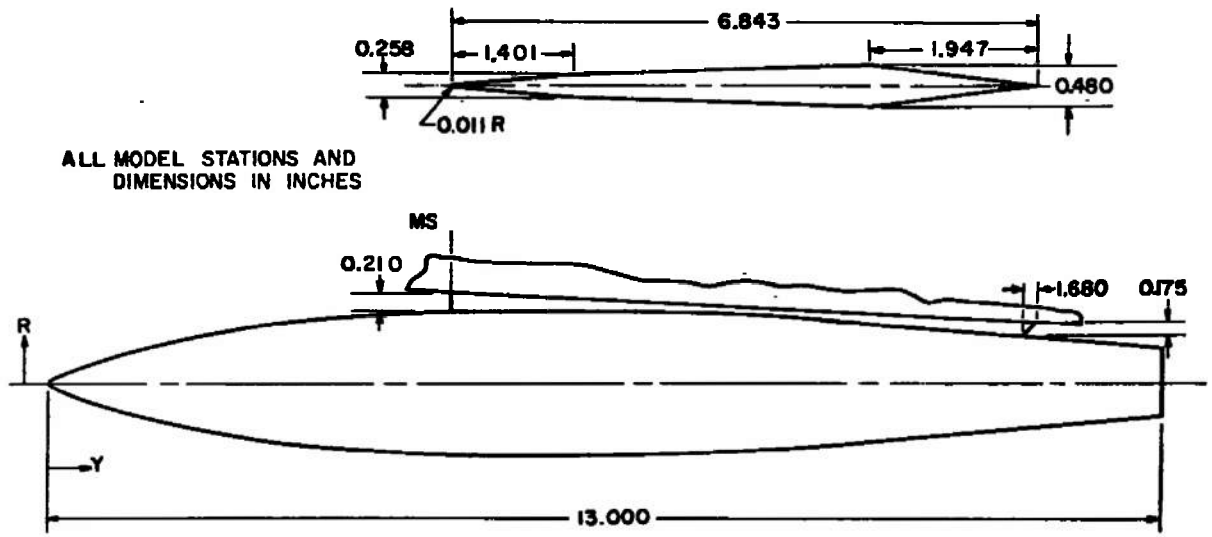

Fig. 10 Details and Dimensions of the 600-gal Dummy Fuel Tank

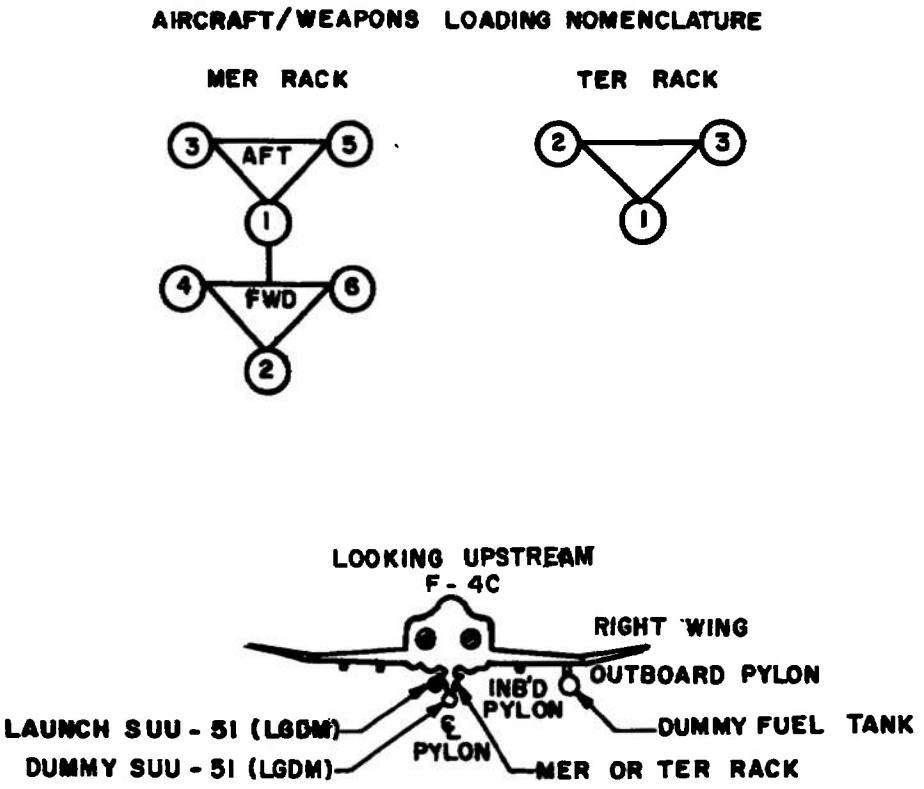

Fig. 11 Aircraft/Weapons Loading Nomenclature

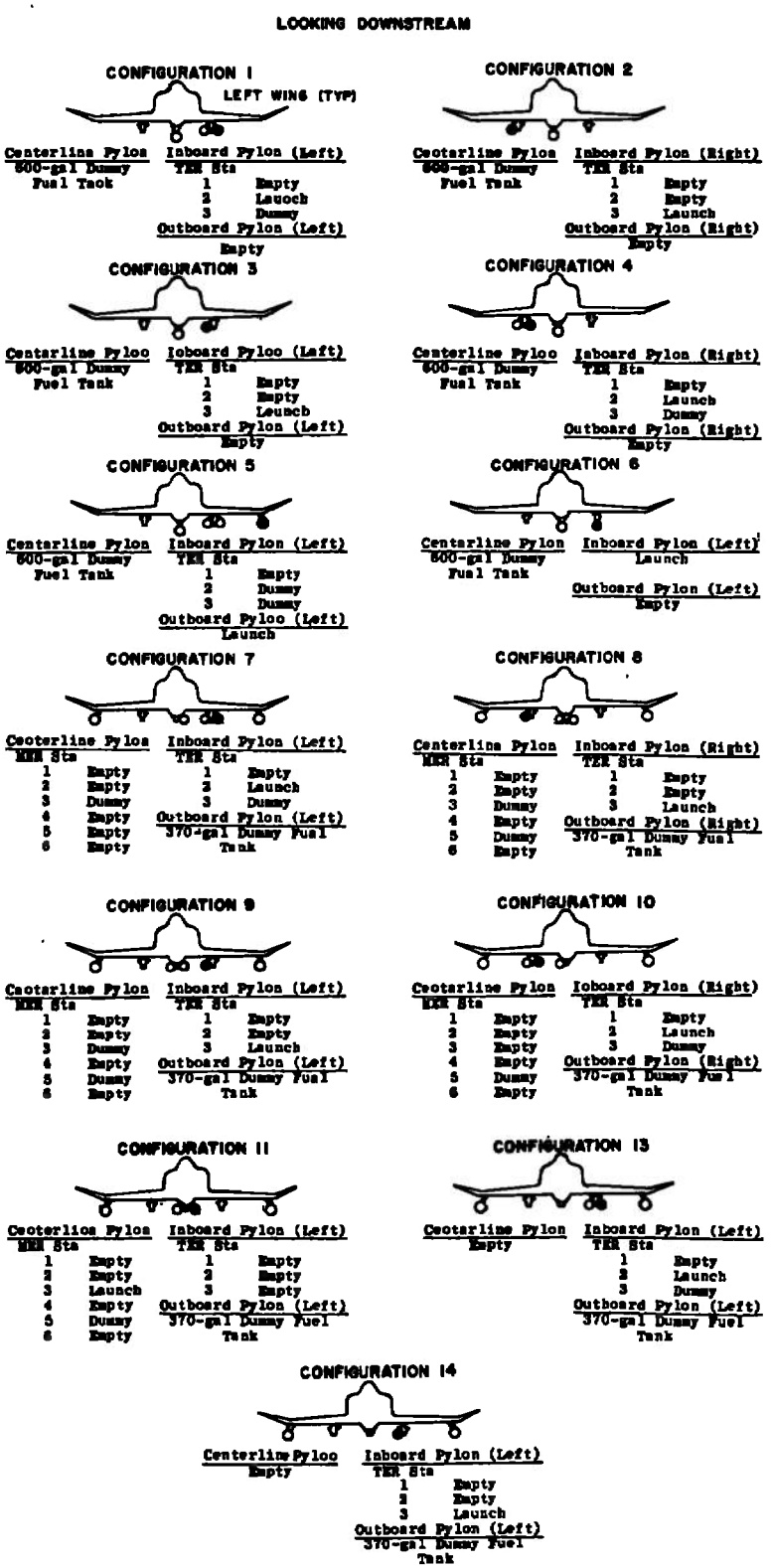

Fig. 12 Schematic of Simulated Aircraft/Weapons Loading Configurations

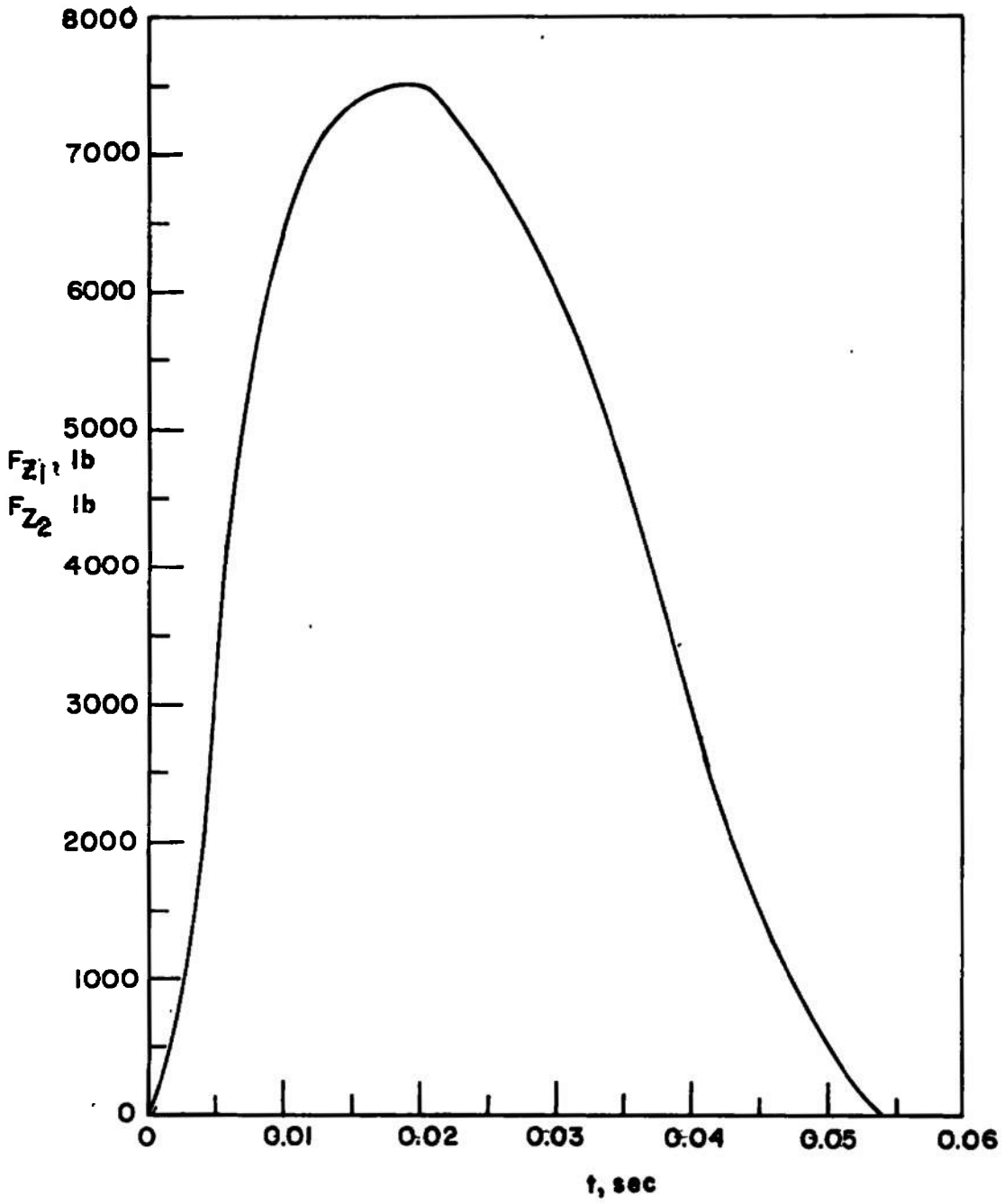

Fig. 13 Pylon Ejector Force Function for Store S-1

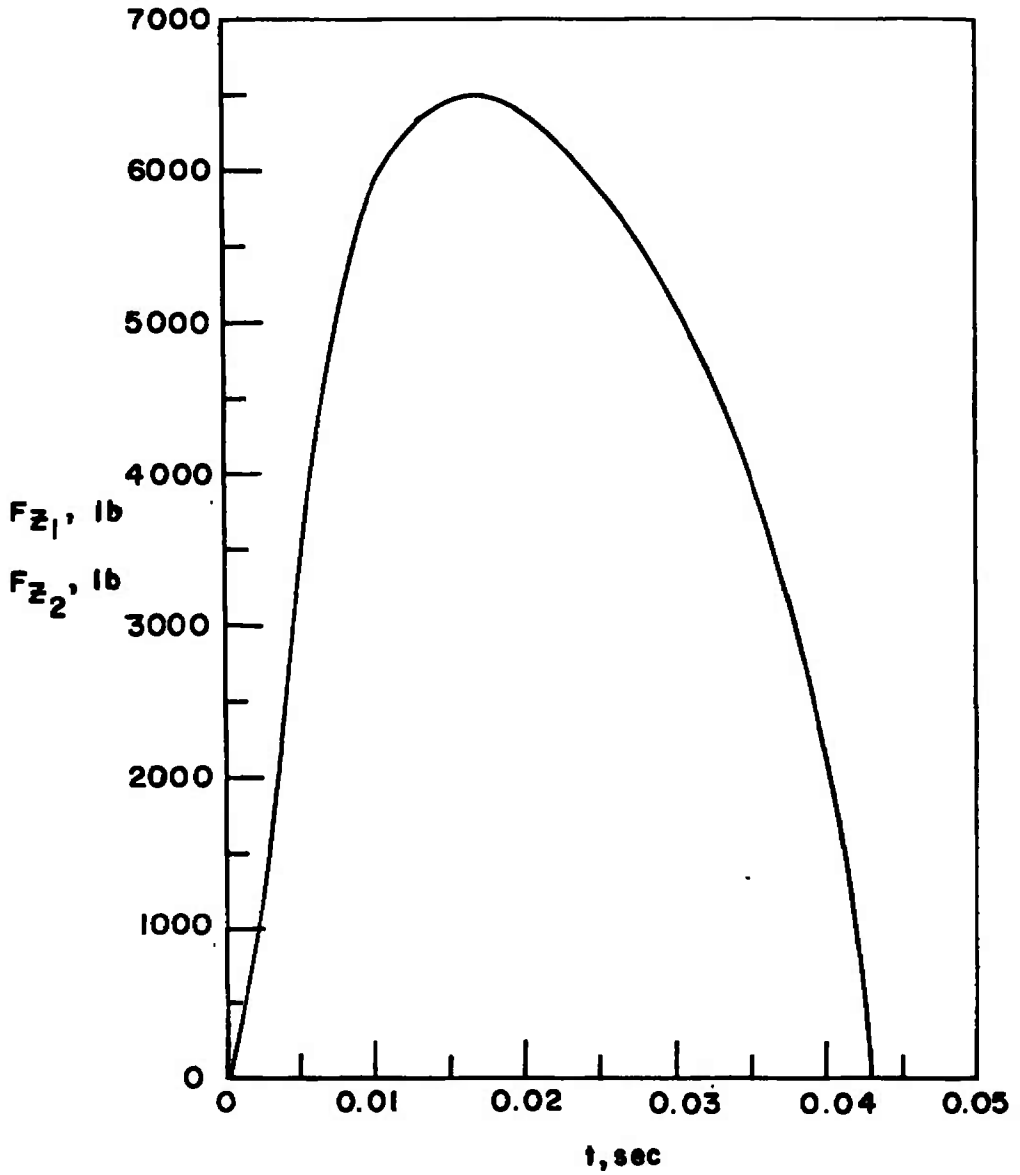

Fig. 14 Pylon Ejector Force Function for Store S-2

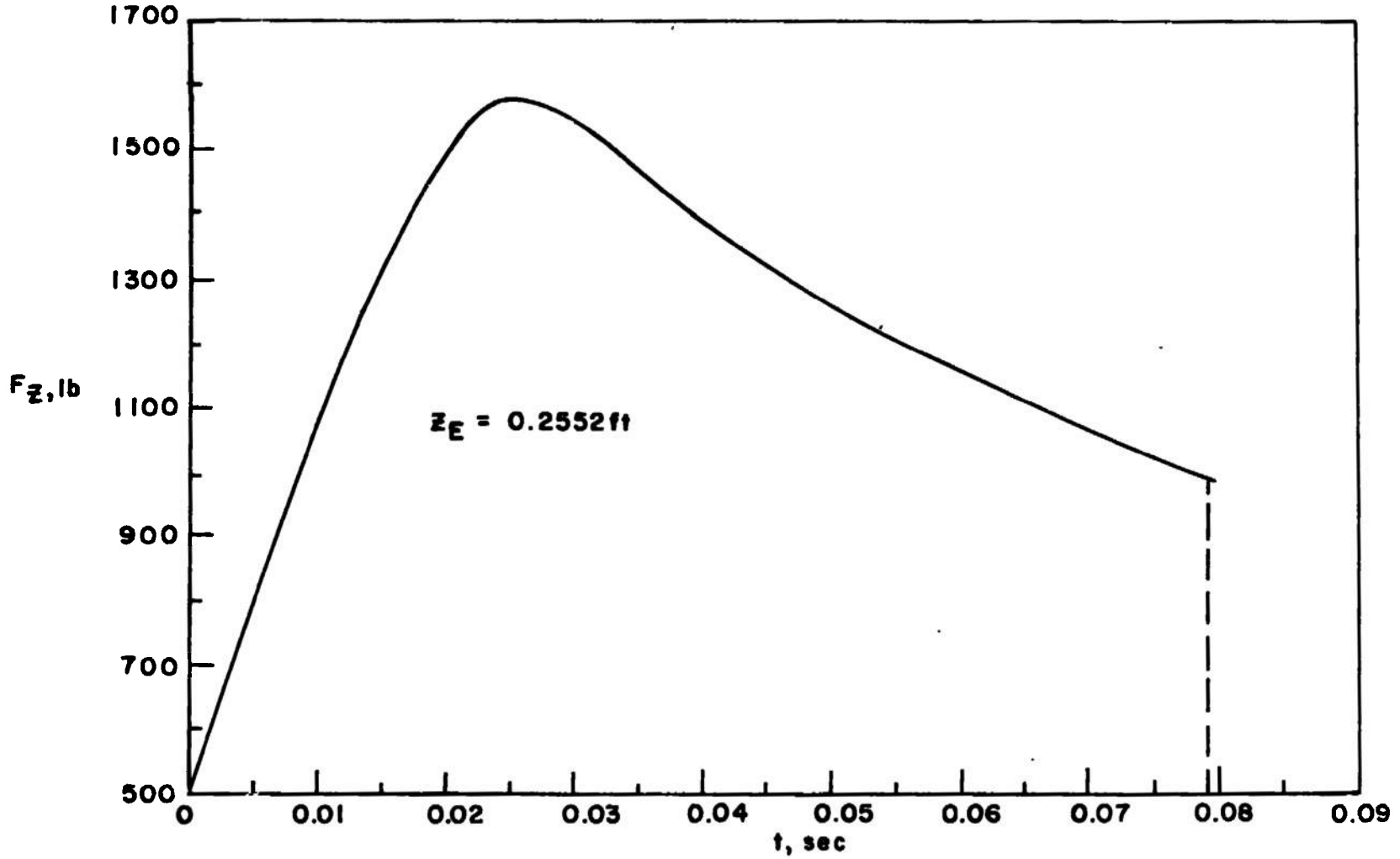

Fig. 15 TER and MER Ejector Force Function for Stores S-1 and S-3

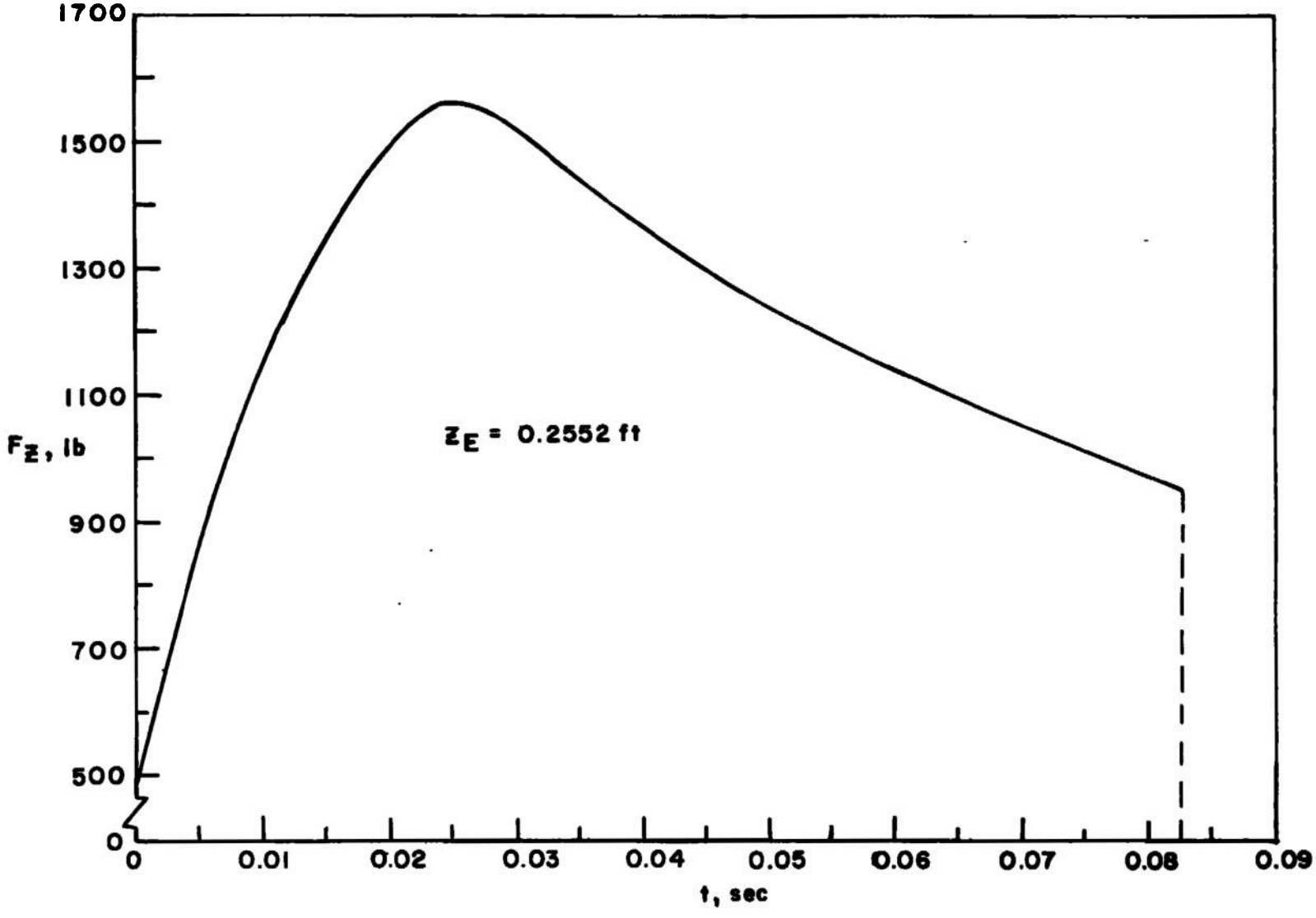

Fig. 16 TER and MER Ejector Force Function for Store S-2

SYM	CONF	M_∞	α_p	$\bar{\phi}$	STORE
□	1	0.66	1.7	0	S-1
○	1	0.66	1.7	0	S-2

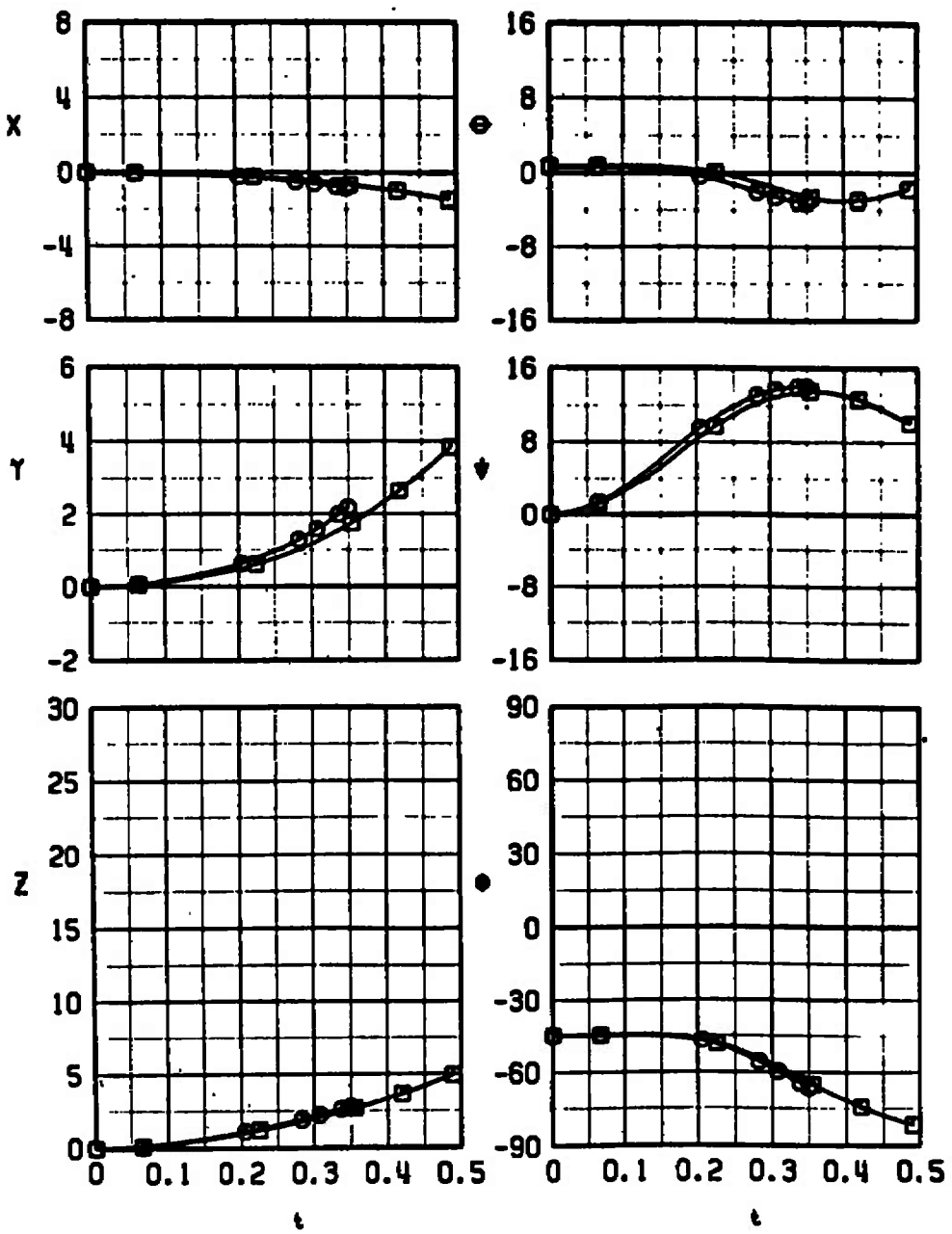

a. Load Configuration 1 (Simulated Left Wing, Inboard TER, Station 2)

Fig. 17 Comparison of Separation Trajectories for Munition Weights of 1000 lb (S-1) and 812 lb (S-2) at Mach Number 0.66

SYM	CONF	M_∞	α_p	$\bar{\alpha}$	STORE
□	5	0.66	1.7	0	S-1
○	5	0.66	1.7	0	S-2

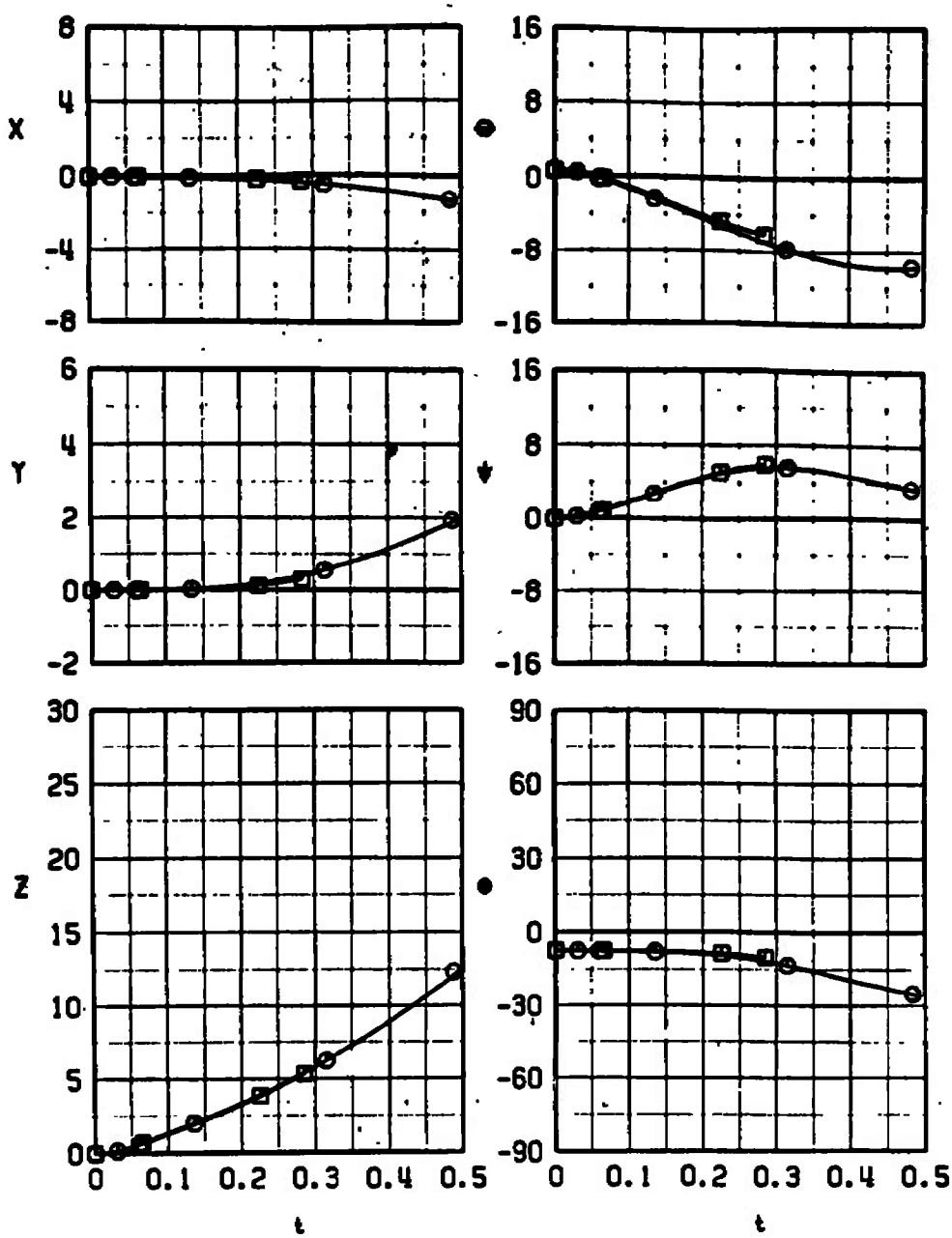

b. Load Configuration 5 (Simulated Left Wing, Outboard Pylon)
Fig. 17 Concluded

SYM	CONF	M_∞	σ_p	$\bar{\theta}$	STORE
□	1	0.66	1.7	0	S-2
◁	1	0.90	0.1	0	S-2

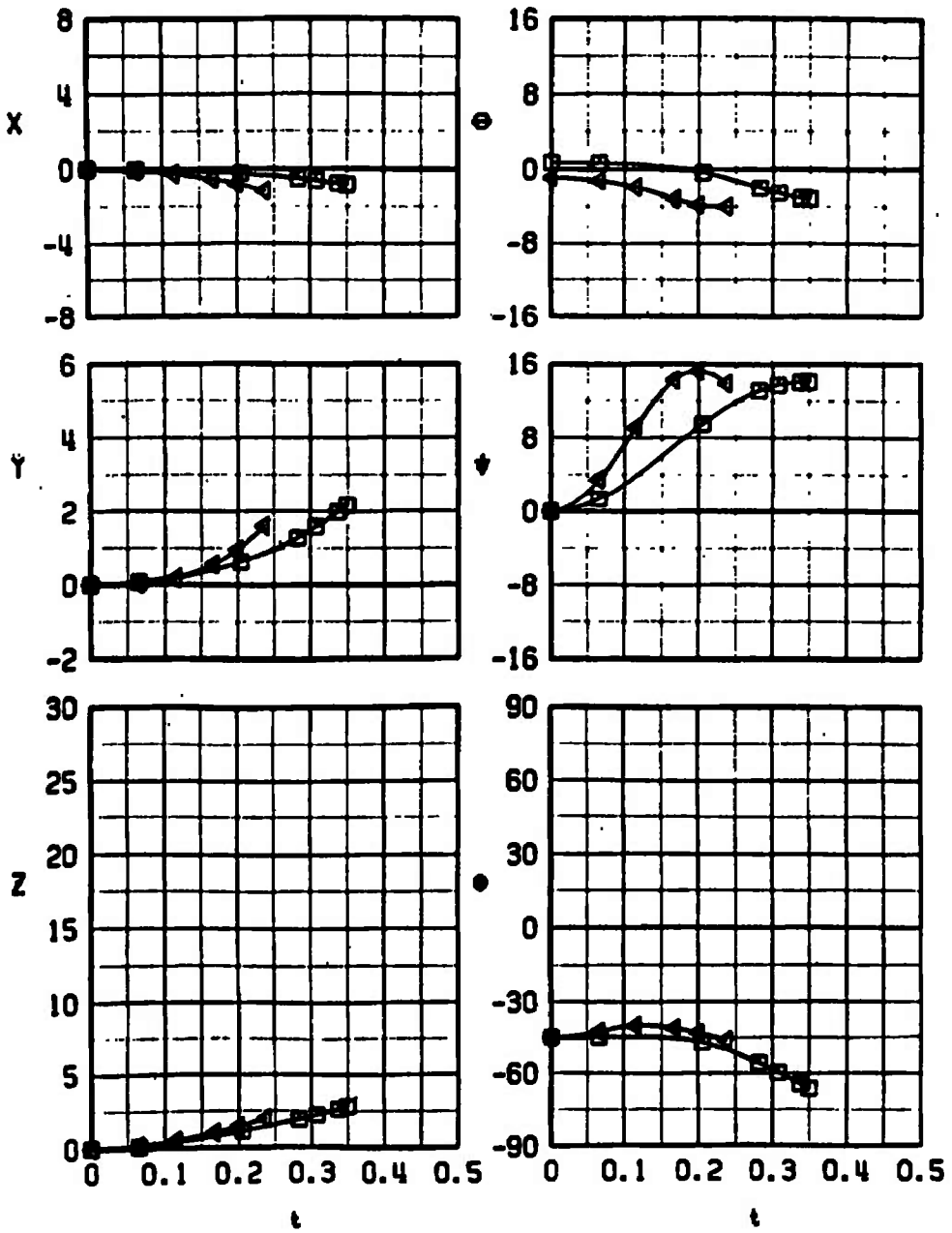

a. $\bar{\theta} = 0$

Fig. 18 S-2 Store Separation Trajectories from Load Configuration 1 (Left Wing, Inboard TER, Station 2)

SYM	CONF	M_∞	α_p	$\bar{\theta}$	STORE
⊡	1	0.66	0.1	-45	S-2

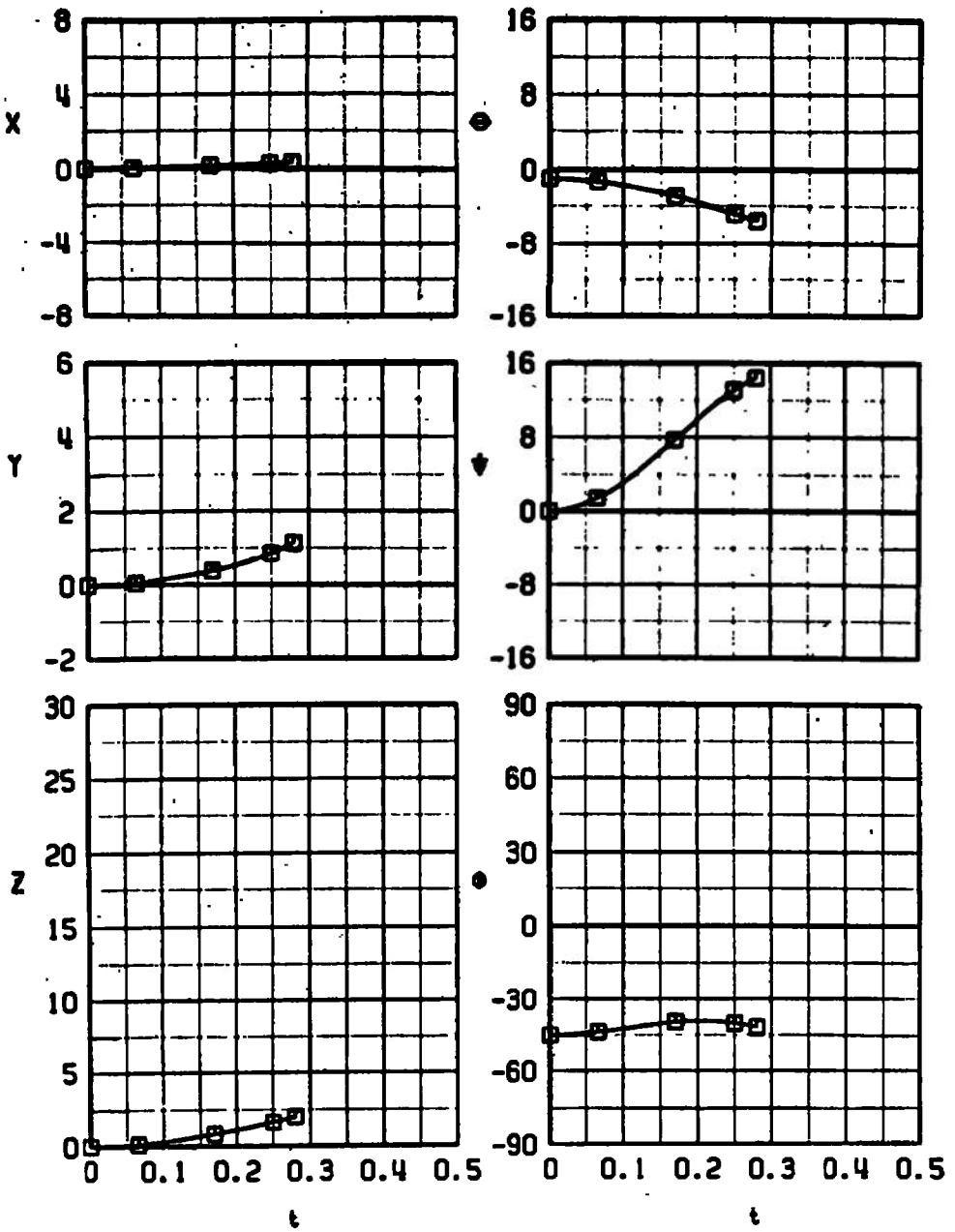

b. $\bar{\theta}$ = -45 deg

Fig. 18 Concluded

SYM	CONF	M_∞	α_p	$\bar{\theta}$	STORE
⊡	2	0.66	1.7	0	S-2
◁	2	0.90	0.1	0	S-2

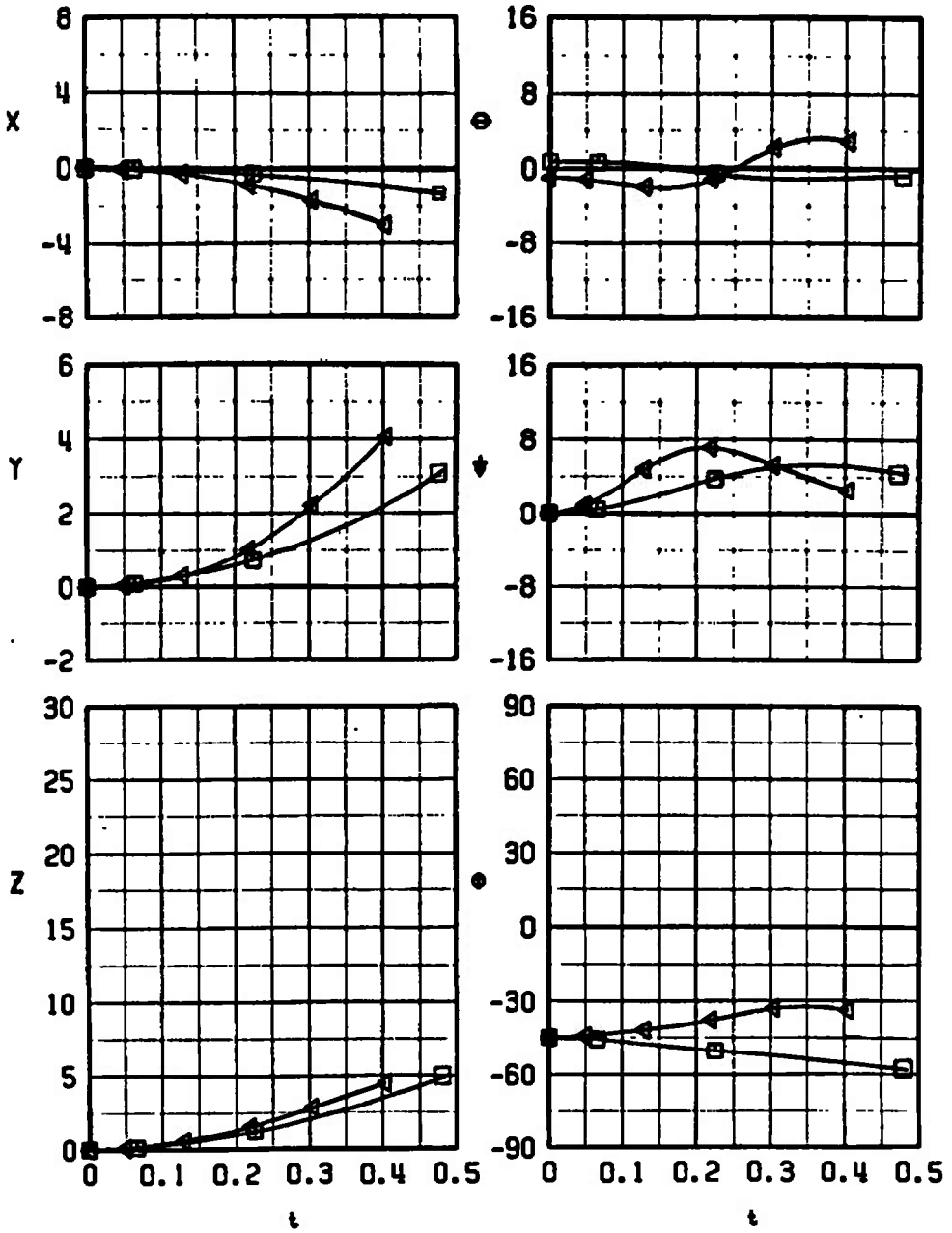

a. $\bar{\theta} = 0$

Fig. 19 S-2 Store Separation Trajectories from Load Configuration 2 (Right Wing, Inboard TER, Station 3)

SYM	CONF	M_∞	α_p	$\bar{\theta}$	STORE
□	2	0.66	0.1	-45	S-2
○	2	0.90	-0.6	-45	S-2

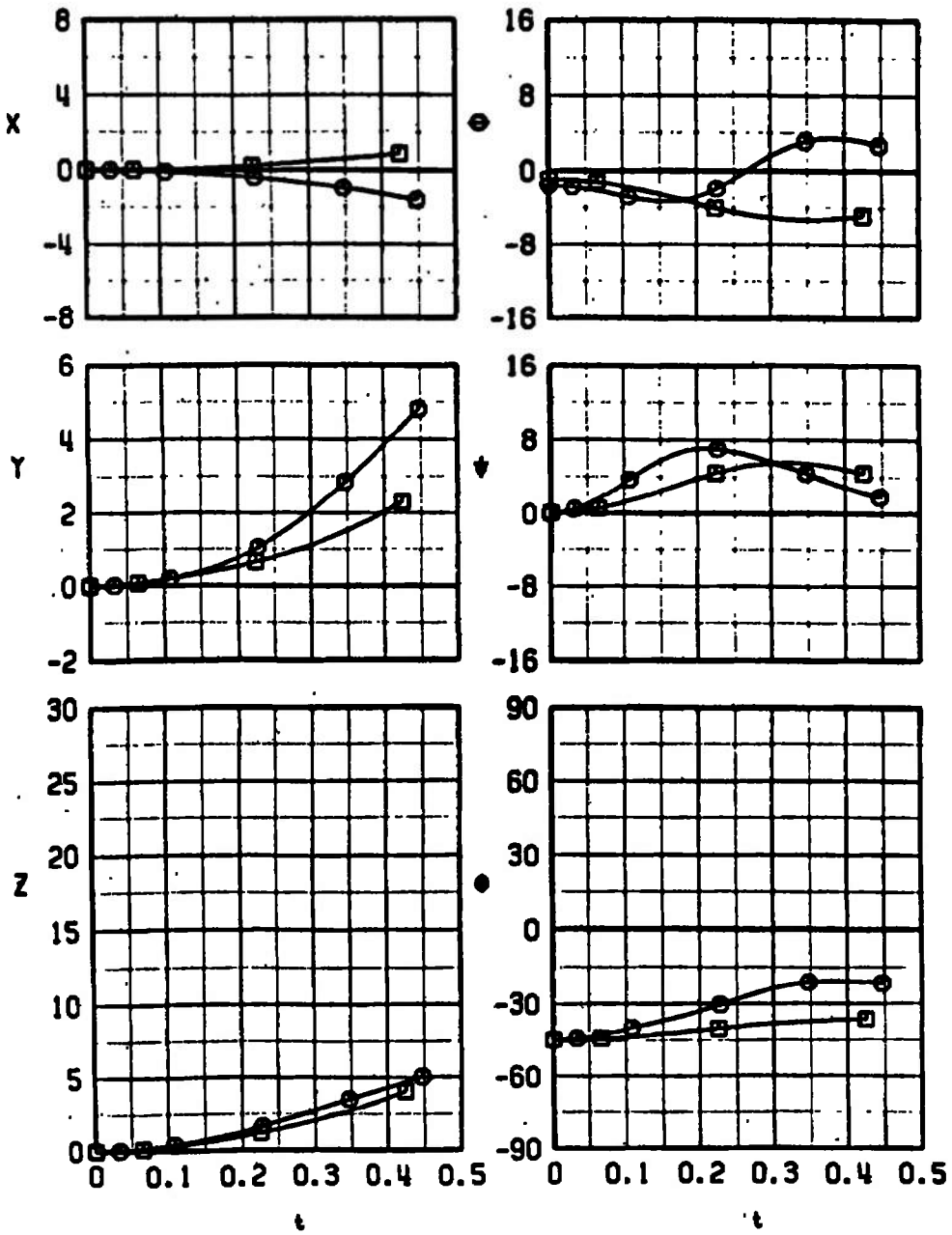

b. $\bar{\theta}$ = -45 deg

Fig. 19 Concluded

SYM	CONF	M_∞	α_p	$\bar{\theta}$	STORE
□	3	0.66	1.7	0	S-2
○	3	0.74	1.0	0	S-2
△	3	0.82	0.5	0	S-2
◁	3	0.90	0.1	0	S-2

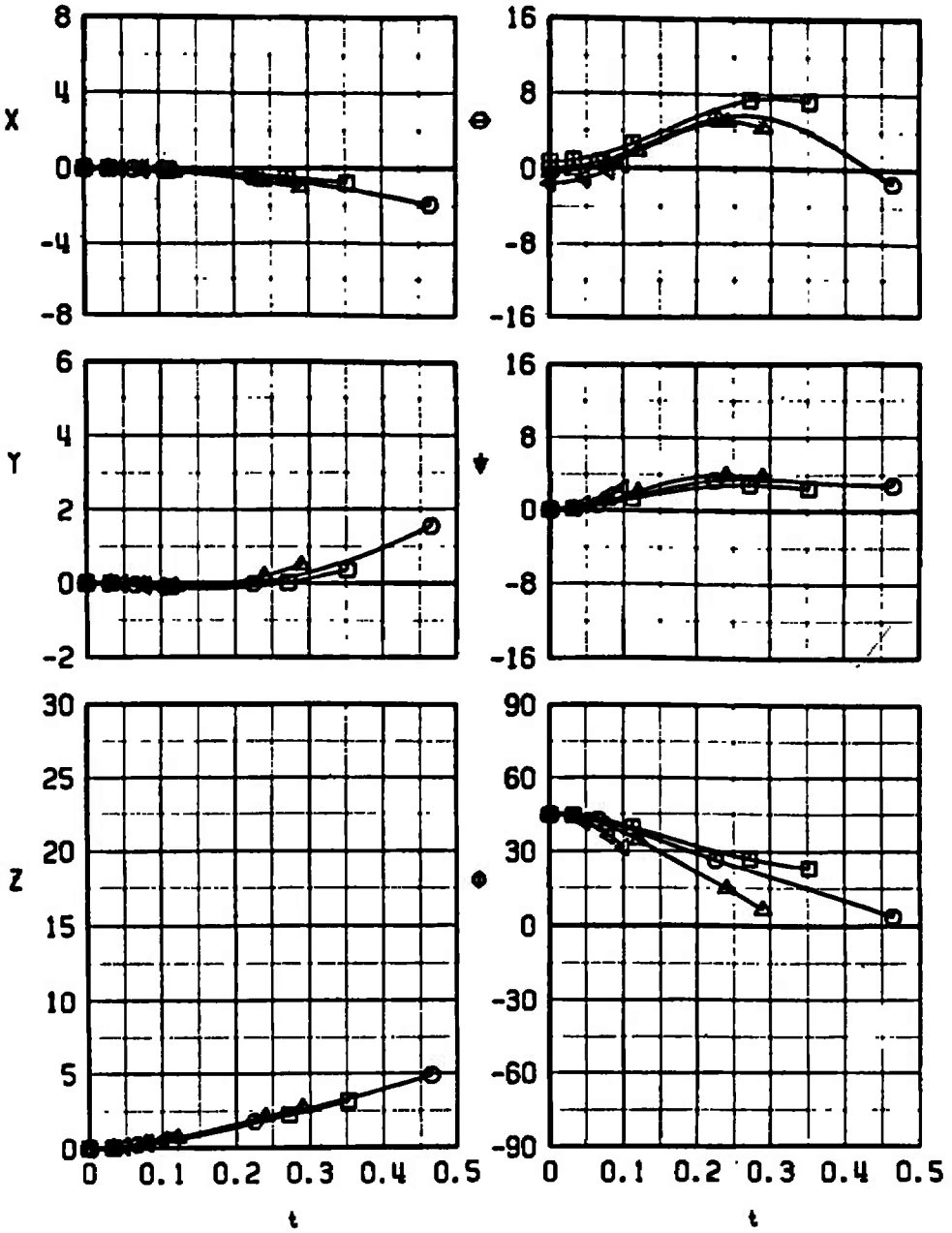

a. $\bar{\theta} = 0$

Fig. 20 S-2 Store Separation Trajectories from Load Configuration 3 (Left Wing, Inboard TER, Station 3)

SYM	CONF	M_∞	α_p	$\bar{\phi}$	STORE
□	3	0.66	0.1	-45	S-2
○	3	0.74	-0.2	-45	S-2
△	3	0.82	-0.4	-45	S-2
◁	3	0.90	-0.6	-45	S-2

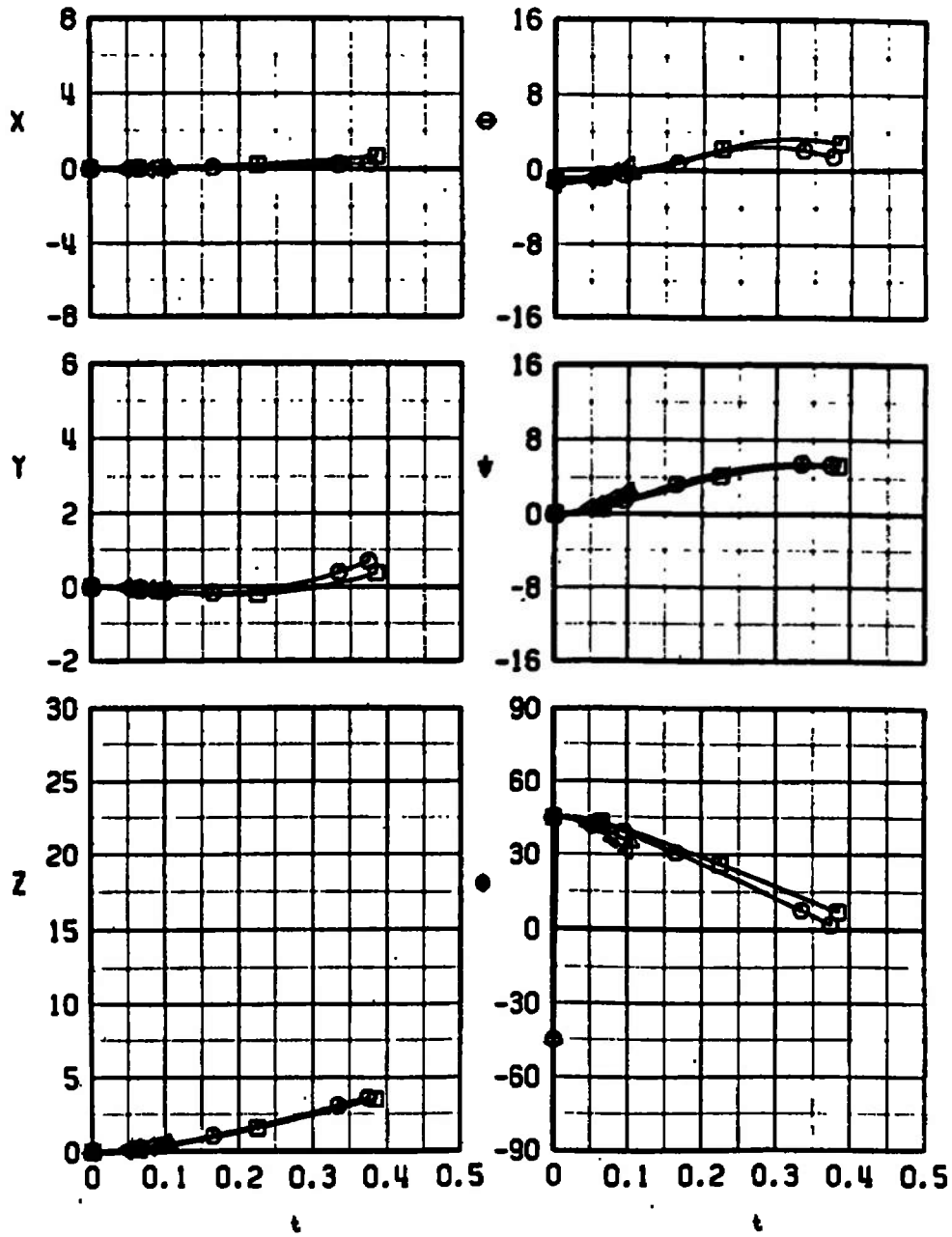

b. $\bar{\theta}$ = -45 deg
Fig. 20 Concluded

SYM	CONF	M_∞	α_p	$\bar{\phi}$	STORE
□	4	0.66	0.1	-45	S-2
○	4	0.90	-0.6	-45	S-2

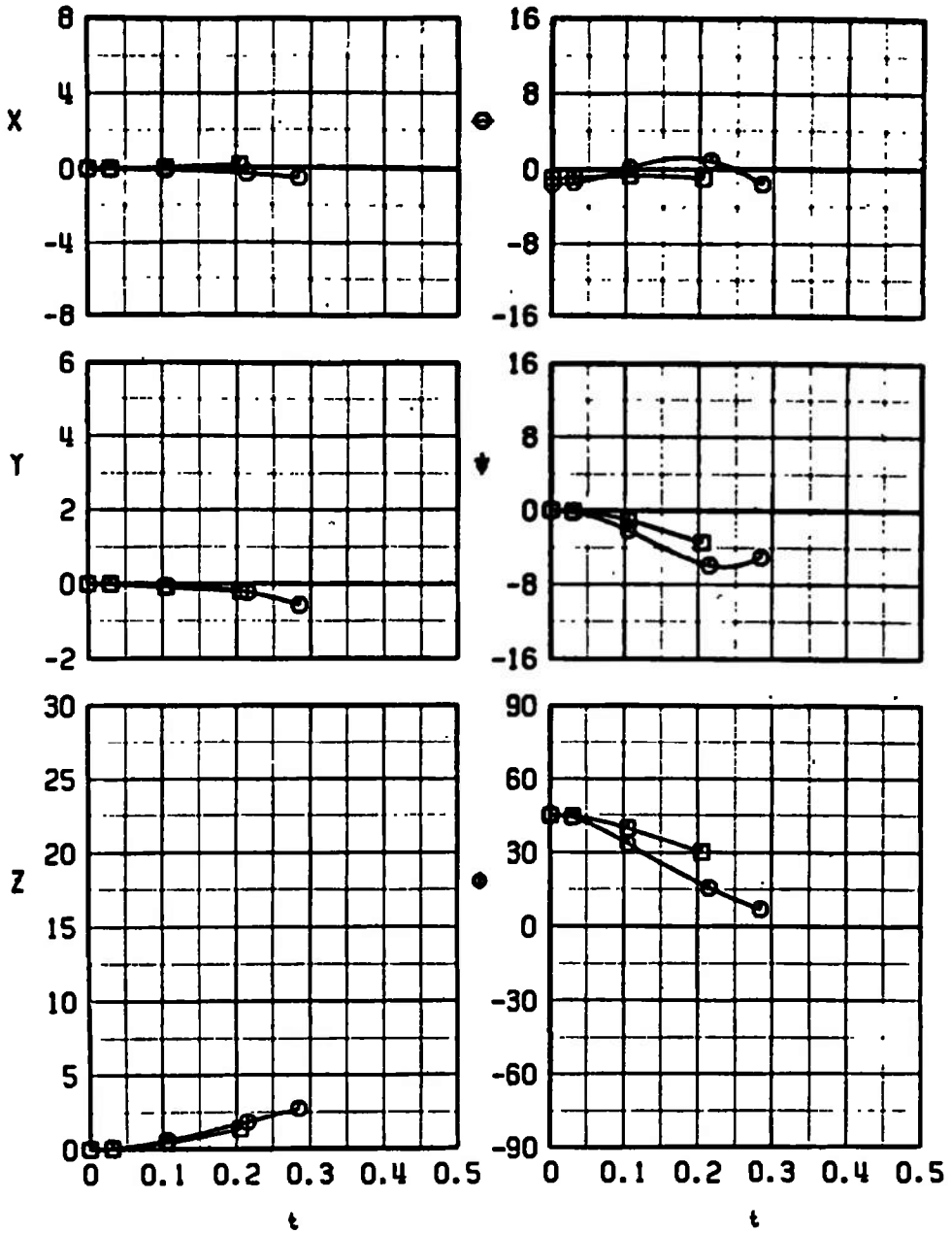

Fig. 21 S-2 Store Separation Trajectories from Load Configuration 4 (Right Wing, Inboard TER, Station 2)

SYM	CONF	M_∞	α_p	$\bar{\theta}$	STORE
□	5	0.66	1.7	0	S-2
◁	5	0.90	0.1	0	S-2

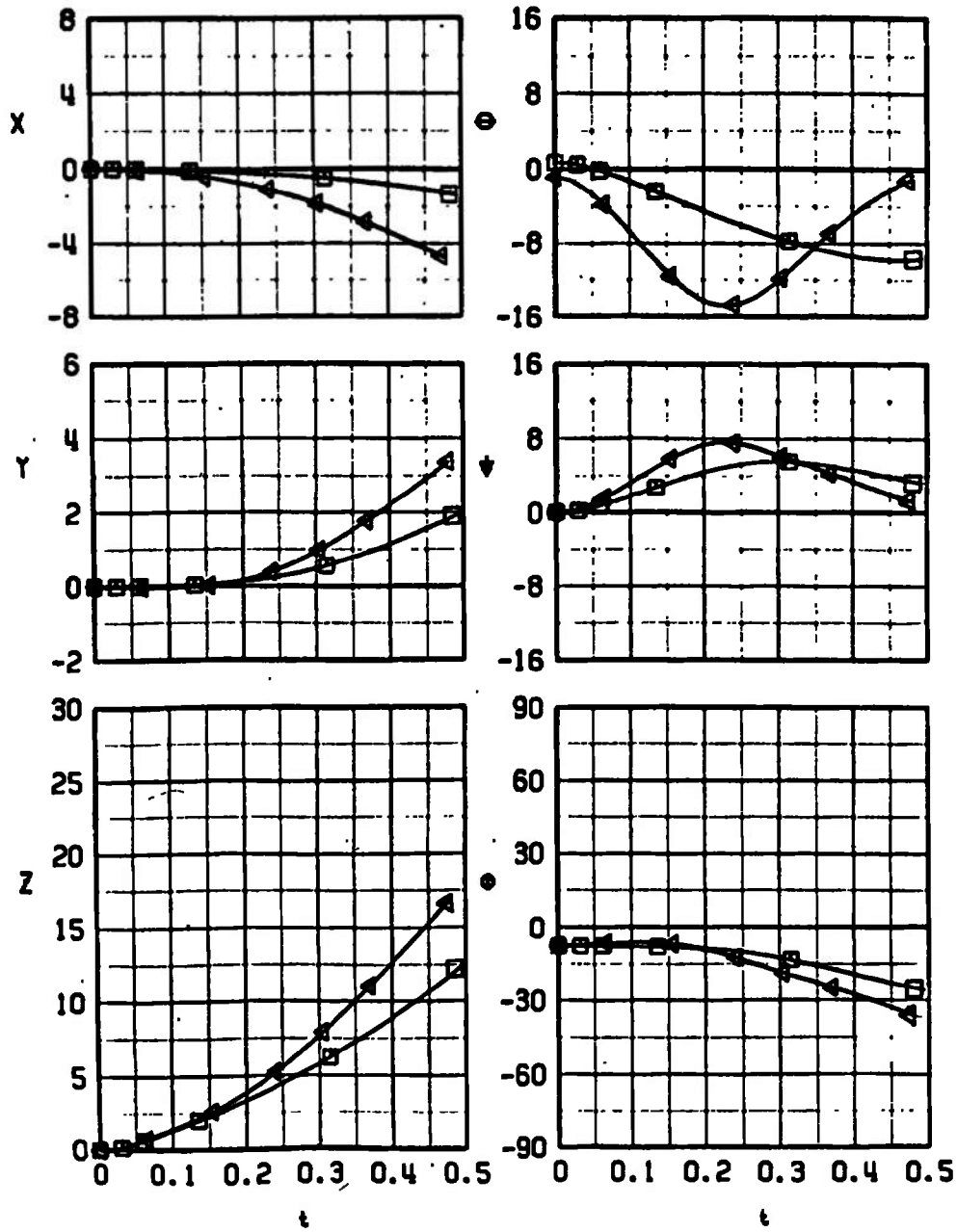

a. $\bar{\theta} = 0$

Fig. 22 S-2 Store Separation Trajectories from Load Configuration 5, (Left Wing, Outboard Pylon)

SYM	CONF	M_∞	α_p	$\bar{\theta}$	STORE
⊡	5	0.66	0.1	-45	S-2
⊙	5	0.90	-0.6	-45	S-2

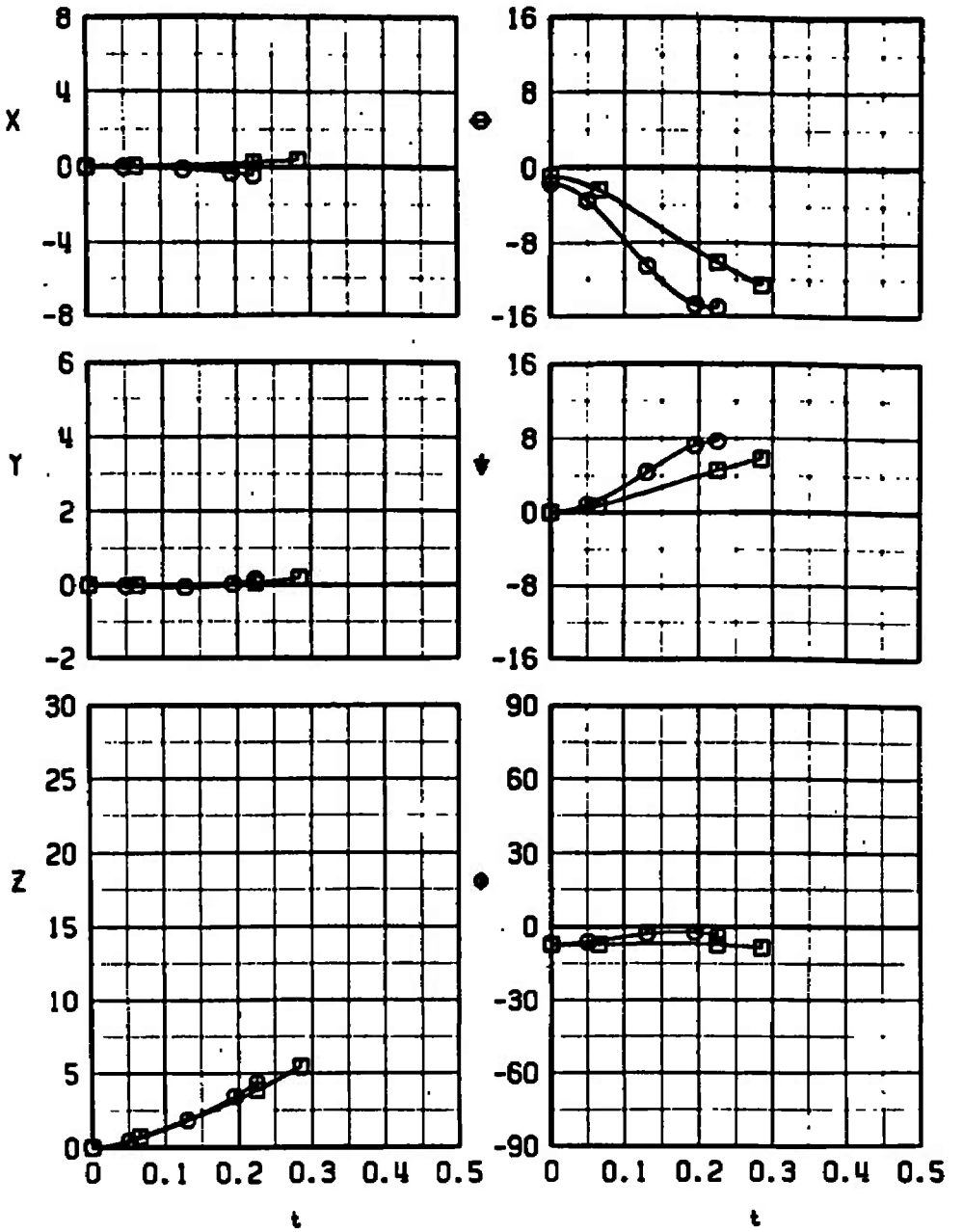

b. $\bar{\theta}$ = -45 deg
Fig. 22 Concluded

SYM	CONF	M_∞	α_p	$\bar{\theta}$	STORE
□	6	0.66	1.7	0	S-2
◁	6	0.90	0.1	0	S-2

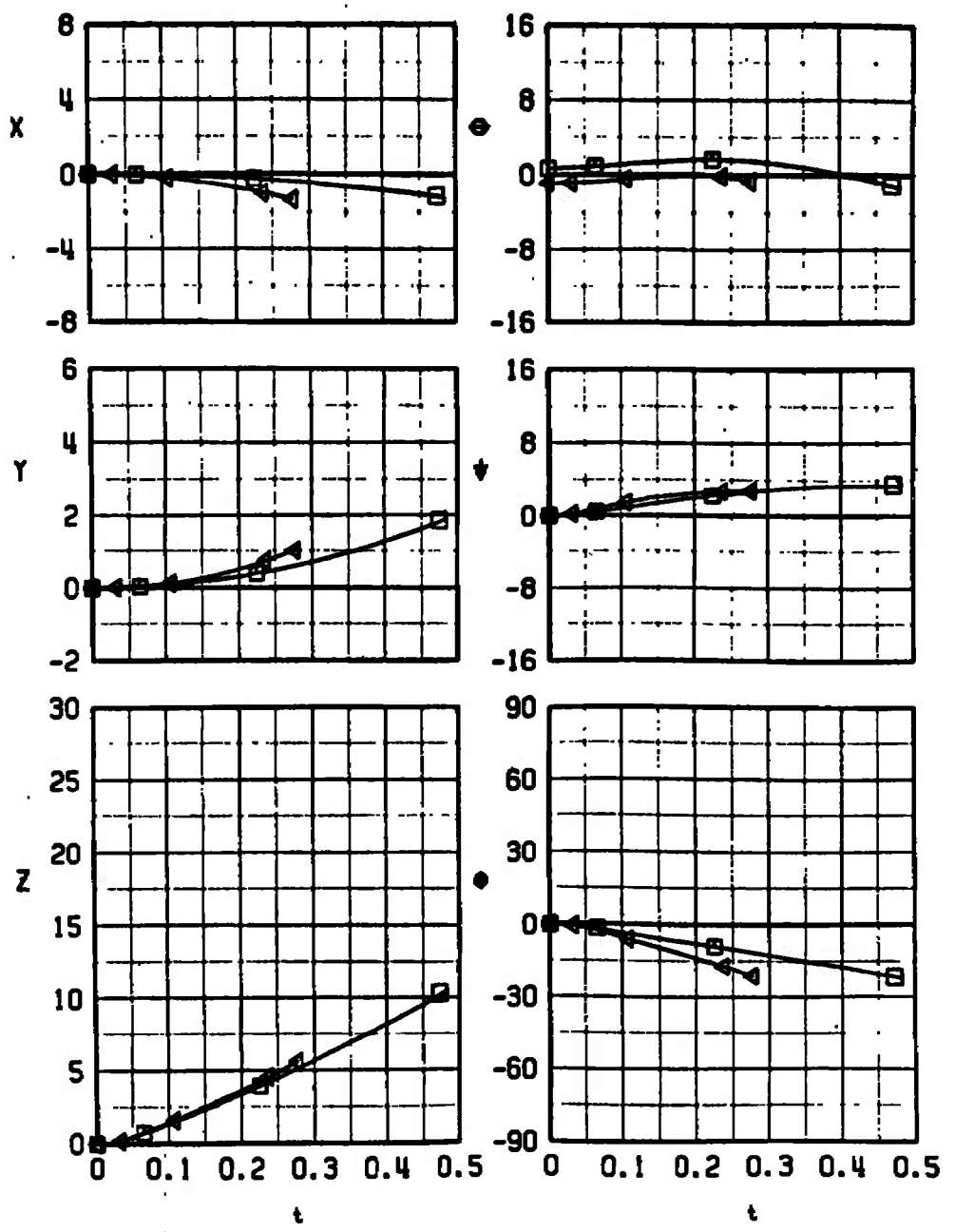

a. $\bar{\theta} = 0$

Fig. 23 S-2 Store Separation Trajectories from Load Configuration 6 (Left Wing, Inboard Pylon)

SYM	CONF	M_∞	α_p	$\bar{\theta}$	STORE
⊡	6	0.90	-0.6	-45	S-2

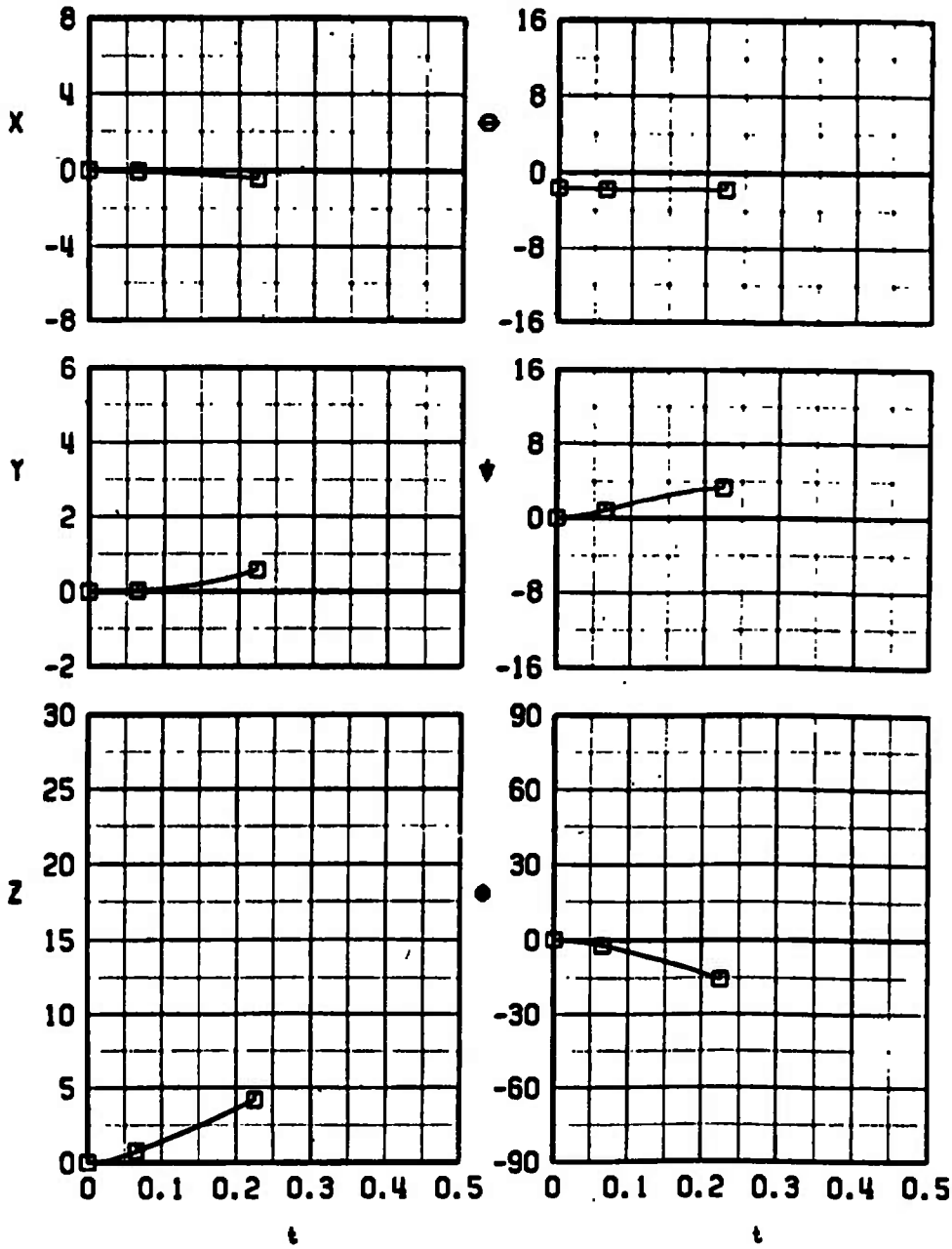

b. $\bar{\theta}$ = -45 deg
Fig. 23 Concluded

SYM	CONF	M_∞	α_p	$\bar{\theta}$	STORE
□	7	0.66	1.7	0	S-3
○	7	0.74	1.0	0	S-3
△	7	0.82	0.5	0	S-3
◁	7	0.90	0.1	0	S-3

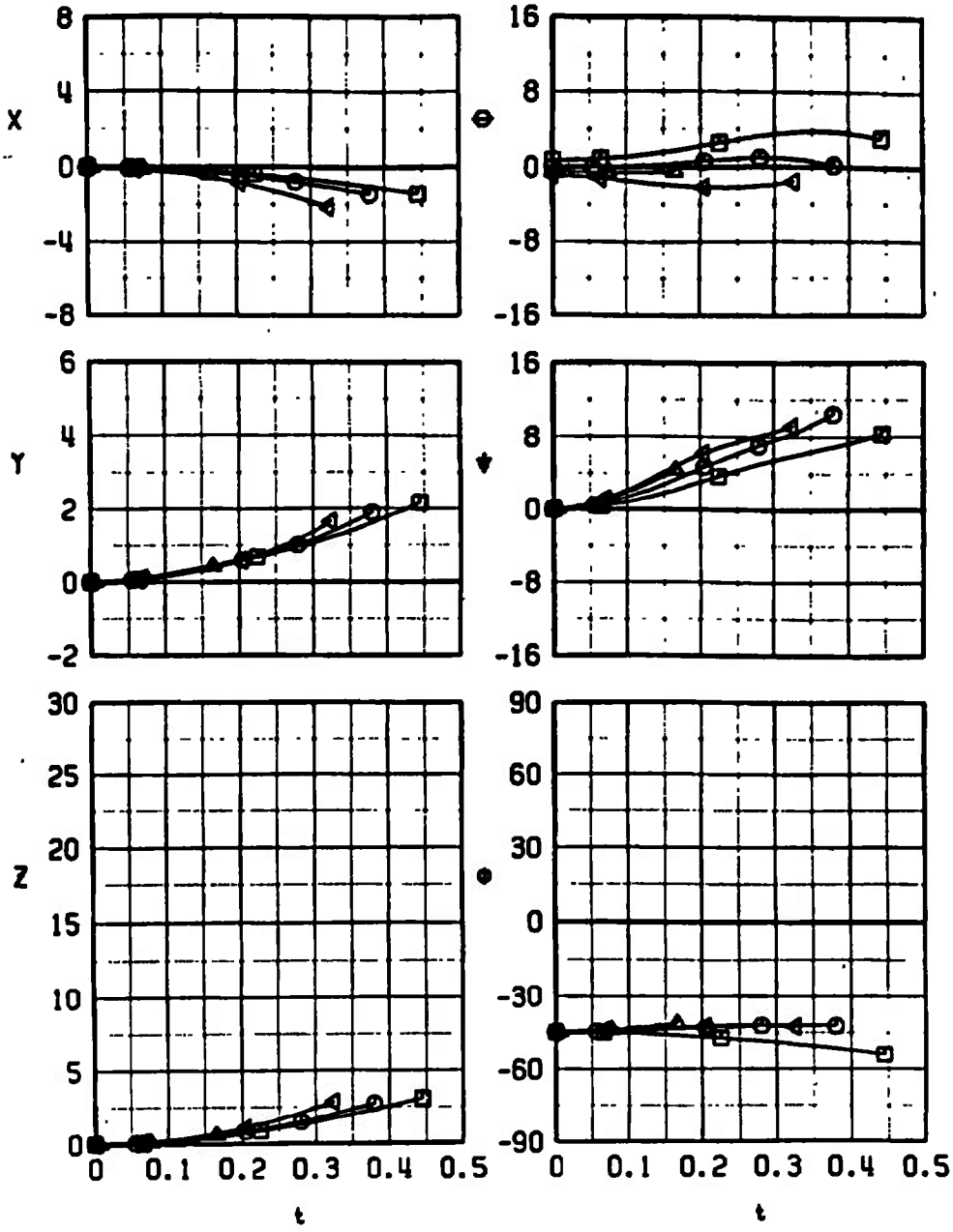

Fig. 24 S-3 Store Separation Trajectories from Load Configuration 7 (Left Wing, Inboard TER, Station 2)

SYM	CONF	M_∞	α_p	$\bar{\theta}$	STORE
⊡	8	0.66	1.7	0	S-3
◁	8	0.90	0.1	0	S-3

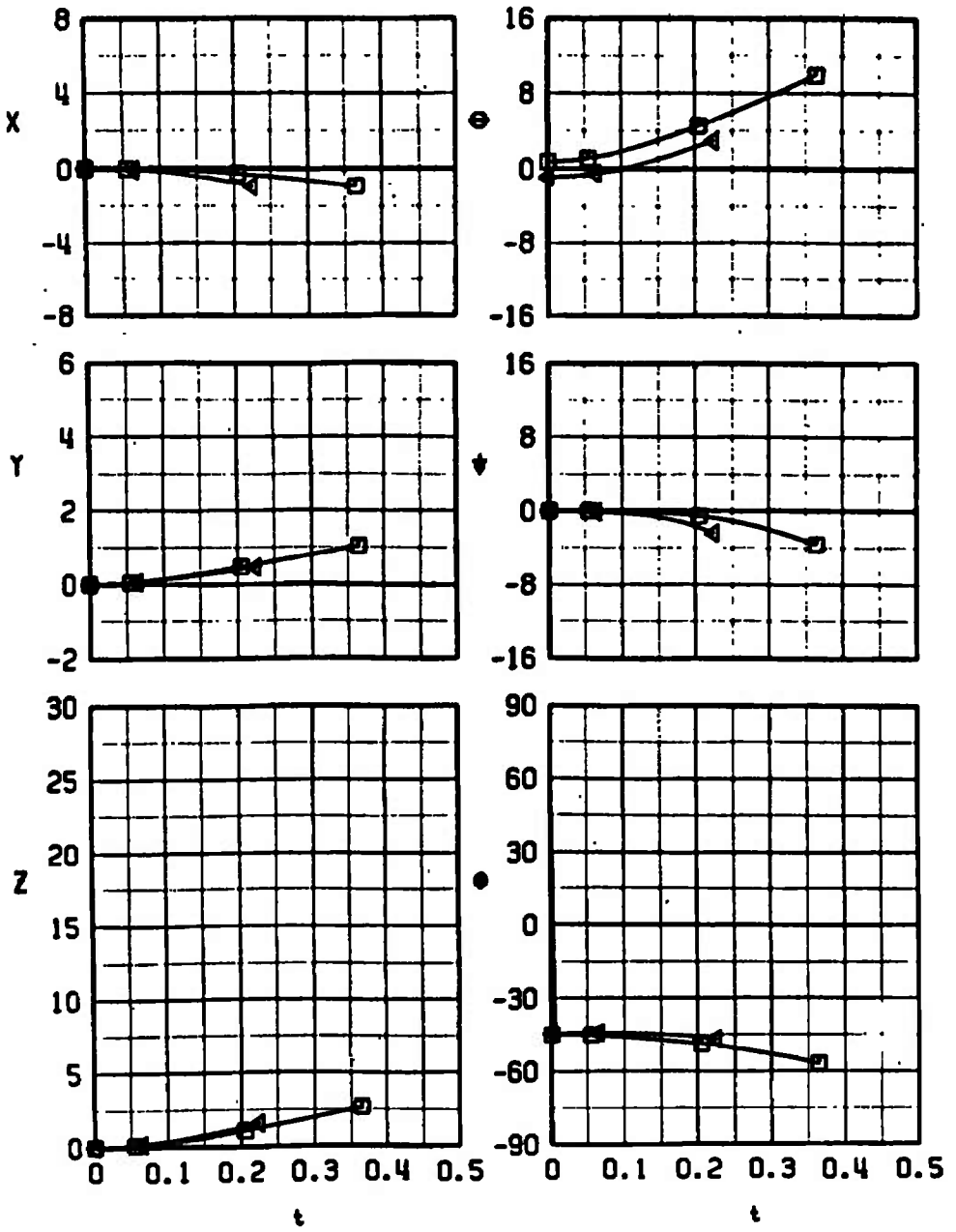

Fig. 25 S-3 Store Separation Trajectories from Load Configuration 8 (Right Wing, Inboard TER, Station 3)

SYM	CONF	M_∞	α_p	$\bar{\theta}$	STORE
□	9	0.66	1.7	0	S-3
◁	9	0.90	0.1	0	S-3

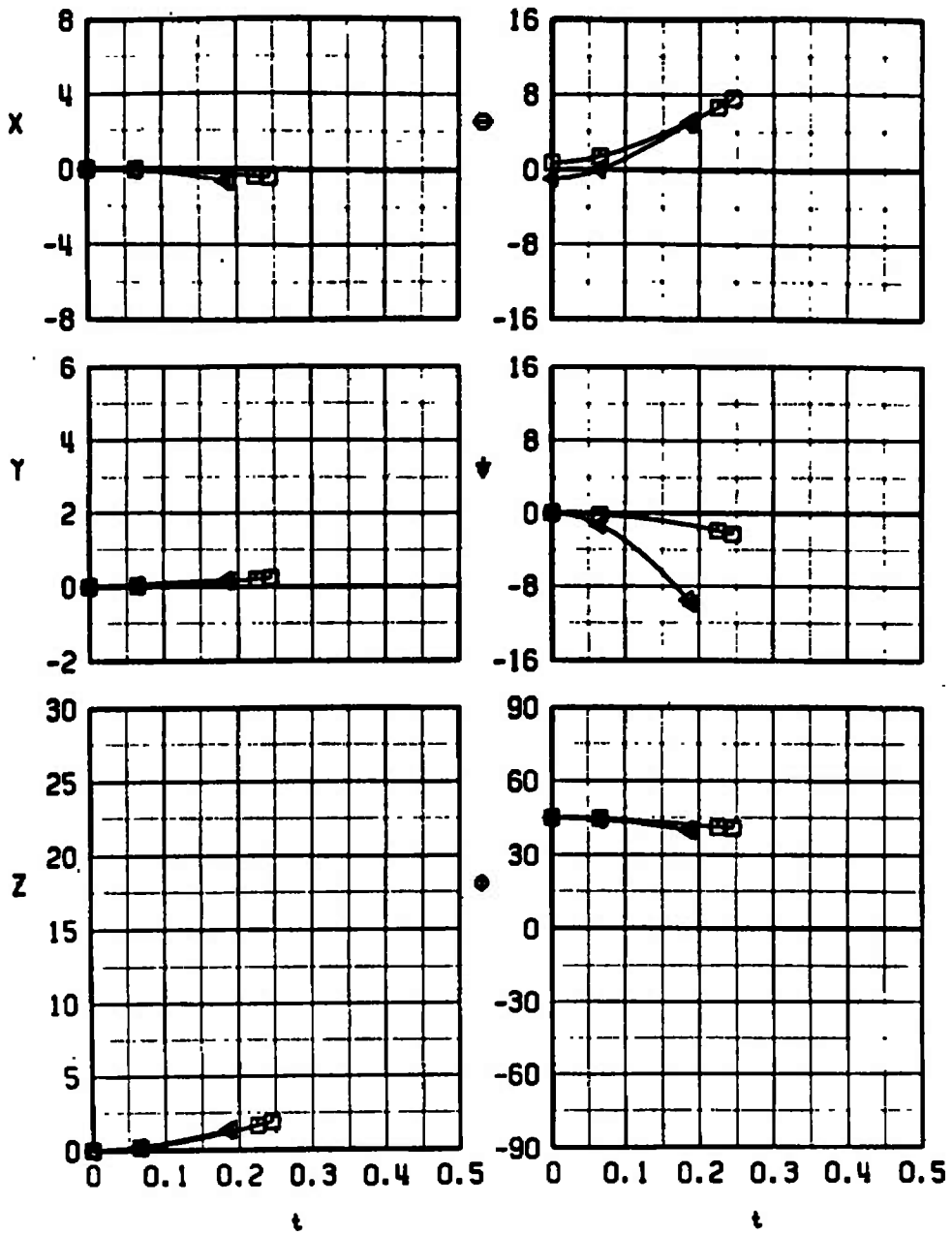

Fig. 26 S-3 Store Separation Trajectories from Load Configuration 9 (Left Wing, Inboard TER, Station 3)

SYM	CONF	M_∞	α_p	$\bar{\theta}$	STORE
□	10	0.66	1.7	0	S-3
◁	10	0.90	0.1	0	S-3

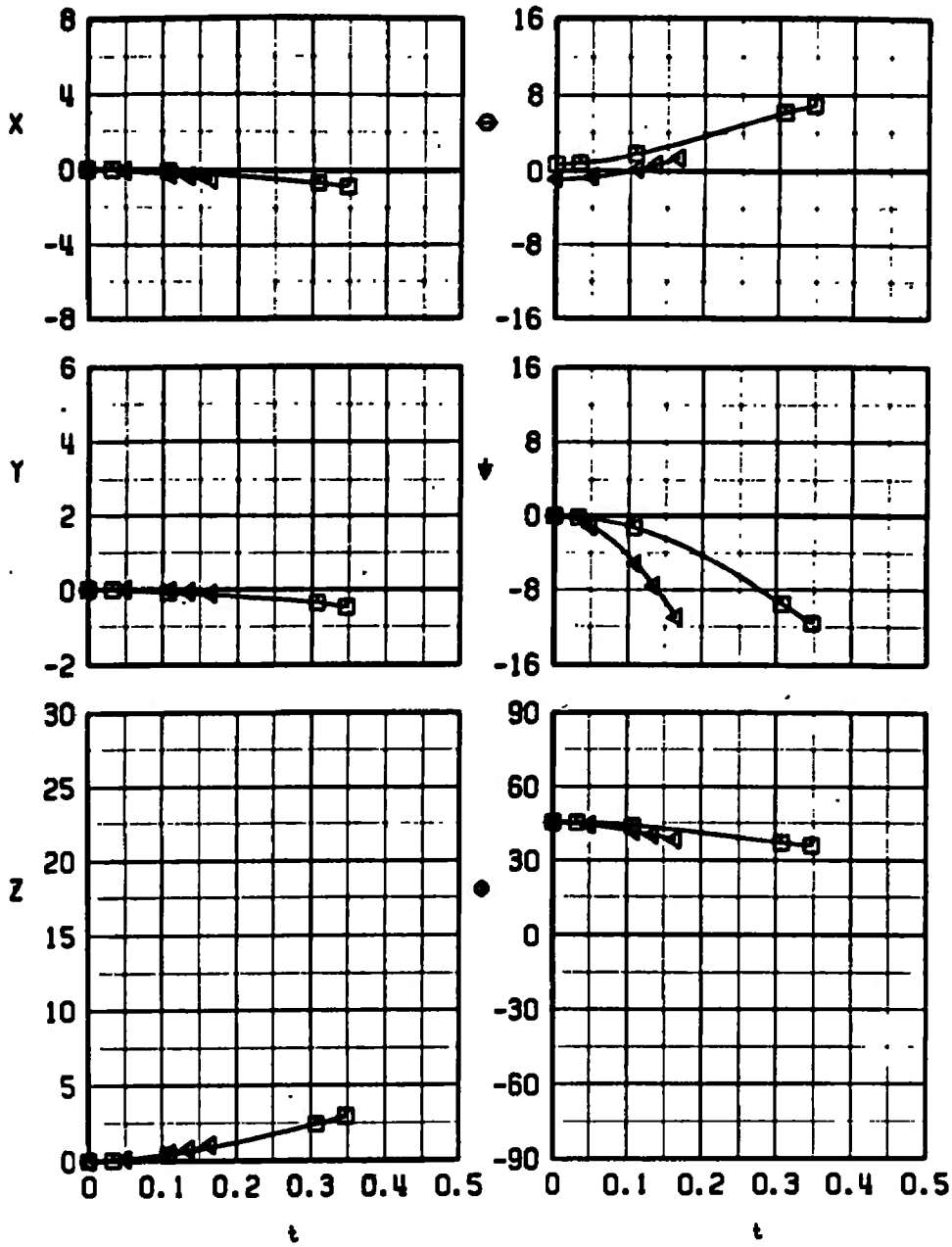

Fig. 27 S-3 Store Separation Trajectories from Load Configuration 10 (Right Wing, Inboard TER, Station 2)

SYM	CONF	M_∞	α_p	$\bar{\phi}$	STORE
□	11	0.66	1.7	0	S-3
◁	11	0.90	0.1	0	S-3

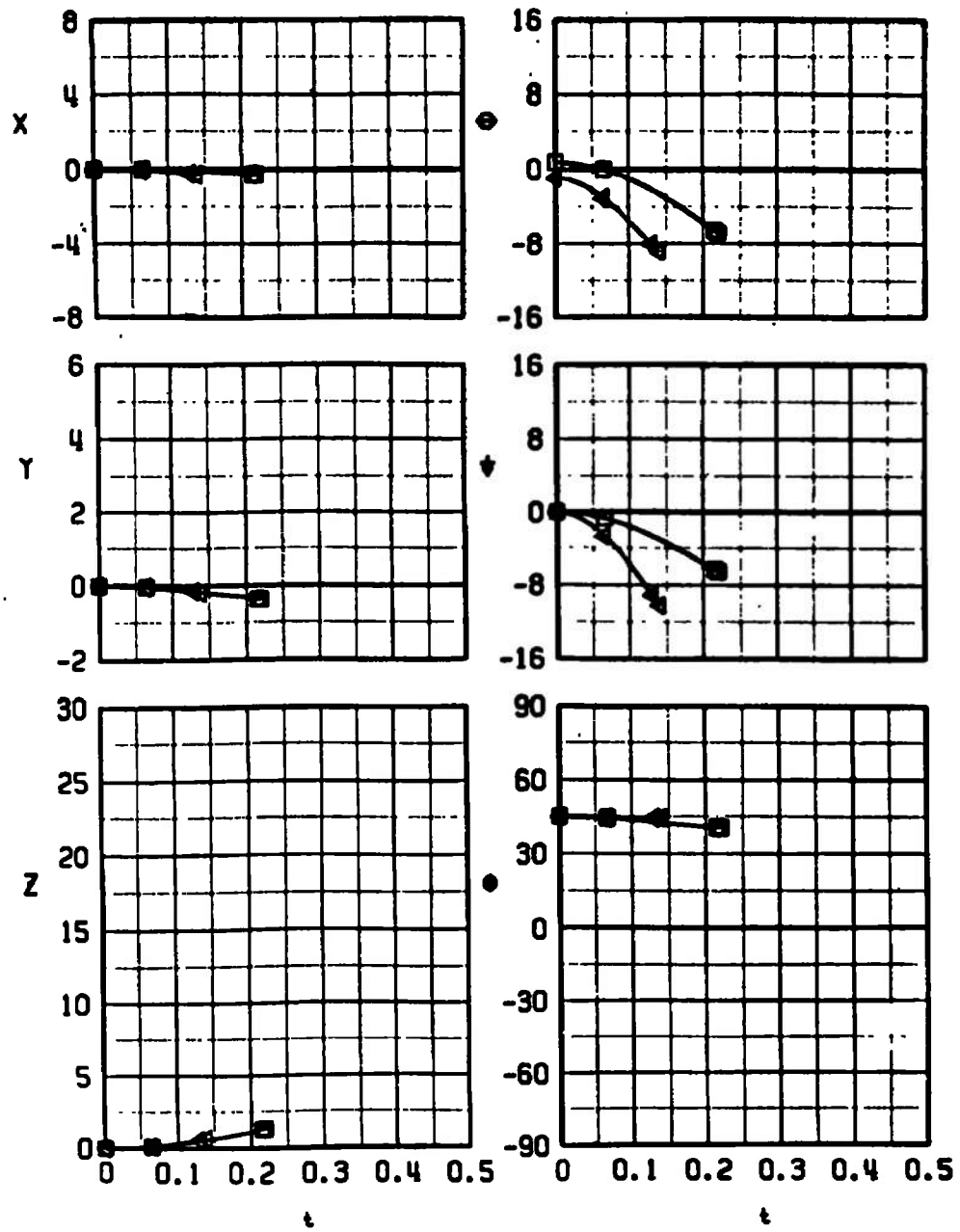

Fig. 28 S-3 Store Separation Trajectories from Load Configuration 11 (Centerline MER, Station 3)

SYM	CONF	M_∞	α_p	$\bar{\theta}$	STORE
□	13	0.66	1.7	0	S-2
◁	13	0.90	0.1	0	S-2

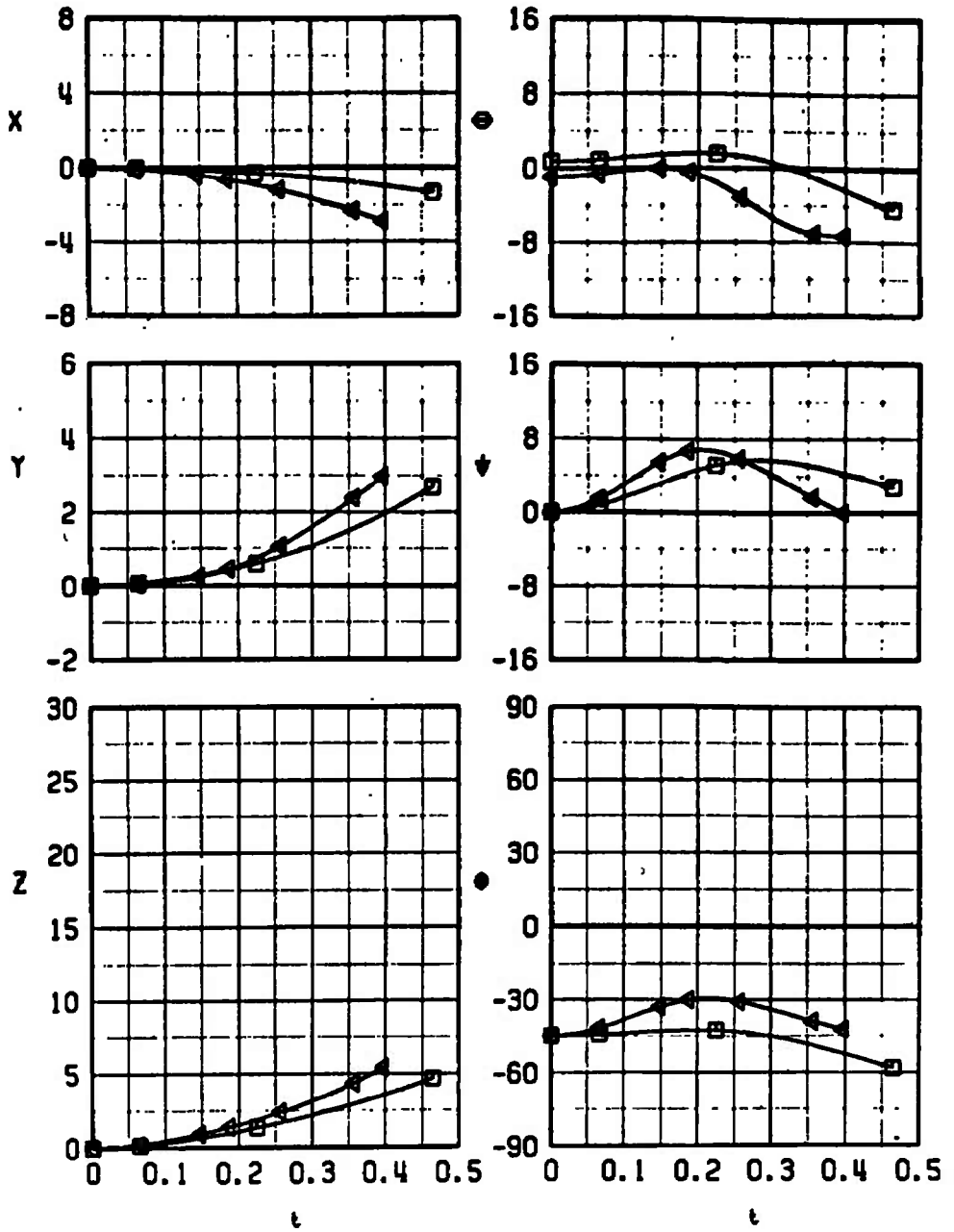

a. $\bar{\theta} = 0$

Fig. 29 S-2 Store Separation Trajectories from Load Configuration 13 (Left Wing, Inboard TER, Station 2)

SYM	CONF	M_∞	α_p	$\bar{\theta}$	STORE
⊡	13	0.90	-0.6	-45	S-2

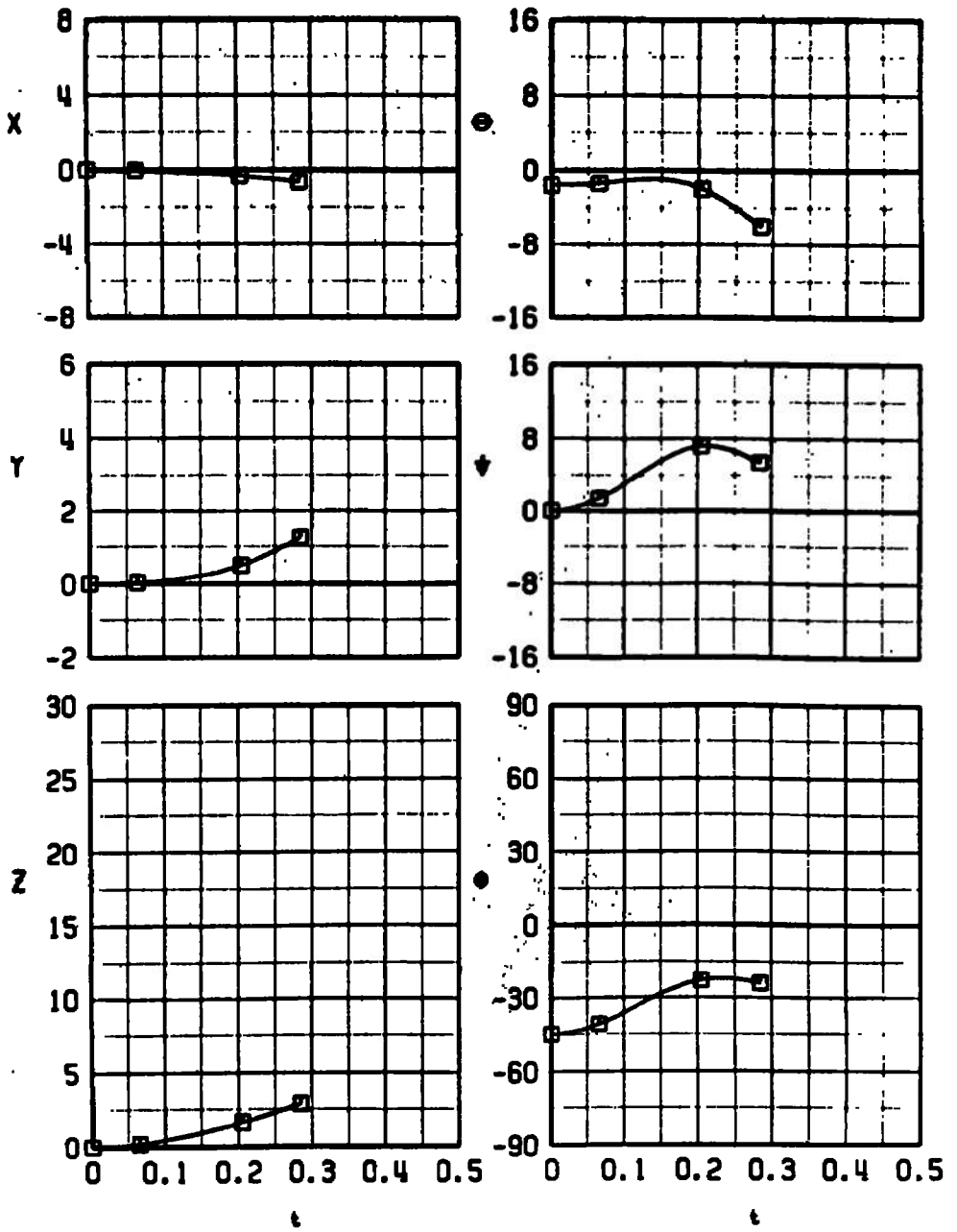

b. $\bar{\theta}$ = -45 deg

Fig. 29 Concluded

SYM	CONF	M_∞	α_p	$\bar{\theta}$	STORE
□	14	0.66	1.7	0	S-2
◁	14	0.90	0.1	0	S-2

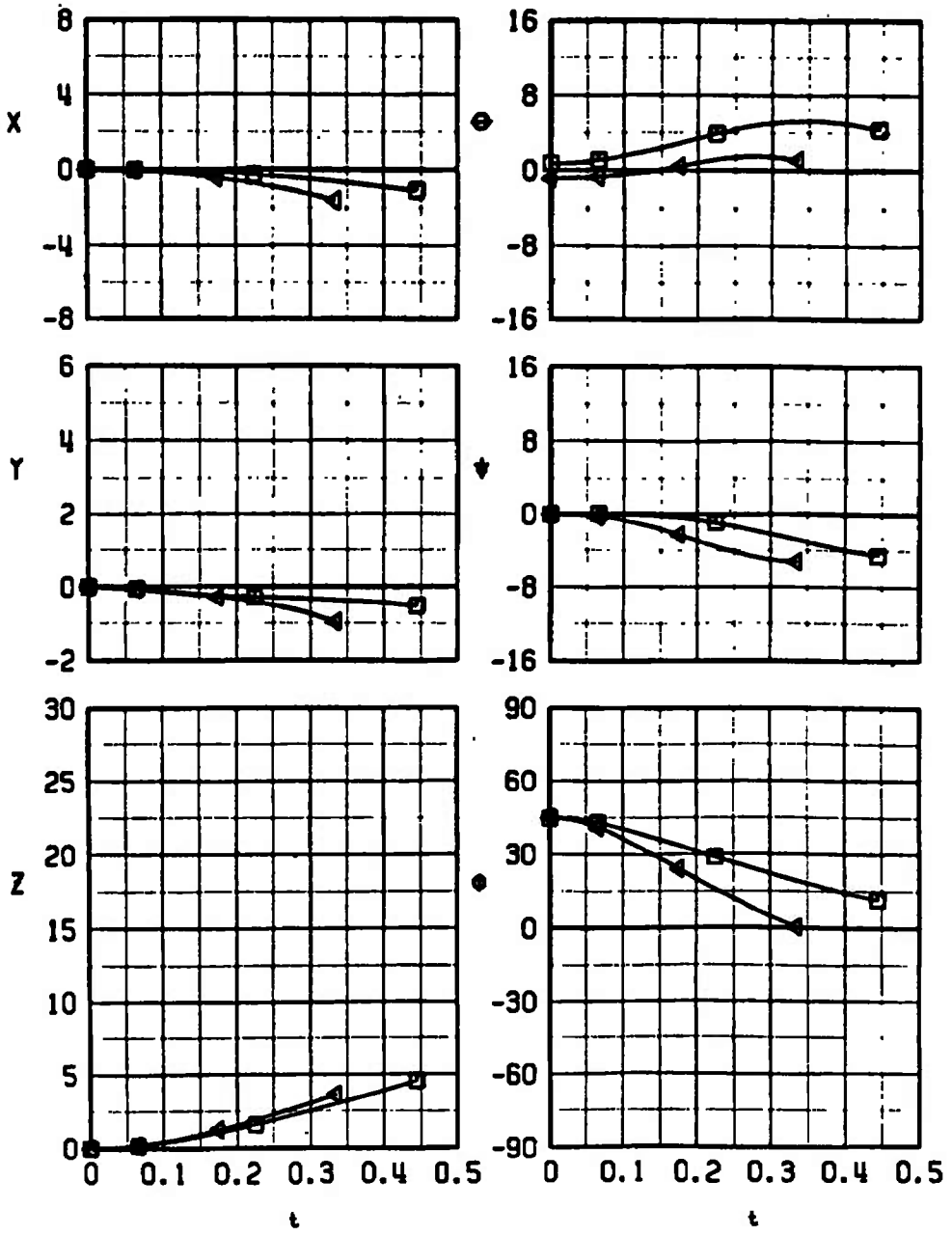

Fig. 30 S-2 Store Separation Trajectories from Load Configuration 14 (Left Wing, Inboard TER, Station 3)

SYM	CONF	M_∞	α_p	$\bar{\phi}$	STORE
⊡	1	0.66	1.7	0	S-2
⊙	13	0.66	1.7	0	S-2

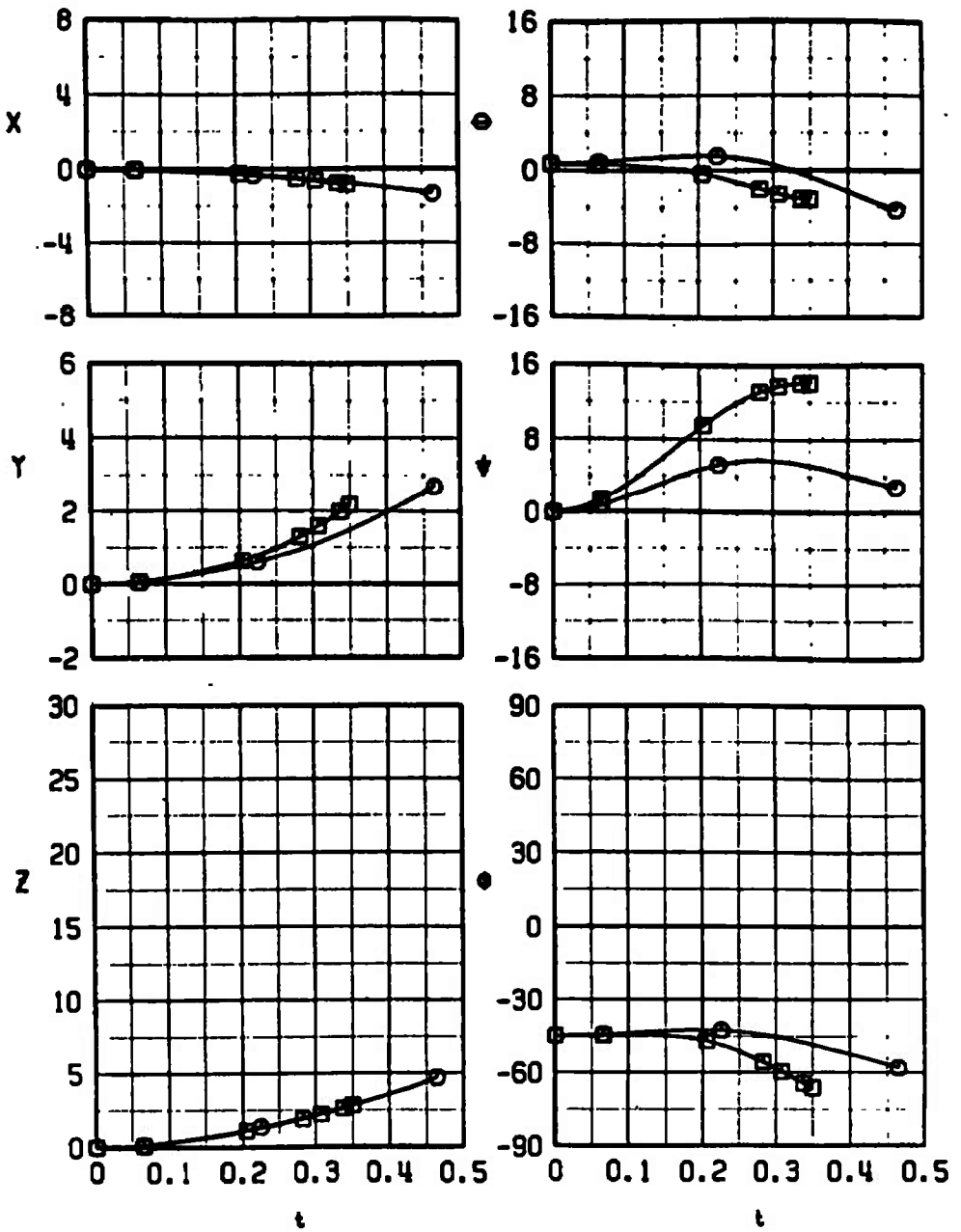

a. $M_\infty = 0.66$

Fig. 31 Effect of Fuel Tank Location on Separation Trajectories (Simulated Left Wing, Inboard TER, Station 2)

SYM	CONF	M_∞	α_p	$\bar{\phi}$	STORE
☐	1	0.90	0.1	0	S-2
○	13	0.90	0.1	0	S-2

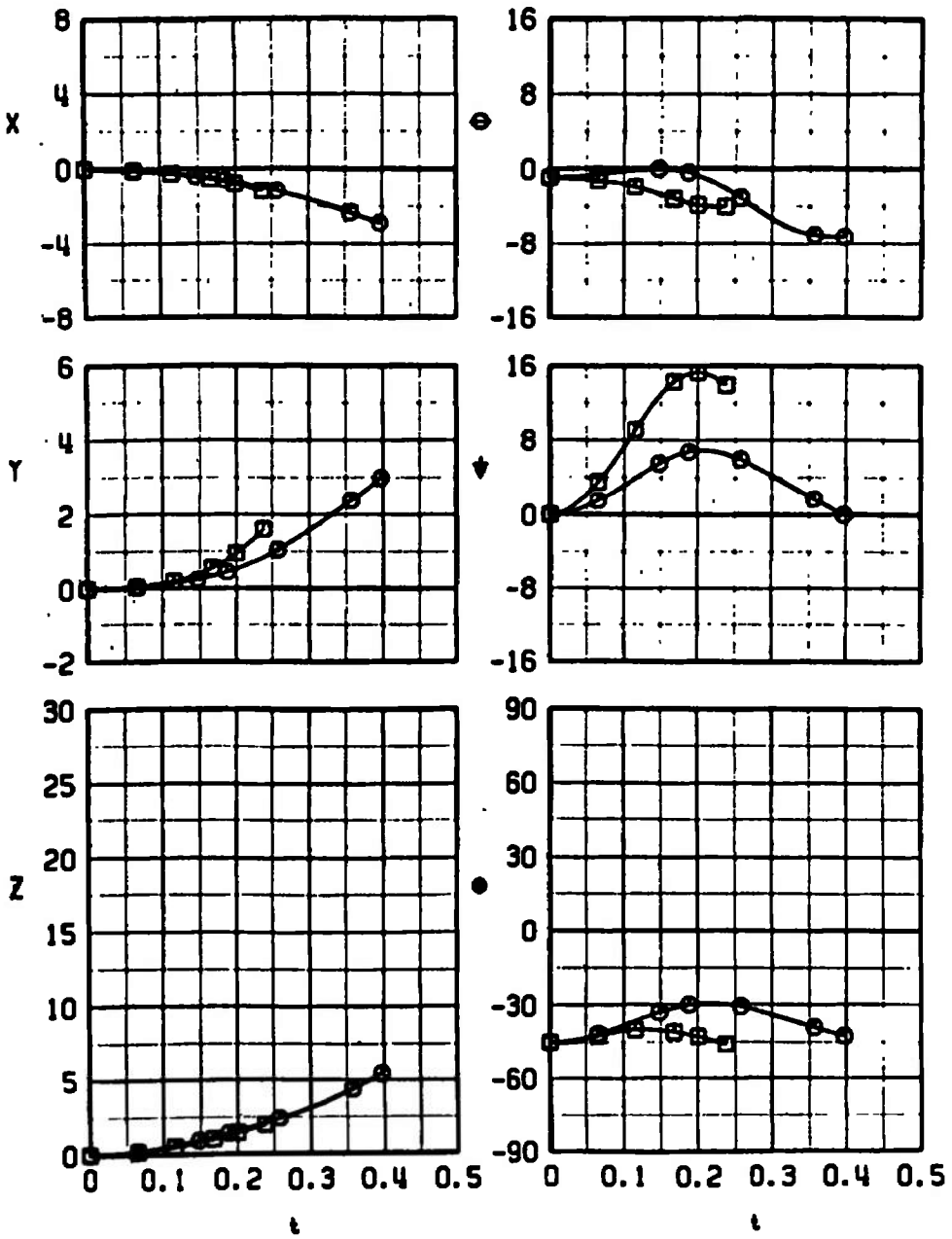

b. $M_\infty = 0.90$

Fig. 31 Concluded

SYM	CONF	M_∞	α_p	$\bar{\phi}$	STORE
□	3	0.66	1.7	0	S-2
○	14	0.66	1.7	0	S-2

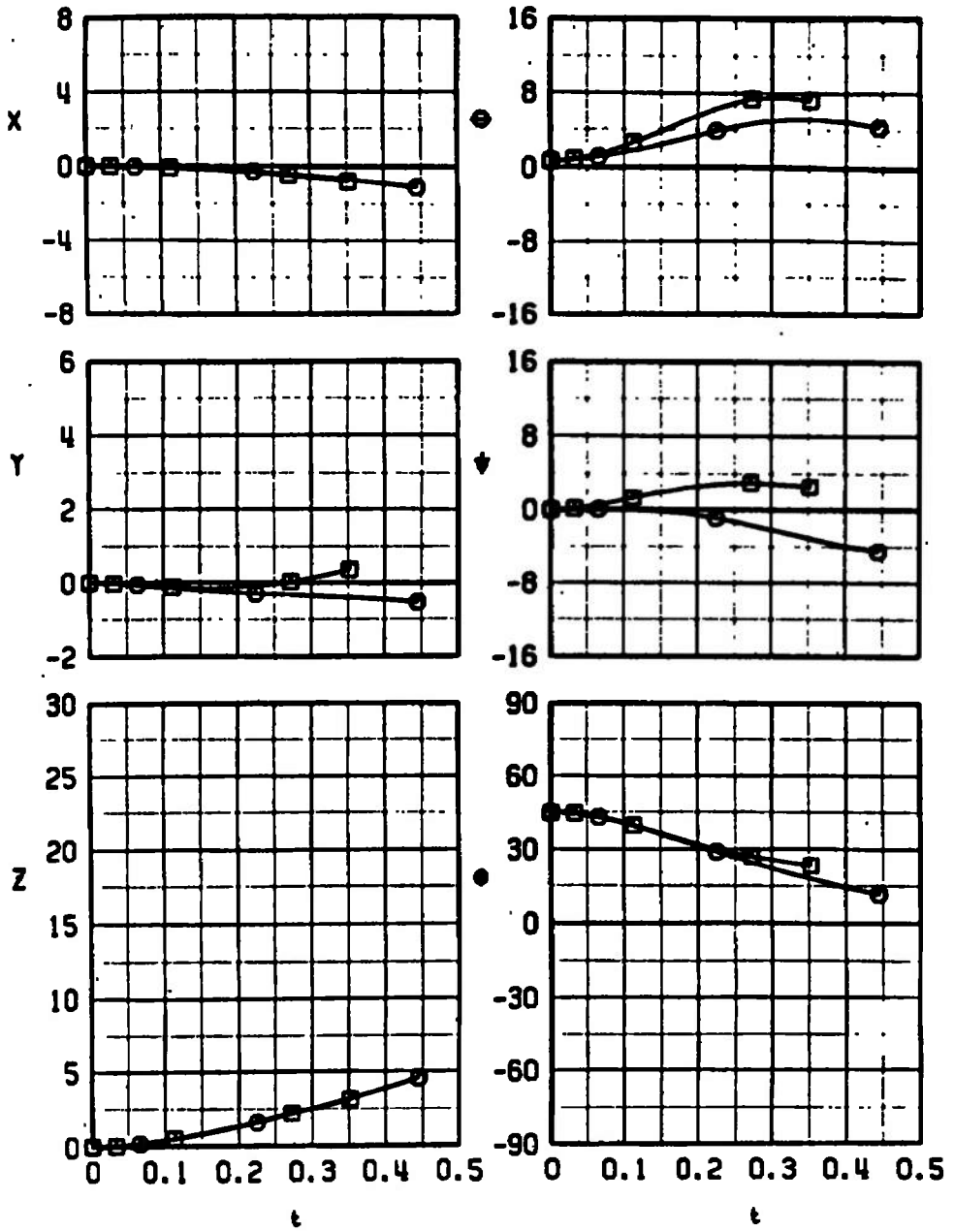

a. $M_\infty = 0.66$

Fig. 32 Effect of Fuel Tank Location on Separation Trajectories (Simulated Left Wing, Inboard TER, Station 3)

SYM	CONF	M_∞	α_p	$\bar{\phi}$	STORE
⊡	3	0.90	0.1	0	S-2
⊙	14	0.90	0.1	0	S-2

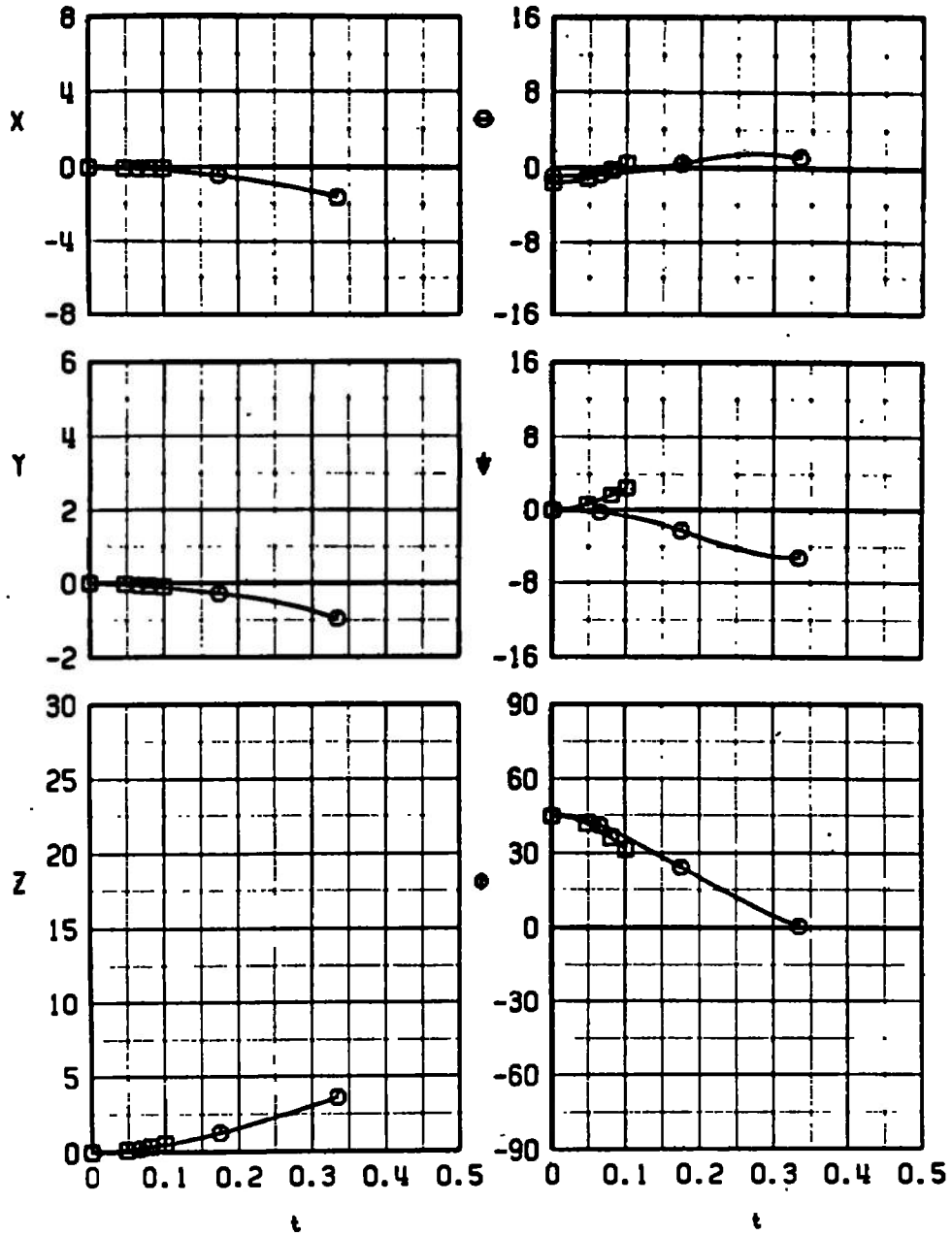

b. $M_\infty = 0.90$

Fig. 32 Concluded

SYM	CONF	M_∞	α_p	$\bar{\theta}$	STORE
□	1	0.90	0.1	0	S-2
○	1	0.90	-0.6	-45	S-2

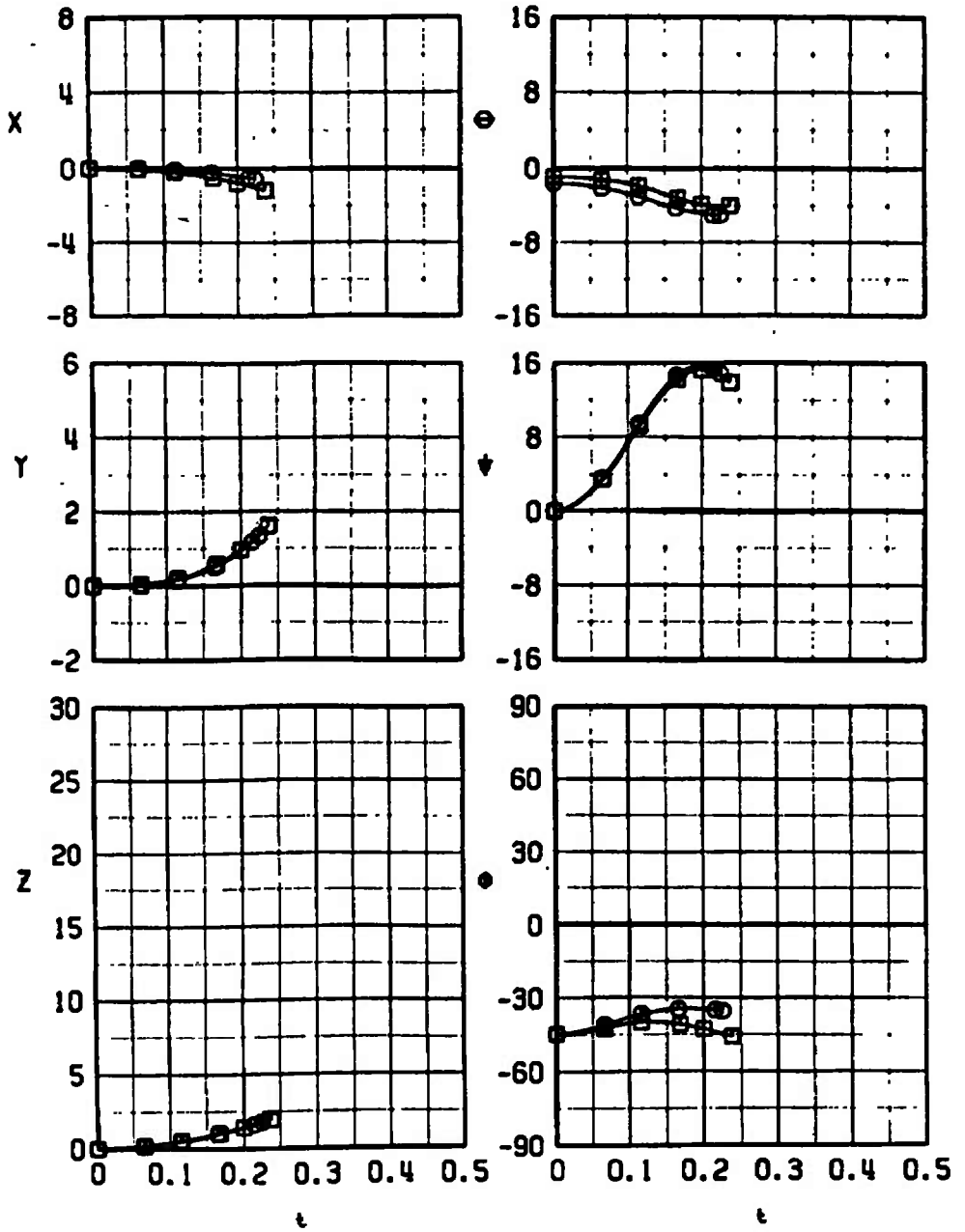

a. Load Configuration 1 (Simulated Left Wing, Inboard TER, Station 2, S-2)

Fig. 33 Effect of Parent-Aircraft Dive Angle on Separation Trajectories from Several Load Configurations at Mach Number 0.90

SYM	CONF	M_∞	α_p	$\bar{\phi}$	STORE
□	2	0.90	0.1	0	S-2
○	2	0.90	-0.6	-45	S-2

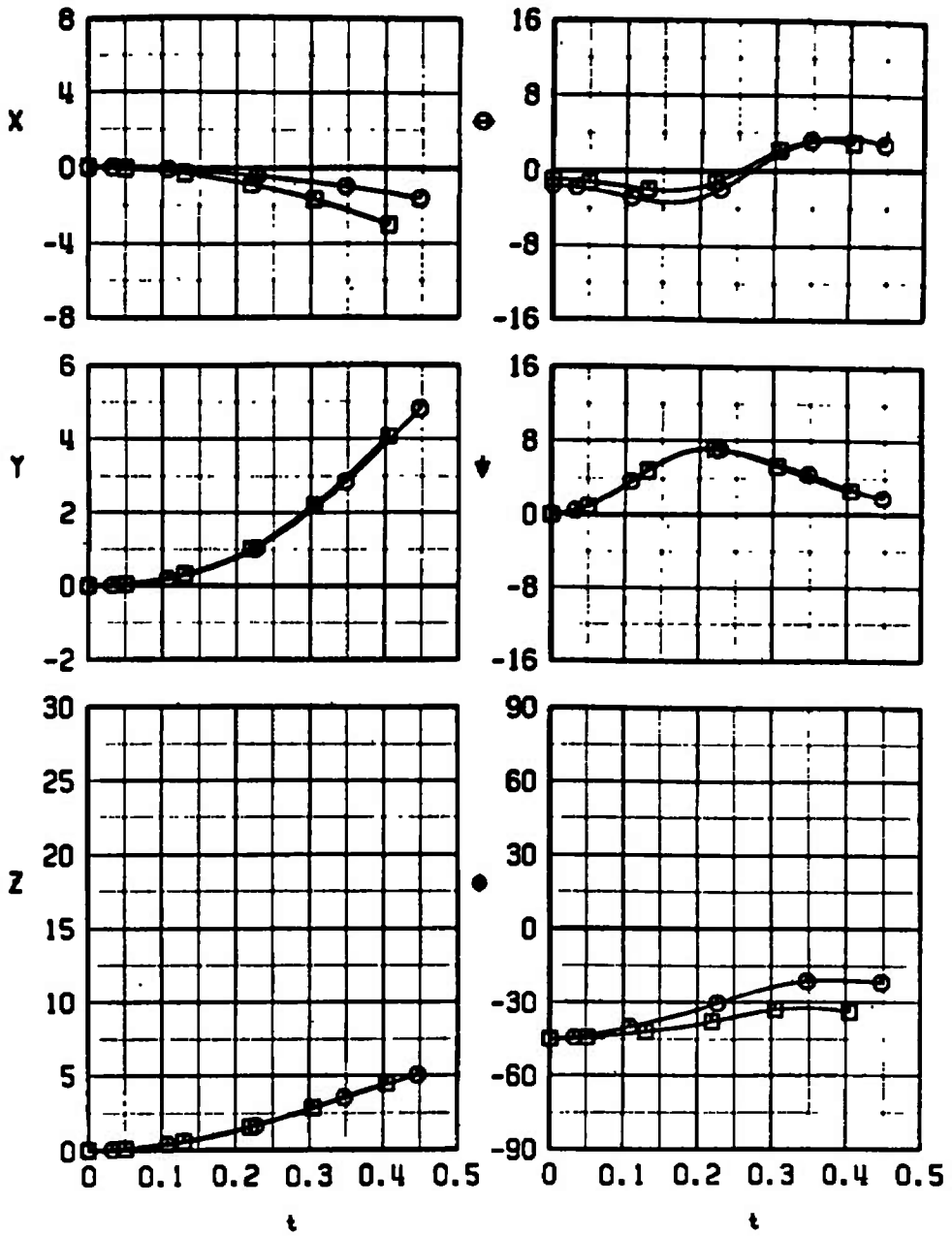

b. Load Configuration 2 (Right Wing, Inboard TER, Station 3, S-2)
Fig. 33 Continued

SYM	CONF	M_∞	α_p	$\bar{\phi}$	STORE
□	4	0.90	0.1	0	S-2
○	4	0.90	-0.6	-45	S-2

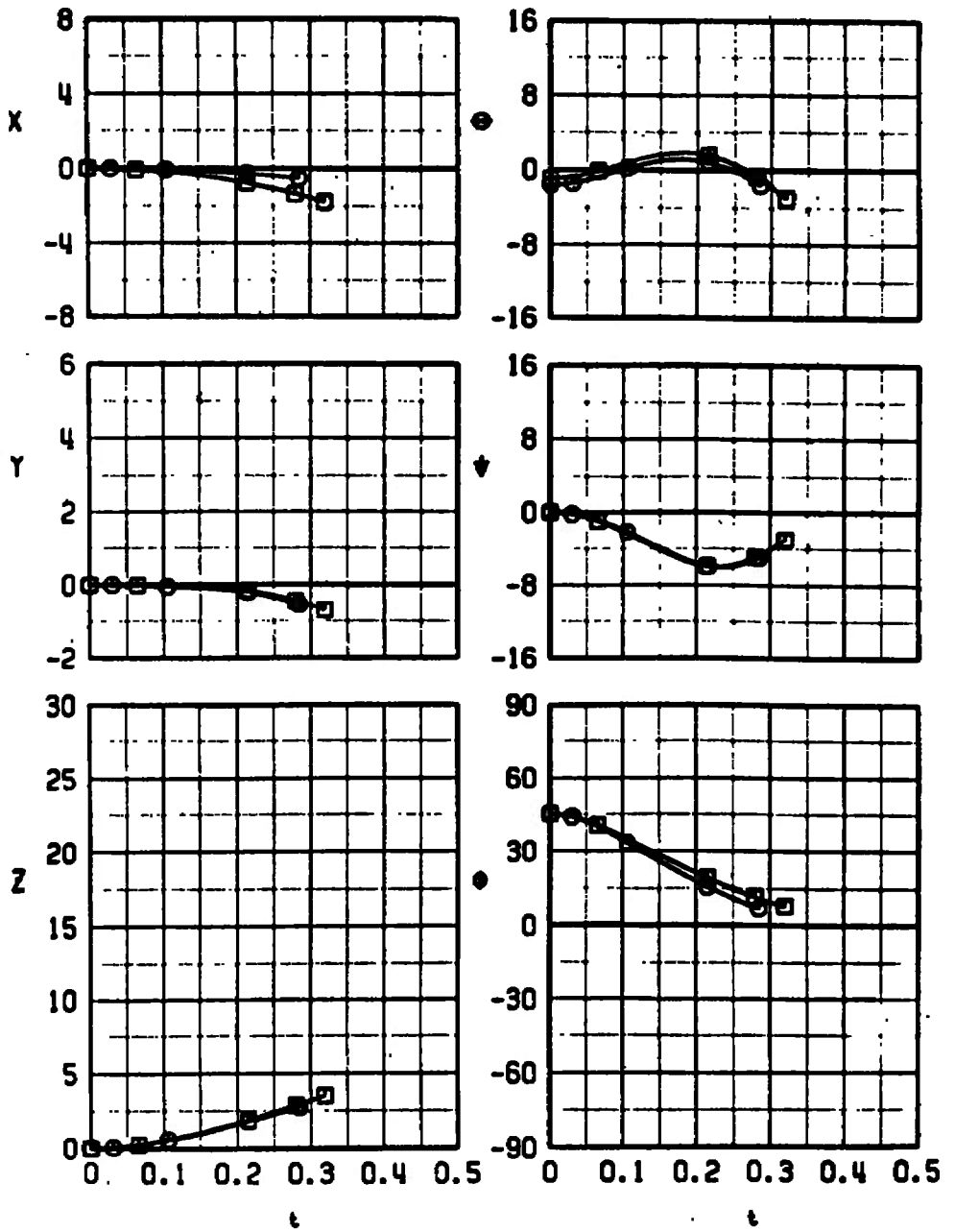

c. Load Configuration 4 (Right Wing, Inboard TER, Station 2, S-2)
Fig. 33 Continued

SYM	CONF	M_∞	σ_p	$\bar{\theta}$	STORE
⊡	5	0.90	0.1	0	S-2
⊙	5	0.90	-0.6	-45	S-2

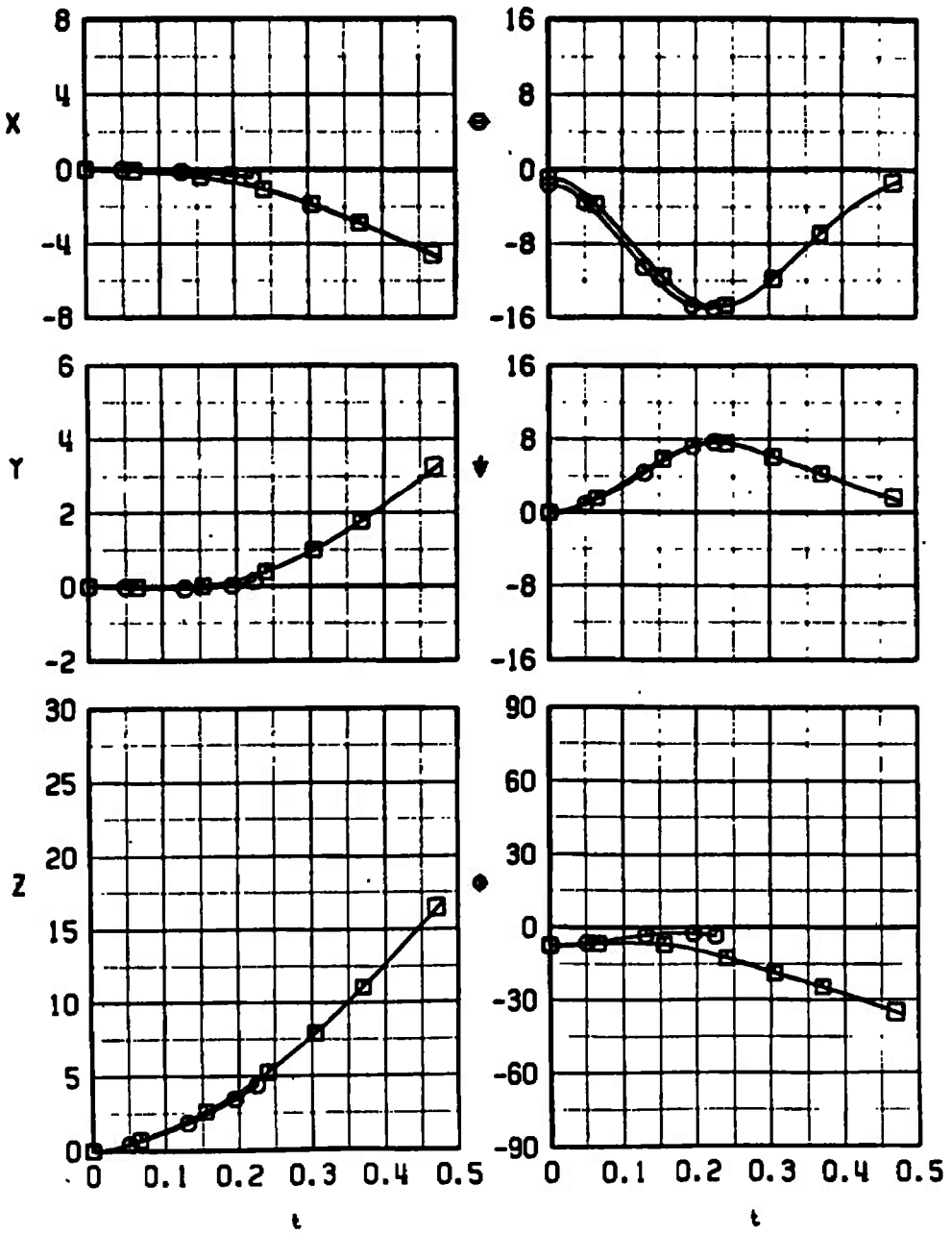

d. Load Configuration 5 (Simulated Left Wing, Outboard Pylon, S-2)
Fig. 33 Continued

SYM	CONF	M_∞	α_p	$\bar{\phi}$	STORE
□	6	0.90	0.1	0	S-2
○	6	0.90	-0.6	-45	S-2

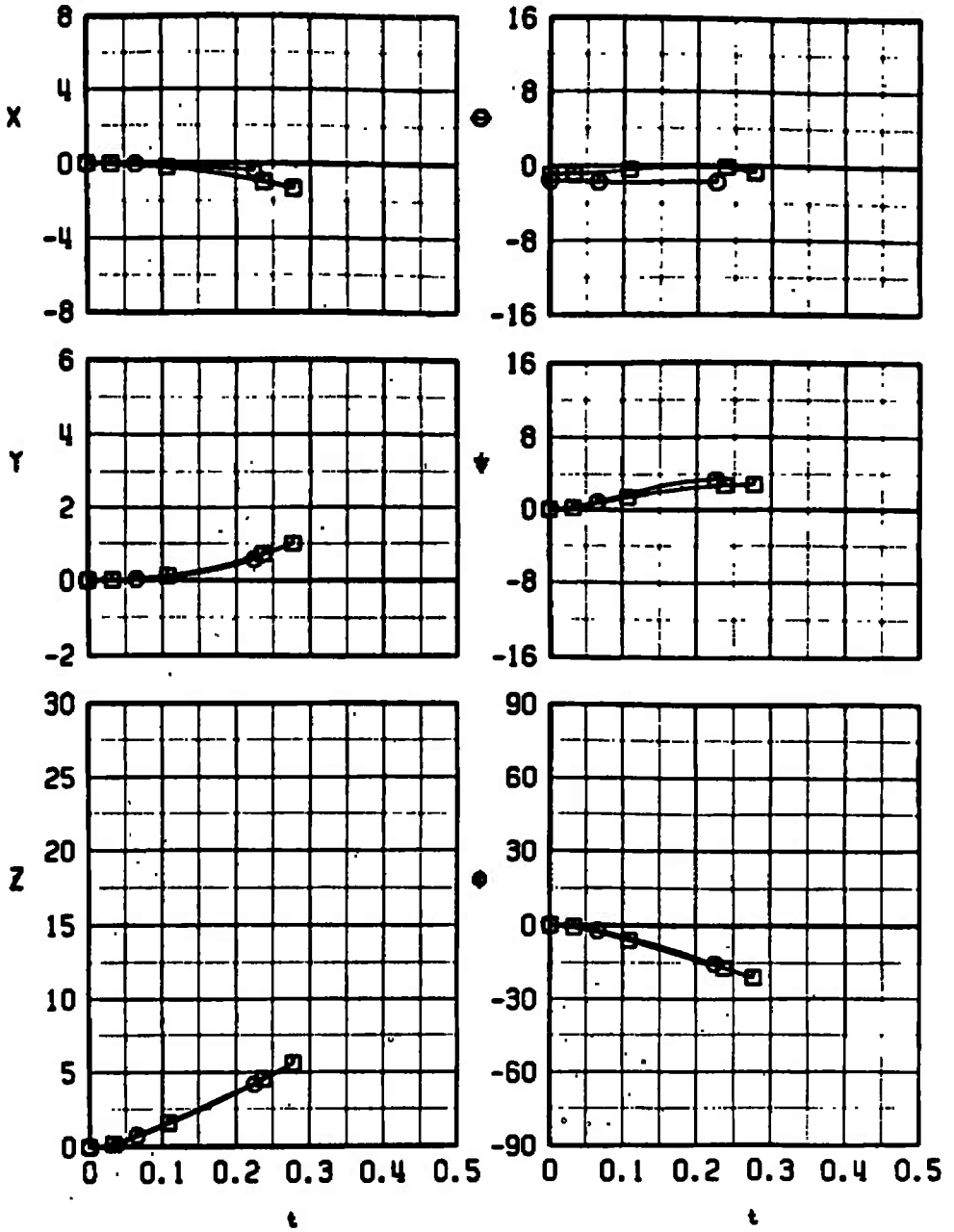

e. Load Configuration 6 (Simulated Left Wing, Inboard Pylon, S-2)
Fig. 33 Continued

SYM	CONF	M_∞	α_p	$\bar{\phi}$	STORE
□	7	0.90	0.1	0	S-3
○	7	0.90	-0.6	-45	S-3

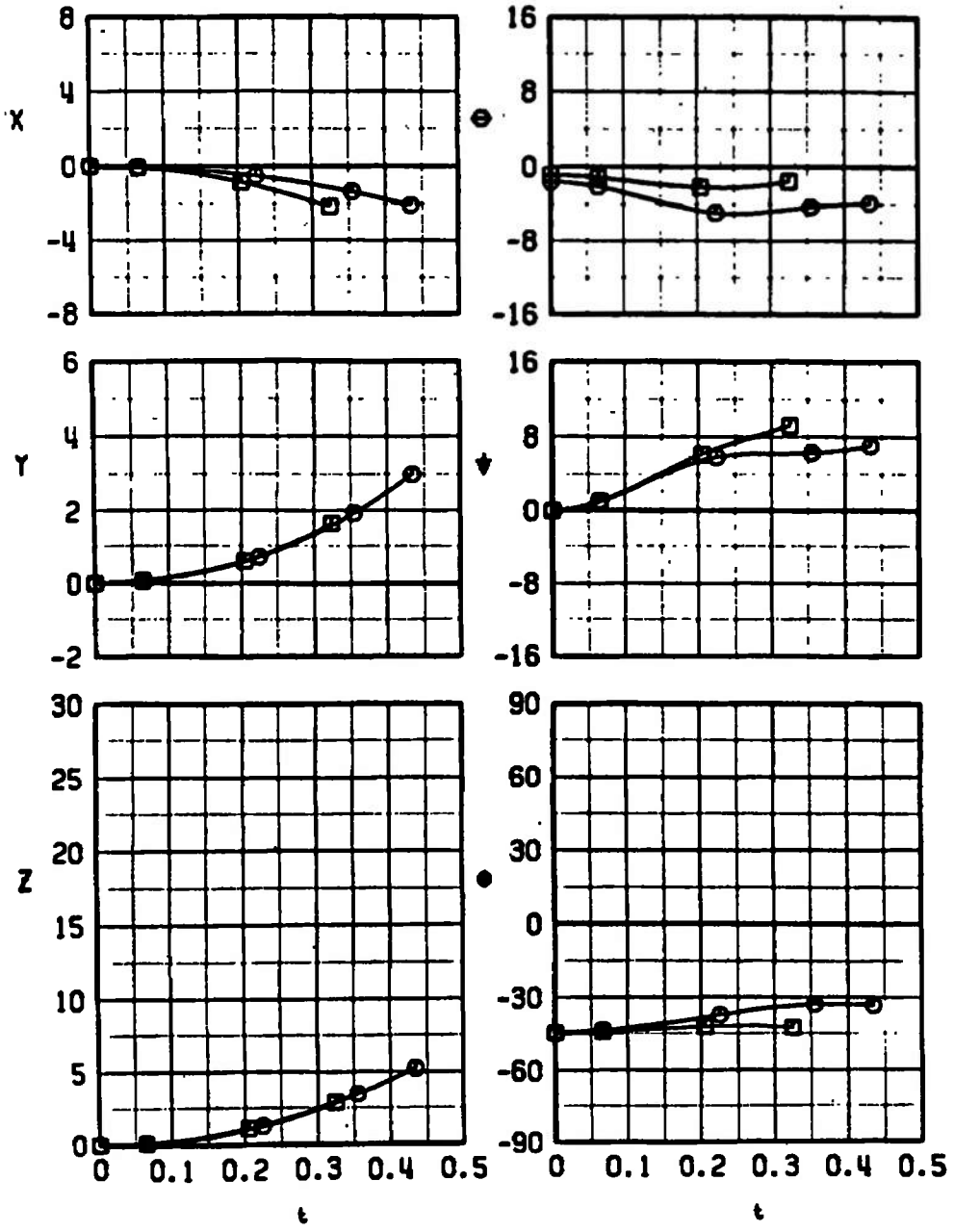

f. Load Configuration 7 (Simulated Left Wing, Inboard TER, Station 2, S-3)
Fig. 33 Continued

SYM	CONF	M_∞	α_p	$\bar{\phi}$	STORE
□	8	0.90	0.1	0	S-3
○	8	0.90	-0.6	-45	S-3

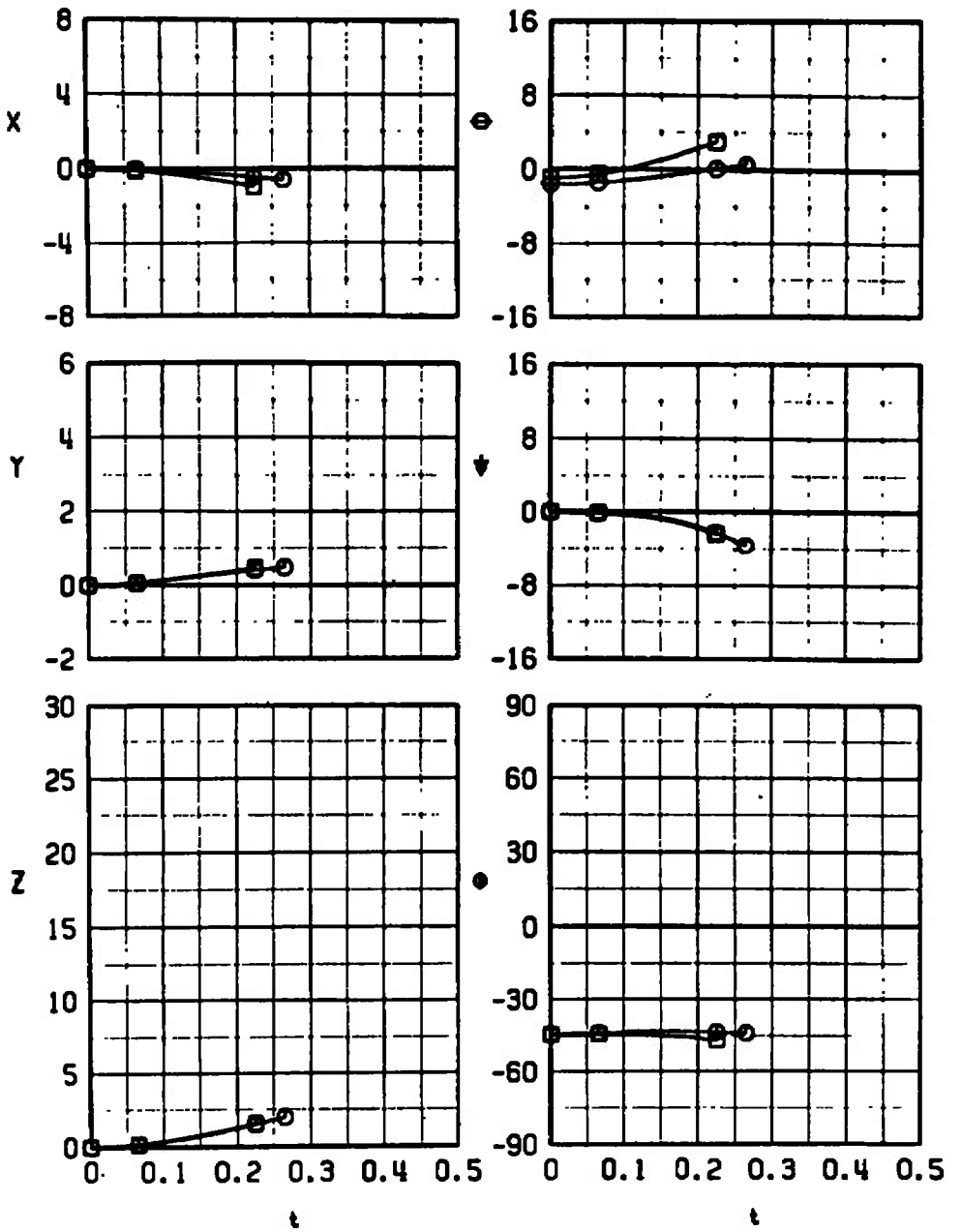

g. Load Configuration 8 (Right Wing, Inboard TER, Station 3, S-3)
Fig. 33 Continued

SYM	CONF	M_∞	α_p	$\bar{\phi}$	STORE
□	9	0.90	0.1	0	S-3
○	9	0.90	-0.6	-45	S-3

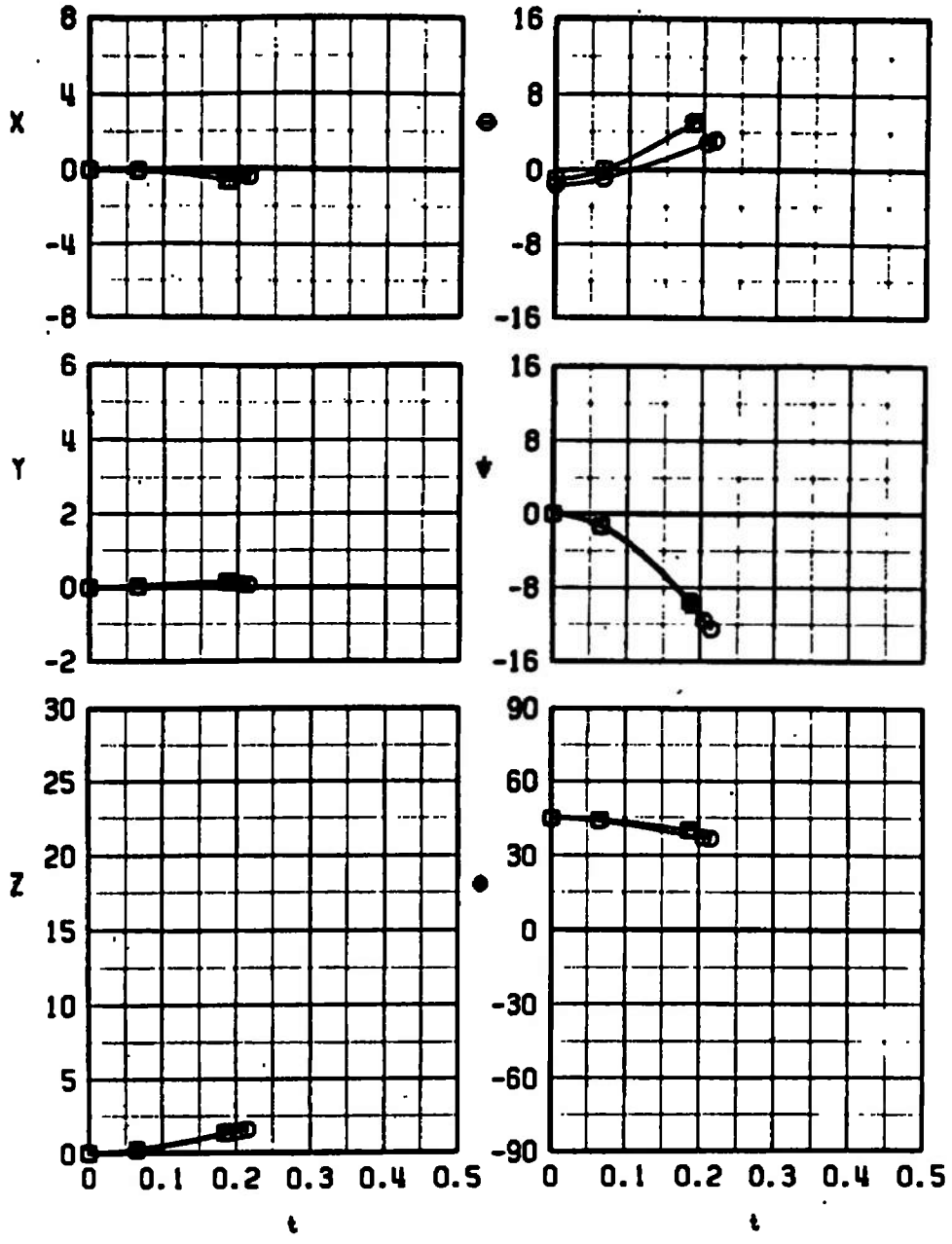

h. Load Configuration 9 (Simulated Left Wing, Inboard TER, Station 3, S-3)
Fig. 33 Continued

SYM	CONF	M_∞	α_p	$\bar{\phi}$	STORE
□	10	0.90	0.1	0	S-3
○	10	0.90	-0.6	-45	S-3

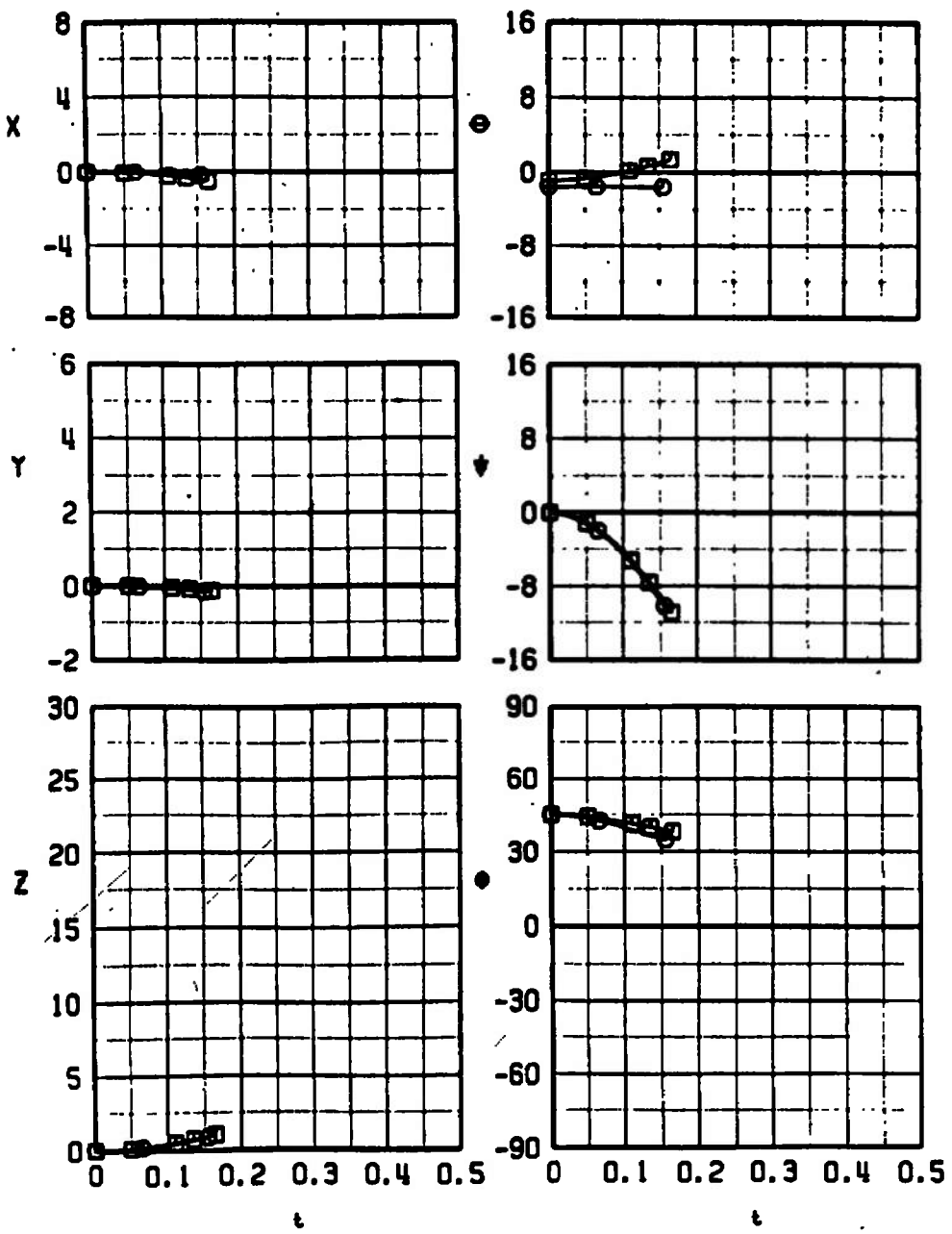

i. Load Configuration 10 (Right Wing, Inboard TER, Station 2, S-3)
Fig. 33 Continued

SYM	CONF	M_∞	α_p	$\bar{\phi}$	STORE
⊡	11	0.90	0.1	0	S-3
⊙	11	0.90	-0.6	-45	S-3

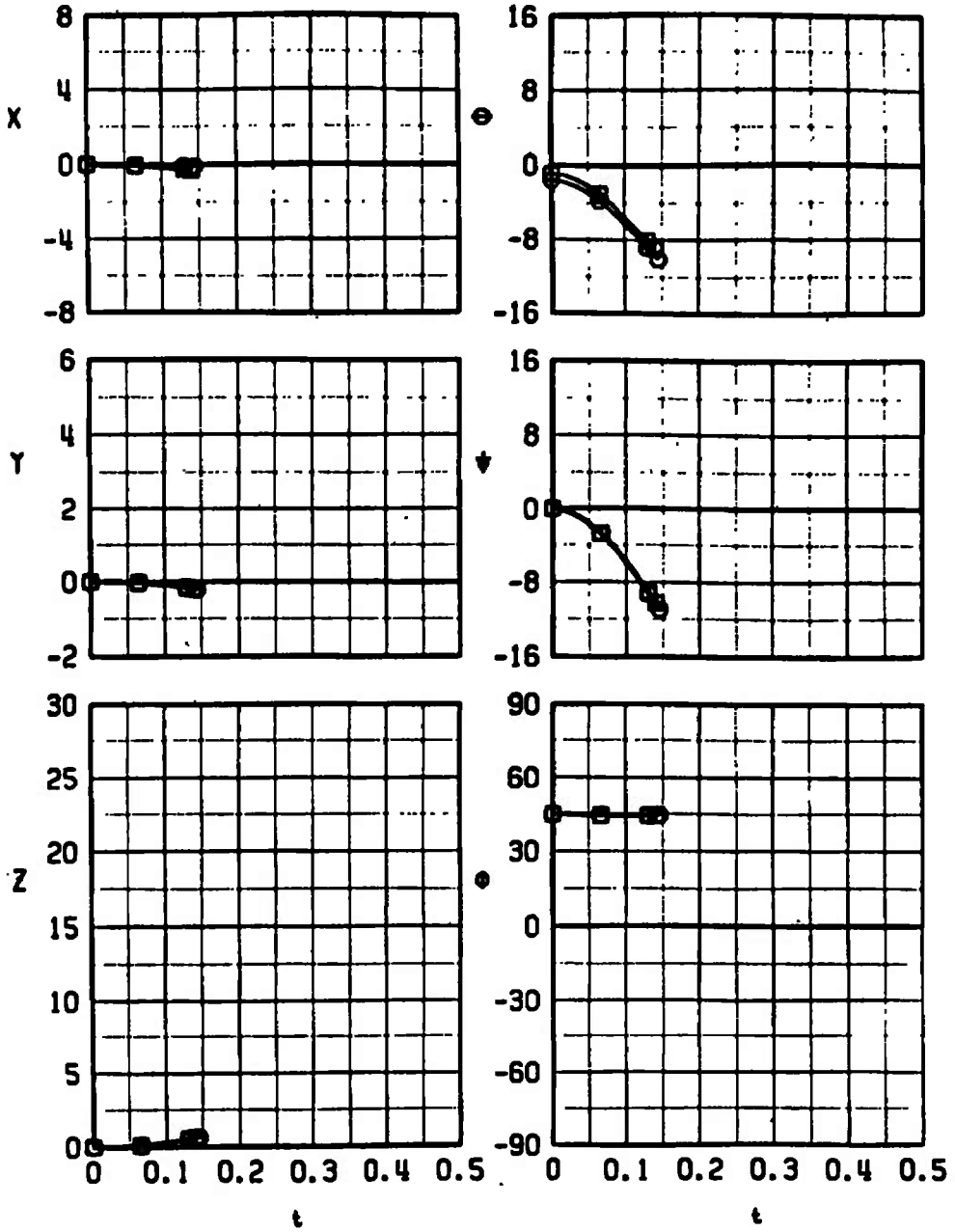

j. Load Configuration 11 (Centerline MER, Station 3, S-3)
Fig. 33 Continued

SYM	CONF	M_∞	α_p	$\bar{\phi}$	STORE
⊡	13	0.90	0.1	0	S-2
⊙	13	0.90	-0.6	-45	S-2

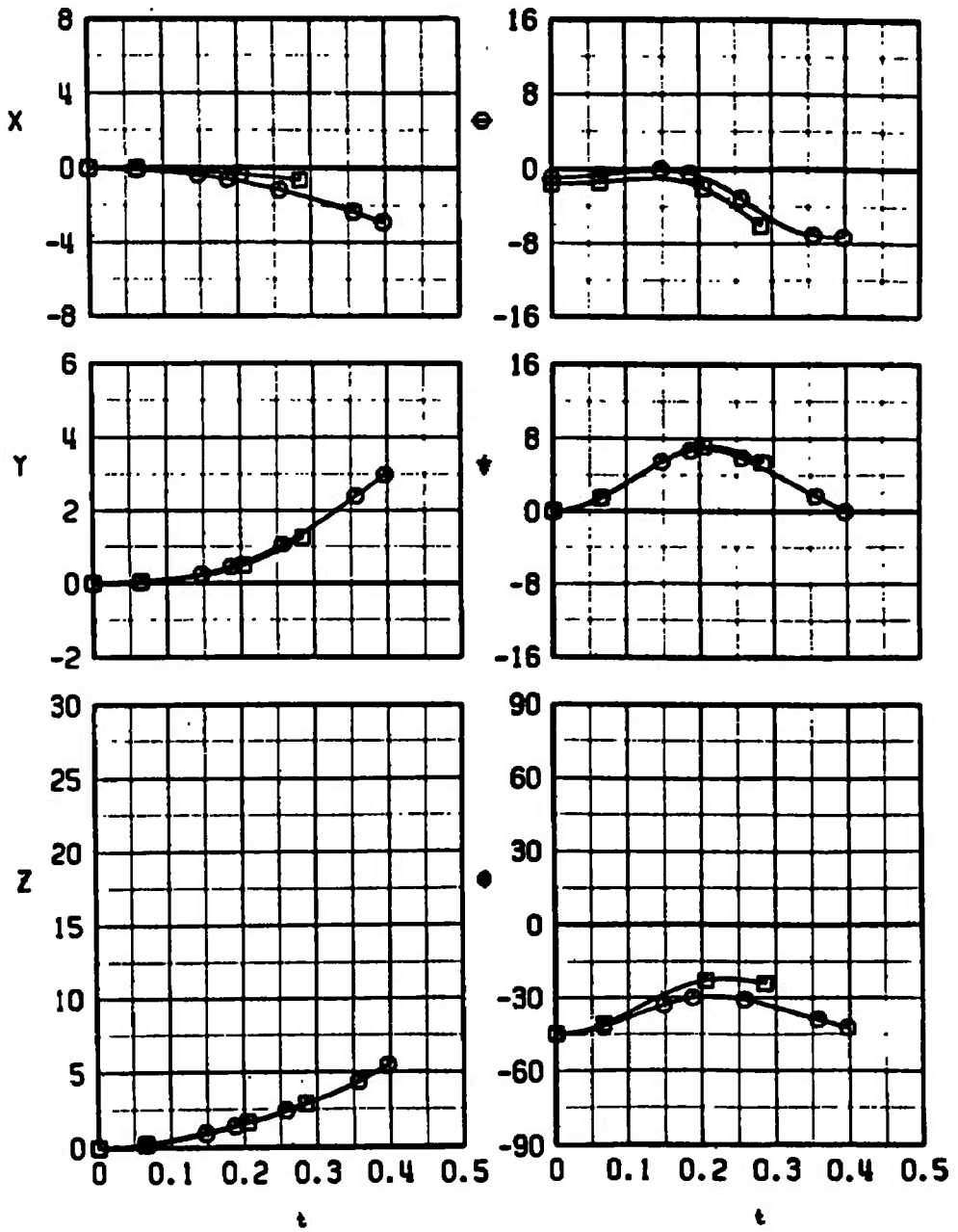

k. Load Configuration 13 (Simulated Left Wing, Inboard TER, Station 3, S-2)
Fig. 33 Concluded

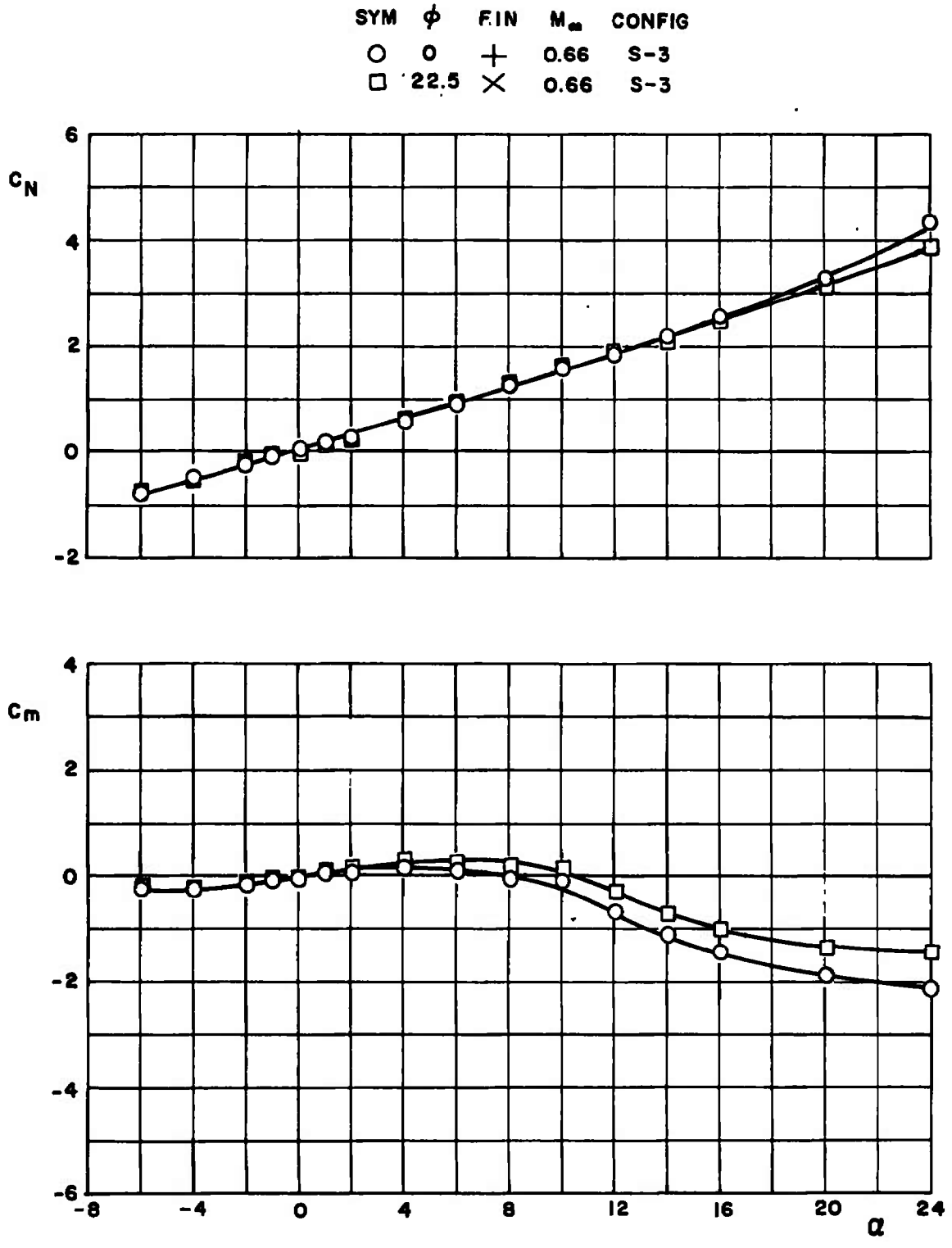

a. $M_\infty = 0.66$

Fig. 34 Free-Stream Static Stability Data for SUU-51 (LGDM) Alternate Design (S-3)

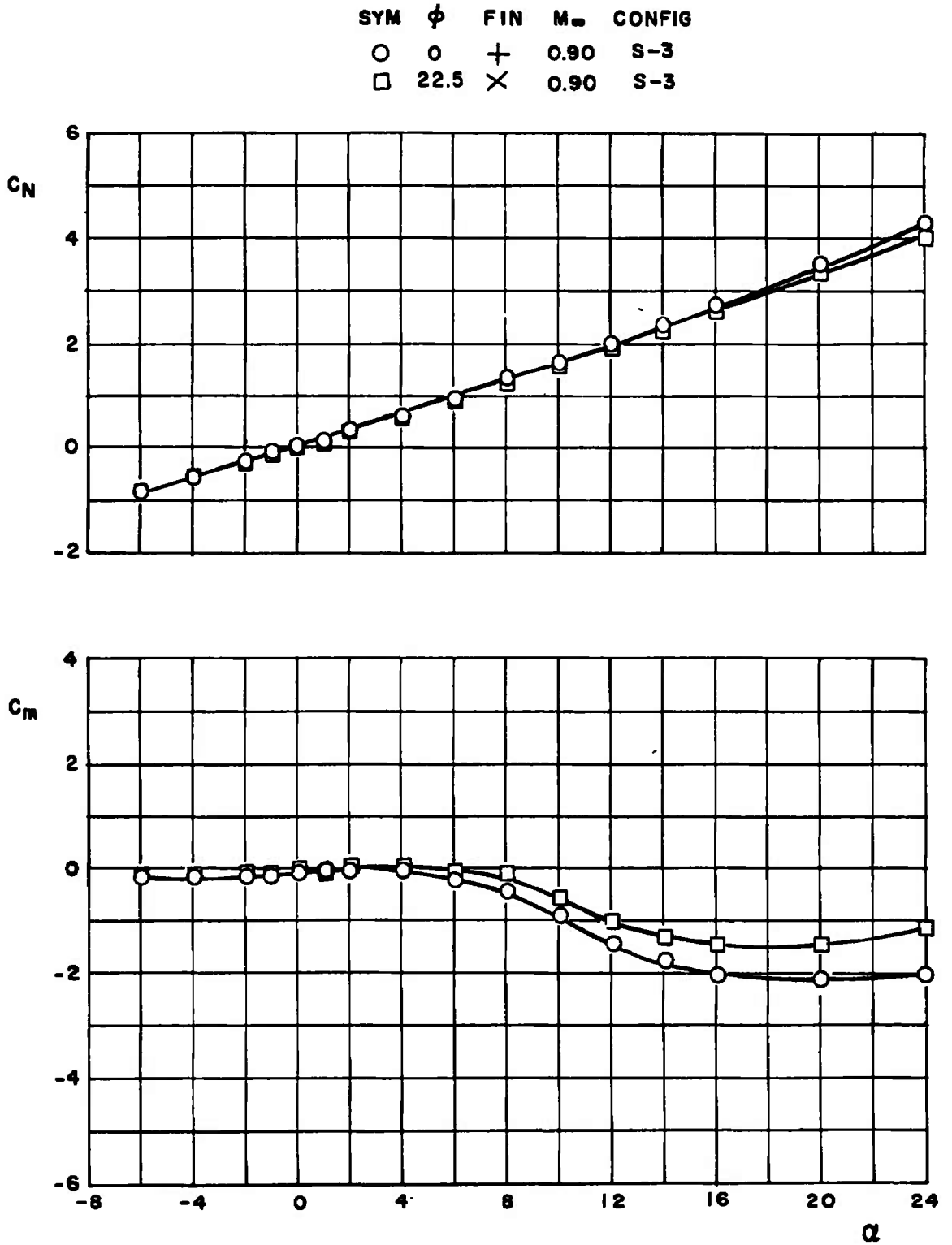

b. $M_\infty = 0.90$

Fig. 34 Concluded

TABLE I
FULL-SCALE STORE PARAMETERS USED IN THE TRAJECTORY CALCULATIONS

Parameter	Store		
	S-1	S-2	S-3
Mass, $\bar{m}$, slugs	31.081	25.241	31.081
Center-of-gravity location, X_{cg}, ft	7.163	7.156	7.207
Location of ejector forces, X_{L_1}, ft (pylon release)	0.854	0.845	---
Location of ejector forces, X_{L_2}, ft (pylon release)	-0.812	-0.821	---
Location of ejector forces, X_L, ft (MER/TER release)	-0.273	-0.160	-0.273
Ejector force cutoff time, T_E, sec (pylon release)	0.054	0.043	---
Ejector stroke length, Z_E, ft (MER/TER release)	0.255	0.255	0.255
Store reference area, S, ft^2	1.396	1.396	1.396
Store reference diameter, b, ft	1.333	1.333	1.333
Roll moment of inertia, I_{xx}, slugs-ft^2	7.8	6.5	7.8
Pitch moment of inertia, I_{yy}, slugs-ft^2	148.8	136.5	155.1
Yaw moment of inertia, I_{zz}, slugs-ft^2	148.3	135.9	154.6
Product of inertia, I_{xz}, slugs-ft^2	-0.27	-0.26	-0.30
Pitch-damping derivative, C_{m_q}, per radian	-324.0	-324.0	-282.0
Yaw-damping derivative, C_{n_r}, per radian	-324.0	-324.0	-282.0
Roll-damping derivative, C_{ℓ_p}, per radian	-6.5	-6.5	-4.0

TABLE II
MAXIMUM FULL-SCALE POSITION UNCERTAINTIES RESULTING
FROM BALANCE PRECISION LIMITATIONS

M_∞	t, sec	ΔX, ft	ΔY, ft	ΔZ, ft	$\Delta\theta$, deg	$\Delta\psi$, deg	$\Delta\phi$, deg
0.66	0.40	±0.04	±0.03	±0.02	±0.3	±0.6	±4
0.90	0.40	±0.07	±0.05	±0.04	±0.6	±1.1	±7

UNCLASSIFIED

Security Classification

DOCUMENT CONTROL DATA - R & D

(Security classification of title, body of abstract and indexing annotation must be entered when the overall report is classified)

1. ORIGINATING ACTIVITY *(Corporate author)*

Arnold Engineering Development Center
Arnold Air Force Station, Tennessee

2a. REPORT SECURITY CLASSIFICATION

UNCLASSIFIED

2b. GROUP

N/A

3 REPORT TITLE

SEPARATION CHARACTERISTICS OF THE SUU-51 LASER-GUIDED DISPENSER MUNITION WITH FIXED TAIL FINS FROM THE F-4C AIRCRAFT

4 DESCRIPTIVE NOTES *(Type of report and inclusive dates)*

August 7 through 13, 1971 - Final Report

5. AUTHOR(S) *(First name, middle initial, last name)*

Jerry Coble, ARO, Inc.

This document has been approved for public release, its distribution is unlimited PER TAB 74-13, dtd 21 JUNE, 1974

6. REPORT DATE	7a. TOTAL NO. OF PAGES	7b. NO. OF REFS
November 1971	73	3

8a. CONTRACT OR GRANT NO.	9a. ORIGINATOR'S REPORT NUMBER(S)
b. PROJECT NO. 1120	AEDC-TR-71-244 AFATL-TR-71-142
c. Program Element 64604F d. Task 09	9b. OTHER REPORT NO(S) *(Any other numbers that may be assigned this report)* ARO-PWT-TR-71-184

10 DISTRIBUTION STATEMENT Distribution limited to U.S. Government agencies only; this report contains information on test and evaluation of military hardware; November 1971; other requests for this document must be referred to Air Force Armament Laboratory (DLGC), Eglin AFB, Florida 32542.

11. SUPPLEMENTARY NOTES	12. SPONSORING MILITARY ACTIVITY
Available in DDC	AFATL (DLGC) Eglin AFB, Florida 32542

13. ABSTRACT Tests were conducted in the Aerodynamic Wind Tunnel (4T) using 0.05-scale models to investigate the separation characteristics of the SUU-51 Laser-Guided Dispenser Munition (LGDM) with fixed tail fins from several carriage configurations of the F-4C aircraft. Releases were studied from the outboard and inboard pylons and from Triple Ejection Rack and Multiple Ejection Rack locations on the inboard and centerline pylons, respectively. Captive-trajectory store separation data were obtained at Mach numbers from 0.66 to 0.90 and a simulated altitude of 5000 ft. At selected test conditions, a parent-aircraft dive angle of 45 deg was simulated. Free-stream force and moment data were also obtained on the SUU-51 (LGDM) model at Mach numbers of 0.66 and 0.90 at store angles of attack from -6 to 24 deg. Generally, the store initially separated from the parent aircraft without store-to-parent contact with most of the trajectories manually terminated. Changing fuel tank positions improved some undesirable trajectories.

Distribution limited to U.S. Government agencies only; this report contains information on test and evaluation of military hardware; November 1971; other requests for this document must be referred to Air Force Armament Laboratory (DLGC), Eglin AFB, Florida 32542.

DD FORM 1 NOV 68 1473

UNCLASSIFIED

Security Classification

14. KEY WORDS	LINK A		LINK B		LINK C	
	ROLE	WT	ROLE	WT	ROLE	WT
F-4C Aircraft						
external stores						
fins (fixed tail)						
separation						
trajectories						
transonic flow						

AFSC
Arnold AFS Tenn